



TAMPEREEN TEKNILLINEN YLIOPISTO
TAMPERE UNIVERSITY OF TECHNOLOGY

Jyrki Kimmel
Studies on Diffractive Mobile Display Backlights



Julkaisu 1053 • Publication 1053

Tampereen teknillinen yliopisto. Julkaisu 1053
Tampere University of Technology. Publication 1053

Jyrki Kimmel

Studies on Diffractive Mobile Display Backlights

Thesis for the degree of Doctor of Science in Technology to be presented with due permission for public examination and criticism in Tietotalo Building, Auditorium TB109, at Tampere University of Technology, on the 16th of June 2012, at 12 noon.

Tampereen teknillinen yliopisto - Tampere University of Technology
Tampere 2012

ISBN 978-952-15-2844-6 (printed)
ISBN 978-952-15-2854-5 (PDF)
ISSN 1459-2045

Abstract

The digital convergence has brought about a new class of mobile devices that allows a compelling, visually rich multimedia experience to the user in a handheld product, such as a mobile telephone. The display in these “smart phones”, “feature phones”, or “multimedia computers”, is a strategically important component that defines the user experience for a great part. While the visual user experience provided by the display can be very good, the power dissipation in the display is the limiting factor in the length of the user interaction with the mobile multimedia content. As the proportion of time of interacting with the visually rich content increases over that of simple voice-driven communication, such commonly used techniques for reducing the overall energy consumption of the device as power-saving modes or time outs cannot be used during a multimedia session without compromising the quality of service to the user.

The conventional mobile liquid-crystal display structure consists of a backlight unit with the associated light sources, the display panel itself, and various optical films that control the state of polarization and viewing characteristics of the display. The backlight unit itself has evolved in the last fifteen years to become a very efficient component to provide uniform illumination to the electro-optic spatial light modulator comprised by the liquid-crystal pixel array. In the conventional structure, the color filter array embedded in the liquid-crystal display panel limits the light throughput in the display system. The backlight unit itself in the conventional configuration is difficult to improve any further, and a system redesign is required to make the display system perform more efficiently than what is currently possible.

One possible way to redesign a display system more effectively is to direct the appropriate primary bands of light through the respective subpixels in the display panel, instead of having these filter white light into the primary colors. This can be done by diffractive means, *i. e.* by placing a grating structure on the light guide plate of the backlight unit. Significant improvement in energy efficiency of a mobile display system can be achieved by this approach, and at the same time, cost savings can be expected due

to the elimination of many beam-shaping films in the backlight unit, as compared to the conventional mobile liquid-crystal display configuration. Further cost savings can be achieved by removing the color filter array, provided that the color purity of outcoupled light is good.

This thesis presents a new pixelated color-separating grating array concept that diffracts the light from red, green, and blue light-emitting diodes in the backlight unit through a subpixel array in a prospective mobile display module. A literature review was conducted and key research studies in the area of diffractive mobile display backlights were reviewed. Experimental studies to verify various constituent elements of this concept are presented, and conclusions are drawn on how the display industry could benefit from this new concept, and what should be taken into account when adopting a new display manufacturing paradigm based on diffractive backlights.

Preface

This study was carried out during the years 2006 to 2012 at Nokia Research Center (NRC), in Tampere, Finland. While no direct support from outside Nokia was applied to the research, this work benefited from several projects funded by the Finnish Funding Agency for Technology and Innovation (Tekes).

I thank my supervisors at Tampere University of Technology (TUT), Rector Markku Kivikoski and Prof. Jukka Vanhala for their support and encouragement, and the Dean of the Faculty of Computing and Electrical Engineering of TUT, Dr. Ulla Ruotsalainen, for her guidance in the finalization of this thesis. I thank with appreciation the pre-examiners of this thesis, Dr. Kälil Käläntär of Global Optical Solutions, Japan, and Prof. Norbert Fruehauf of University of Stuttgart, Germany, for their valuable comments. I also extend my thanks to my superiors at Nokia Research Center, Dr. Martin Schrader, Ms. Marja Salmimaa, and Dr. Jyri Huopaniemi for their continuing support during the work. I also thank the principal of the NRC's PhD program, Dr. Jari Kangas for his interest and helpful discussions. The Immersive Interaction Technologies Team of the NRC Media Technology Laboratory have been very helpful throughout the project, and I thank them all, especially Mr. Toni Järvenpää and Dr. Pekka Äyräs, as well as Mr. Markus Virta of the NRC Prototyping Unit for their unfailing help regarding the laboratory work. Further thanks are due to our colleagues at NanoComp Oy, Dr. Pasi Laakkonen (currently of Rocsole, Ltd.), Dr. Sami Siitonen, and Mr. Tuomo Rytönen. I am also grateful to Dr. Johan Bergquist of Nokia Chief Technology Officer unit in Tokyo, Dr. Pasi Saarikko, currently in Microsoft Corp., as well as Dr. Andrea Giraldo and Mr. Nicholas Bergeron at Liquavista BV (now a subsidiary of Samsung Corp.), who have been coauthors in my publications, and helpful in many other ways. I am also deeply grateful for the instrumental inspiration, influence, and insight of Dr. Tapani Levola, currently at Microsoft Corp. who designed all the gratings for this thesis during his work at NRC.

Finally, I have my love and deepest gratitude to my dear wife Ulla-Maija, as well as my son Arttu-Sakari and daughter Kaisa-Maria without whose continuous support, encouragement, patience, and coaching this thesis would never have been written.

Tampere, April 24th, 2012

Jyrki Kimmel

Contents

ABSTRACT	I
PREFACE.....	III
CONTENTS	V
LIST OF PUBLICATIONS	VII
AUTHOR'S CONTRIBUTION	VIII
CONVENTIONS AND LIST OF ABBREVIATIONS.....	IX
1 INTRODUCTION	1
2 DISPLAYS FOR PORTABLE AND HANDHELD ELECTRONIC DEVICES	4
2.1 DISPLAYS IN MOBILE COMMUNICATIONS.....	4
2.1.1 <i>Background</i>	4
2.1.2 <i>Mobile Display Technology</i>	6
2.1.3 <i>Requirements for Mobile Displays</i>	8
2.2 TRANSFLECTIVE DISPLAYS FOR MOBILE APPLICATIONS	9
2.2.1 <i>Transflective LCD Structures and LC Optics</i>	10
2.2.2 <i>Light Sources</i>	13
2.2.3 <i>Incoupling Structures</i>	15
2.2.4 <i>LGPs and Reflectors</i>	15
2.2.5 <i>Beam-Forming Optics and Polarizers</i>	16
2.2.6 <i>Compensation Films</i>	17
2.2.7 <i>Integration of Films</i>	17
2.2.8 <i>Top Coatings and Touch Structures</i>	18
2.3 ALTERNATIVE AND EMERGING TECHNOLOGY	18
2.3.1 <i>OLED Displays</i>	18
2.3.2 <i>Field-Sequential Color Displays</i>	19
2.3.3 <i>Electrowetting Displays</i>	20
2.3.4 <i>Microelectromechanical System Displays</i>	21
2.3.5 <i>Electrophoretic Information Displays</i>	21
2.4 ENERGY AND POWER SAVINGS CONSIDERATIONS.....	22
3 DESCRIPTION OF WORK.....	24
3.1 CONVENTIONS AND COORDINATE SYSTEMS IN DIFFRACTIVE BACKLIGHT DESIGN.....	24
3.2 LITERATURE ON DIFFRACTIVE BACKLIGHT TECHNOLOGIES	26
3.3 BINARY AND SLANTED SMALL-AREA GRATING ARRAYS FOR DIFFRACTIVE BACKLIGHTS	26
3.3.1 <i>Concept Verification by Binary Striped Grating Array</i>	26
3.3.2 <i>Color-Separating Pixelated Slanted Grating Array</i>	30

3.4	BACKLIGHT DEMONSTRATOR STUDIES.....	34
3.4.1	<i>Diffractive Pixelated Backlight Array</i>	34
3.4.2	<i>Diffractive Pixelated Grating Array in Electrowetting Display Application</i>	38
3.5	EMBEDDED SOLUTION FOR DIFFRACTIVE BACKLIGHT	39
4	DISCUSSION AND CONCLUSIONS	46
	REFERENCES	51
	PUBLICATIONS	

List of Publications

This thesis consists of an introductory part and six publications [P1-P6]. The publications of this thesis are listed below.

- [P1] J. Kimmel, "Diffractive Backlight Technologies for Mobile Applications," *Journal of the Society for Information Display*, Vol. 20, No. 5, pp. 245-258, 2012.
- [P2] J. Kimmel, T. Levola, P. Saarikko, and J. Bergquist, "A Novel Diffractive Backlight Concept for Mobile Displays," *Journal of the Society for Information Display*, Vol. 16, No. 2, pp. 351-357, 2008.
- [P3] J. Kimmel, T. Levola, and P. Laakkonen, "Diffractive Backlight Grating Array for Mobile Displays," *Journal of the Society for Information Display*, Vol. 16, No. 8, pp. 863-870, 2008.
- [P4] J. Kimmel, T. Levola, S. Siitonen, and T. Rytönen, "A New Diffractive Backlight for Mobile Displays," *Proceedings of the International Display Research Conference 2008*, pp. 290-293, 2008.
- [P5] J. Kimmel, T. Levola, A. Giraldo, N. Bergeron, S. Siitonen, and T. Rytönen, "Diffractive Backlight Light Guide Plates in Mobile Electrowetting Display Applications," *SID Symposium Digest*, Vol. XV, pp. 826-829, 2009.
- [P6] J. Kimmel and T. Levola, "Mobile Display Backlight Light Guide Plates Based on Slanted Grating Arrays," *Journal of Photonics for Energy*, Vol. 2, pp. 024501-1 - 024501-11, 2012.

[P1-P5]: ©Society for Information Display. Reprinted with permission. [P6]: ©Society of Photo-Optical Instrumentation Engineers. Reprinted with permission.

Author's Contribution

Publication 1, “Diffractive Backlight Technologies for Mobile Displays” is a review paper researched and written solely by the author.

Publication 2, “A Novel Diffractive Backlight Concept for Mobile Displays:” the author was the principal writer. He devised the original concept, designed the experimental characterization setup and performed the measurements as well as analyzed the results.

Publication 3, “Diffractive Backlight Grating Array for Mobile Displays:” the author was the principal writer. He devised the original concept and grating array geometry, designed the experimental characterization setup, manufactured the grating samples and performed the measurements as well as analyzed the results.

Publication 4, “A New Diffractive Backlight for Mobile Displays:” the author was the principal writer. He devised the original concept and grating array geometry, subcontracted the manufacturing of the test samples, designed the experimental characterization setup and performed the measurements as well as analyzed the results.

Publication 5, “Diffractive Backlight Light Guide Plates in Mobile Electrowetting Display Applications:” the author was the principal writer. He devised the original concept and grating array geometry, subcontracted the manufacturing of the test samples, designed the experimental characterization setup and performed the measurements as well as analyzed the results.

Publication 6, “Mobile Display Backlight Light Guide Plates Based on Slanted Grating Arrays:” the author was the principal writer. He invented the concept and subcontracted the manufacturing of the test demonstrator, then designed the experimental characterization setup and performed the measurements. The analysis of the results was done jointly with the coauthor.

Conventions and List of Abbreviations

SI units are used except where conventions in the industry prefer English units, such as in characterizing the display size by diagonal inches, and pixel pitch by “points per inch” (ppi), and units conventionally used in the industry in describing data transfer speed *e. g.* in 1000 bits per second (kbit/s). Units, names of elements of the periodic table and their inorganic compounds, glass types, and registered trademarks are not listed in the list of abbreviations below.

2G	second generation
3G	third generation
4G	fourth generation
ALD	atomic layer deposition
ALS	ambient light sensor
AM	active matrix
AMLCD	active-matrix liquid-crystal display
AMOLED	active-matrix organic light-emitting diode
B	blue
BEF	brightness-enhancing film
BLU	backlight unit
Caller ID	caller identification
CBU	color breakup
CCFL	cold-cathode fluorescent lamp
CFA	color filter array
CIE	Committee International d’Eclairage
CSTN	color supertwist nematic
DBEF	dual brightness-enhancing film
EBR	electronic book reader
EPID	electrophoretic information display
ESR	enhanced specular reflector
EWD	electrowetting display
FFS	fringe-field switching
FSC	field-sequential color
G	green
GPRS	general packet radio service

GSM	global system of telecommunications
HD	high definition
HSCSD	high-speed circuit-switched data
HSDPA	high-speed downlink packet access
HSPA+	evolved high-speed packet access
IPS	in-plane switching
LC	liquid crystal
LCD	liquid-crystal display
LED	light-emitting diode
LGP	light-guide plate
LTE	long-term evolution
MEMS	micro-electromechanical system
MIP	memory-in-pixel
MVA	multidomain vertical alignment
NTSC	National Television System Committee
OCB	optically compensated bend
OLED	organic light-emitting diode
PDA	personal digital assistant
PM	passive matrix
PMMA	poly (methyl methacrylate)
R	red
RGB	red-green-blue
RIBE	reactive ion-beam etching
SEM	scanning electron microscope
SI	international system of units
SMS	short messaging service
STN	supertwist nematic
TE	transverse electric
TIR	total internal reflection
TM	transverse magnetic
TN	twisted nematic
TV	television
UI	user interface
UV	ultraviolet
WAP	wireless application protocol
WCDMA	wideband code division multiple access
WVGA	wide video graphics array

1 Introduction

Mobile display technology has been an area of intensive research in the recent years, and rapid progress has been made in creating display modules that provide good image quality for the user at an affordable package for the mobile device maker. There are a few remaining questions that require answers, depending on the actual needs of the end user. One of these questions relates to the power dissipation of the display, which constitutes a major limitation on the available time of continuous use of a cellular telephone, for instance. Most mobile displays on the market are based on liquid crystals (LCs). In transmissive and transfective mobile liquid-crystal displays (LCDs), the backlight provides the illumination for the electro-optic LC modulator that decodes the information on the display for the user to see. Transfective mobile displays can also take advantage of ambient illumination due to the integral reflector structure of the display panel. The power dissipation of the backlight constitutes the main portion of the energy usage of the whole user interface, and in dim ambient illumination conditions, also the transfective display relies on the backlight to provide an intelligible image to the user.

Organic light-emitting diode (OLED) displays have recently appeared on the market in mobile phones, with good image quality, and for live video use, their power dissipation already can be lower than that of a comparable LCD. However, for bright display content, for example predominantly white internet browser windows, and for menus with white background, OLEDs will have higher power dissipation than what can be achieved with an LCD in similar use. In addition, OLEDs need to be driven to high luminance in outdoors illumination conditions, further increasing the power dissipation of the display in mobile use.

In order to make a display with significantly lower power dissipation than what is available in mobile displays today, an electro-optical modulator based display, such as a liquid-crystal display, can offer an advantage, but a radical redesign of the display system is required. Instead of filtering the white light that is emitted by the light-

emitting diodes (LEDs) in the display backlight, color-separating or selecting principles should be applied. Transflective liquid-crystal displays have been traditionally made by stacking a set of optical films and the display panel together in a single package, and it has been difficult to redesign the display system to take into account the light propagation in the display at the subpixel level. In separating the colors, diffractive backlights can be applied to direct the light in the main primary color spectral bands to the corresponding subpixels in the display matrix. This is the basic rationale that has guided the work presented in this thesis.

This thesis is a result of experimental work on pixelated grating array based backlight structures that was carried out at the Nokia Research Center in Tampere, Finland, between 2006 and 2012. In this research, backlight structures with striped and pixelated grating array light-guide plates are used for coloring the pixels. Both binary and slanted gratings have been applied for the grating structures.

Chapter 2, an introduction to portable displays, sets the broader context for the thesis. The Chapter describes the motivation for improving the power efficiency of a mobile display module, and how different display technologies and display addressing methods can be used to attain this goal.

Chapter 3 is the description of the individual constituent publications (P1-P6), the research and experimental work performed, and the results obtained within the individual publications. Chapter 4 presents a discussion of the results and draws conclusions from the work.

The constituent publications (P1-P6) have been appended at the end of the thesis. Publication P1 is a review paper of diffractive backlights in the mobile display context. The research for the review was done concurrently with the experimental studies. Consequently, it also contains a subsection dealing with the research presented in the remaining Publications. In Publication P2, a one square centimeter test structure with binary gratings for outcoupling of green and blue light separately was manufactured and the output light distribution was characterized. It was shown that blue and green primary bands of light can be separated and directed toward the user effectively. In Publication P3, also a square centimeter sized test structure was made, this time with slanted gratings for red, green, and blue primaries, and the outcoupled light distribution showed

that all colors could be separated spatially with a high degree of direction toward the user. In Publication P4, a full display sized grating array was fabricated and characterized, and in Publication P5 this grating array was coupled to an electrowetting display prototype. Finally, based on the results of these previous studies, in Publication P6 an embedded grating array structure was fabricated by etching on a high refractive index glass substrate. This time, the characterization was done by using laser light sources which were prism-coupled to the light guide. The measurements were performed with a photodetector arrangement.

The goal of research in display backlights, as evidenced *e. g.* by the literature review of P1, is to improve the energy efficiency, light uniformity, and color purity of a display module. The research question in this thesis is whether it is possible to reach one or several of these goals by using a diffractive approach. Consequently, Publications 2-6 aimed to experimentally demonstrate steps toward making an energy-efficient backlight for electro-optically modulated mobile displays based on color-separating grating arrays. The central problems dealt with finding the proper type of grating geometry, pixel geometry, and solutions for integrating the backlight within the display structure itself. An additional consideration raised by Publications 3-6 was the indication that it may be possible to design a solution with no color filter array in the display panel itself.

The results of this work show that it is possible to couple light out of the grating arrays in a precise fashion, as through a display array, toward the user. The light separation in the grating array has been good, but some effects of light scattering and unwanted crosstalk have been observed. The results have been encouraging, and it seems that a prospect of a new display system paradigm based on pixelated grating array light-guide plates not only reduces power dissipation but also simplifies the display module design by eliminating some of the films used for controlling light distribution, and by the possibility to remove the color filter array in the display glass design. The downside is the added difficulty in designing display modules with integrated diffractive grating array back substrates. It remains to be seen if the display industry can embrace this new system paradigm in the design of future mobile display modules.

2 Displays for Portable and Handheld Electronic Devices

2.1 Displays in Mobile Communications

2.1.1 Background

The development of mobile telephony is a prime example of the digital convergence, or integration of features of many different classes of digital devices within one communication terminal. Especially after the transformation of cellular telephone technology from the analog signaling networks to the so-called “second generation” (2G) digital networks in the 1990s, it became feasible to integrate functions of digital still cameras, short-range communication devices, handheld navigators, and gaming terminals in mobile telephones [1]. This trend has continued through the third generation (3G) of mobile telephony as well, and today, the mobile “feature phones” and “smart phones” can even be called “mobile computers” [2]. Many of the functions included in today’s mobile terminals require high performance of the display of the device, as the user can expect a good image quality in viewing photographs, video clips, browser content, and navigation screens. Mobile games also require high visual image quality of the display. [3, 4]

Concurrently with the evolution of mobile terminals, the capacity of the mobile and broadband networks has increased, so that the mobile device user can expect an internet experience on the mobile device that rivals a basic home network internet connection [4]. Figure 1 depicts the development of cellular data bandwidth to a stationary mobile user. From the Figure, it can be inferred that today’s network capability allows high-quality visual data delivery to a mobile user. Further on, the development of the “long term evolution” (LTE), or 4th generation (4G) networks lends itself to communication experience that can benefit *e. g.* from cloud storage of content and remote computing applications [5]. Still, the expectations on the visual quality of the user interface (UI) will remain very high.

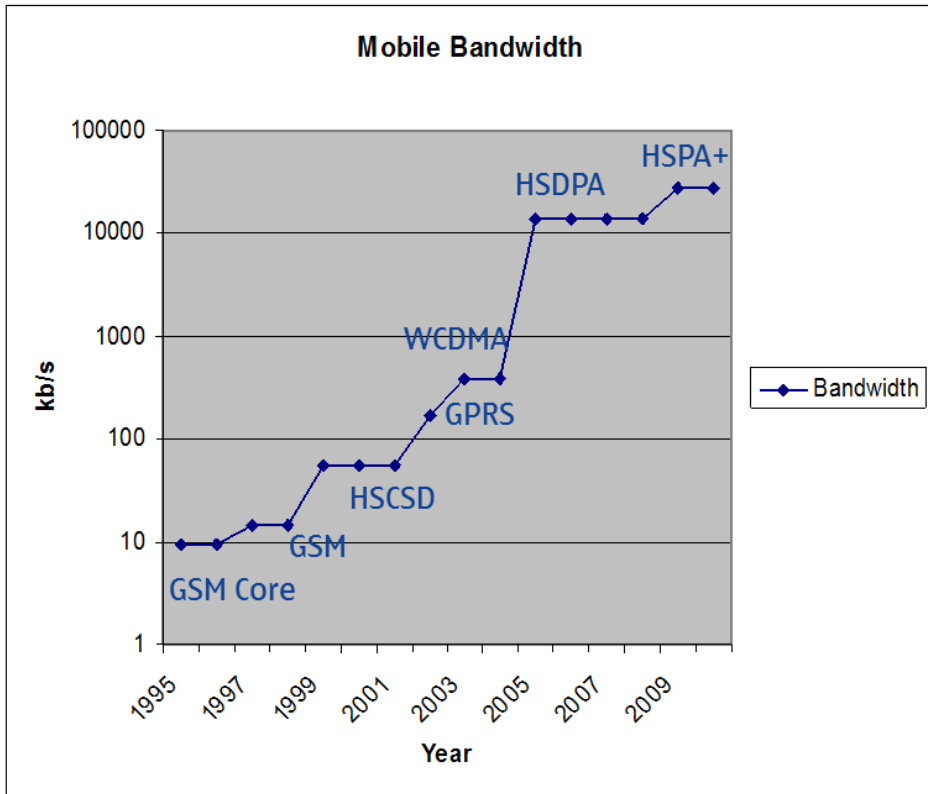


Figure 1. Development of data bandwidth of digital mobile telephone systems over time. GSM: Global System for Mobile Telephony; HSCSD: High Speed Circuit-Switched Data; GPRS: General Packet Radio System; WCDMA: Wideband Code Division Multiple Access; HSDPA: High-Speed Downlink Packet Access; HSPA+: Evolved High-Speed Packet Access. From [2], reprinted with permission.

The mobile phone market determines the sales of mobile displays for a large part. The volume of phones sold worldwide overwhelms the market for all other classes of portable devices. In 2012, the prediction of the market volume for mobile phones is about 1.4×10^9 units [5]. Therefore, when discussing mobile phone displays, the applicability of argumentation can be readily extended to other classes of handheld devices. Display requirements, for instance, can be very similar for *e. g.* handheld navigation devices and digital camera products. Since many mobile devices have several displays, it can be estimated that the market for mobile displays exceeds 1.5×10^9 units [5]. With regard to the display requirements, the electronic book reader (EBR) can be viewed as a special case, as it benefits from a quasi-static low-power display, instead of a video-speed multimedia display.

The purpose of the display in the mobile user interface was originally to provide a visual feedback of the keys punched for calling another party. The caller identification (caller ID) function also was very useful, and these two functions could be realized by just an alphanumeric or even a seven-segment directly driven display [4]. Light-emitting diodes (LEDs) and later, liquid-crystal displays (LCDs) were used to provide this function in the UI. In addition to this information, icons were used to display remaining battery charge, signal strength, and some special states of the device [4, 6]. As the mobile terminals for 2G networks were being designed, other functions became useful as well, such as the short messaging service (SMS), and this functionality required alphanumeric multi-line LCDs. Even further on, simple games were implemented in the mobile devices, and a matrix-driven display became necessary. Mobile browsing applications were also launched, for instance using the Wireless Application Protocol (WAP) browsers [4]. Although limited use was found with other passive-matrix color displays such as with the electrically controlled birefringence (ECB) mode [7], starting from circa 1998, the first mobile color displays with passive matrix (PM) supertwist nematic (STN) LCDs became available on the Japanese market. From then on, the mobile display development was a steady improvement toward large, full-color video displays as found on smart phones today [4]. Active matrix (AM) driving was already required for high-resolution screens in the early 2000s. This development led, however, to increased power dissipation in the display. Multimedia sessions on mobile terminals are therefore now power-limited, and mobile devices need to be charged more frequently than what was necessary in the days of the monochrome STN display [3].

2.1.2 Mobile Display Technology

Today's multimedia-capable mobile devices mainly employ active-matrix LCDs (AMLCDs) and organic light-emitting diode (OLED) displays. LCD technology variants are most often used in mobile phones. Other types of display devices in the portable device space mainly occur in electronic book readers. There, electrophoretic information displays (EPIDs) have a presence, especially in monochrome devices. The liquid-crystal displays on mobile phones are either transmissive or transreflective. Reflective displays appeared on personal digital assistant (PDA) devices in the beginning of the 2000s, but they did not last long in the marketplace. The main reason

for this was that the displays required a frontlight, and degraded reflectivity and viewing artifacts due to the frontlight structure became annoying to the users [8].

Transmissive LCDs have a backlight that provides the illumination to the user. The liquid crystal (LC) layer in the display acts as an electro-optically modulating medium for light emanating from the backlight unit (BLU). Both passive and active addressing can be used to drive an LCD, but in modern mobile LCDs, active matrix driving is preferred. Transflective displays can, in addition to utilizing the BLU, benefit from the ambient light to display information in bright illumination conditions, such as outdoors on a sunny day. Figure 2 depicts the comparison between transmissive and transflective displays.

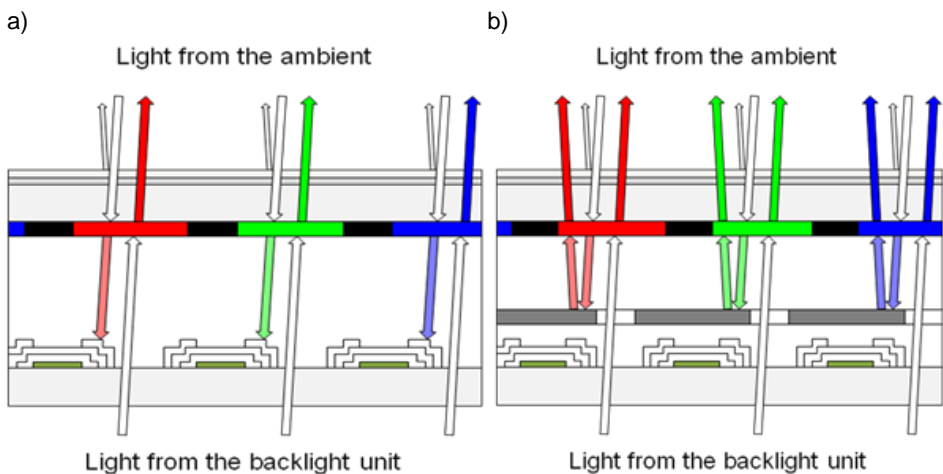


Figure 2. Conceptual representation of a) transmissive and b) transflective LCDs. In a) the reflection of ambient light is prominent at the surface of the display, and light entering the cell is for the most part absorbed. In b) the ambient light reflects from the reflector structure fabricated on top of the backplane. (Not to scale.) [3] ©Springer Verlag, reprinted with permission.

As can be seen in Figure 2, the integral reflector structure of a transflective display allows the use of the ambient illumination for image formation. The reflector structure can be optimized to take into account different use cases for a mobile device. Backlight utilization efficiency is somewhat lower than in transmissive displays, due to the need to pass the light from the BLU through an aperture in the subpixel structure.

2.1.3 Requirements for Mobile Displays

The main requirements that mobile displays need to fulfill today are summarized in Table 1. In developing mobile displays, tradeoffs need to be made, as many of these requirements are somewhat contradictory. For instance, high image quality at video speeds does not comply with a low power dissipation requirement. Low cost in mobile displays is also a requirement that conflicts with many other characteristics of a mobile display that manifest themselves in delivering the high image quality of the display. Developing mobile display modules against these requirements has, however, led to high-quality displays that have appealing visual image characteristics, low weight, small outer dimensions, and acceptable power dissipation and cost to the integrator. Besides the mechanical dimensions and image quality characteristics, the display also has to withstand harsh environmental conditions. Reliability of a mobile phone is still a leading development goal, as the user needs to be able to rely on the mobile phone to place a call even in the most distressing situations.

Table 1. Mobile display requirements*. [3] ©Springer Verlag, reprinted with permission.

Characteristic	Requirement	Unit
Size	Typically 1.8" to 4.3"	Diagonal inches
Resolution	160 by 128 to WVGA (480 by 800)	Number of pixels, horizontal by vertical; WVGA: Wide Video Graphics Array; other computer-based resolution designations are used frequently as well
Pixel pitch	100–350 ppi	Pixels per inch (ppi)
Number of colors	256 k to 16 M	Number of addressable color levels, "k" designates thousands, "M" millions
Colour gamut	70–125% NTSC	Percent of color area of the NTSC gamut on the CIE diagram
Brightness	100–300 cd/m ²	Luminance; cd/m ²
Contrast	100–5,000	Contrast ratio; number
Viewing angle	+/- 20° to +/-90°	Degrees about the azimuth
Speed	15–60 fps	Frames per second

*NTSC: National Television System Committee; CIE: Committee International d'Eclairage.

The power dissipation of current multimedia-capable mobile displays is in the order of 300-500 mW. As the panel power consumption is in the range of tens of mW, it can be concluded that the BLU is responsible for the majority of the power dissipation in a mobile liquid-crystal display. [8]

The requirements for mobile displays presented in Table 1 can be most readily achieved by applying AMLCD panels in building a mobile product. In the mobile technology space today, several other technologies have a presence. As it has been already mentioned, OLEDs have already made their mark on the smart phone display market, and EPIDs are frequent in the EBR products. Of the LCD variants on the mobile market, there still exist low-end display modules with monochrome supertwist nematic (STN) LCDs, and passive matrix color supertwist nematic (CSTN) LCD panels. Table 2 presents a comparison of these display variants, as applicable on the mobile display market today.

Table 2. Mobile display technology comparison*. [3] ©Springer Verlag, reprinted with permission.

Technology	General characteristics	Note
Monochrome STN	High reflectivity, good contrast, simple and cost-effective technology	Low market volume, as advanced features in phones proliferate
CSTN	Low reflectivity, poor color gamut	Still in use in low-end phones
PM OLED	Low information content with regard to associated expense	In use in secondary displays
AM OLED	High resolution, good power efficiency in live video and TV viewing, extremely good color gamut. Outdoor performance is poor	Few sources available and associated cost is quite high
AM Transmissive LCD	Good resolution and color gamut, no reflective/outdoor use, viewing experience as good in small space as for HD TV panels today	Established technology, very cost-effective
AM Transflective LCD	Good reflectivity, outdoor use possible. Good color gamut in backlit mode	Excellent combination of viewing properties for varied ambient environments
Electrophoretic displays (EPID)	Good reflectivity, generally requires an ambient light source	Characteristics approach "newspaper legibility." Main display technology for EBRs

*HD: High definition; TV: Television.

2.2 Transflective Displays for Mobile Applications

In order to adapt the viewing characteristics of a mobile display into a wide range of ambient illuminance levels, mobile phone integrators apply transflective displays in their products. Whereas a transmissive display excels in dim and dark ambient conditions, the backlight in a transmissive display cannot always provide enough luminance to overcome the reflections from the ambient environment in bright outdoors

conditions. This means that colors get washed out and text becomes illegible on transmissive displays. The same phenomenon affects OLED displays as well, as their operation solely relies on the emissive property of the individual subpixels. Figure 3 depicts a comparison of transmissive and transflective LCDs in conceptually different ambient illuminance levels. As is evident from Figure 3, a transflective display can provide the information required by the user in a more varied range of ambient illumination. The reason for this is the reflective structure that is an integral part of every subpixel [9]. Transflective displays are mainly quite small, suitable for mobile phones, but some devices in the 10" diagonal class have been manufactured for notebook computer use [10].

2.2.1 Transflective LCD Structures and LC Optics

The modern transflective display is based on an integrated internal reflector structure, in order to prevent any parallax artifacts that would result from an external reflector [11]. The internal reflectors are manufactured under the respective color filter areas in the subpixel matrix. For the illumination from the backlight to get through, a hole is manufactured in the reflector. Figure 4 presents a schematic view of a transflective display. As can be seen in Figure 4, the light from the ambient passes the color filter array (CFA) twice. Light propagating in the LC layer also experiences double retardation, if the cell gap stays the same for both paths of light. Transflective display design needs to have this aspect taken into account. Otherwise, the image contrast is reversed in backlit and reflective operation, which is undesirable to the user. One approach to account for this is to halve the cell gap of the LC area in the reflective mode, as is shown in Figure 5 a. This kind of a structure is more difficult to manufacture than a single cell gap structure, shown in Figure 5 b. For single cell gap transflective LCDs, the LC mode needs to be selected in such a way that the image characteristics in both transmissive and reflective use are retained. In-plane switching (IPS), fringe-field switching (FFS), and multidomain vertical alignment (MVA) LC modes are frequently used in mobile transflective single cell gap LCDs [12]. These modes usually are selected for normally black operation, giving good contrast. The wide viewing angle operation of these LC modes can also be appealing to many consumers in mobile use.

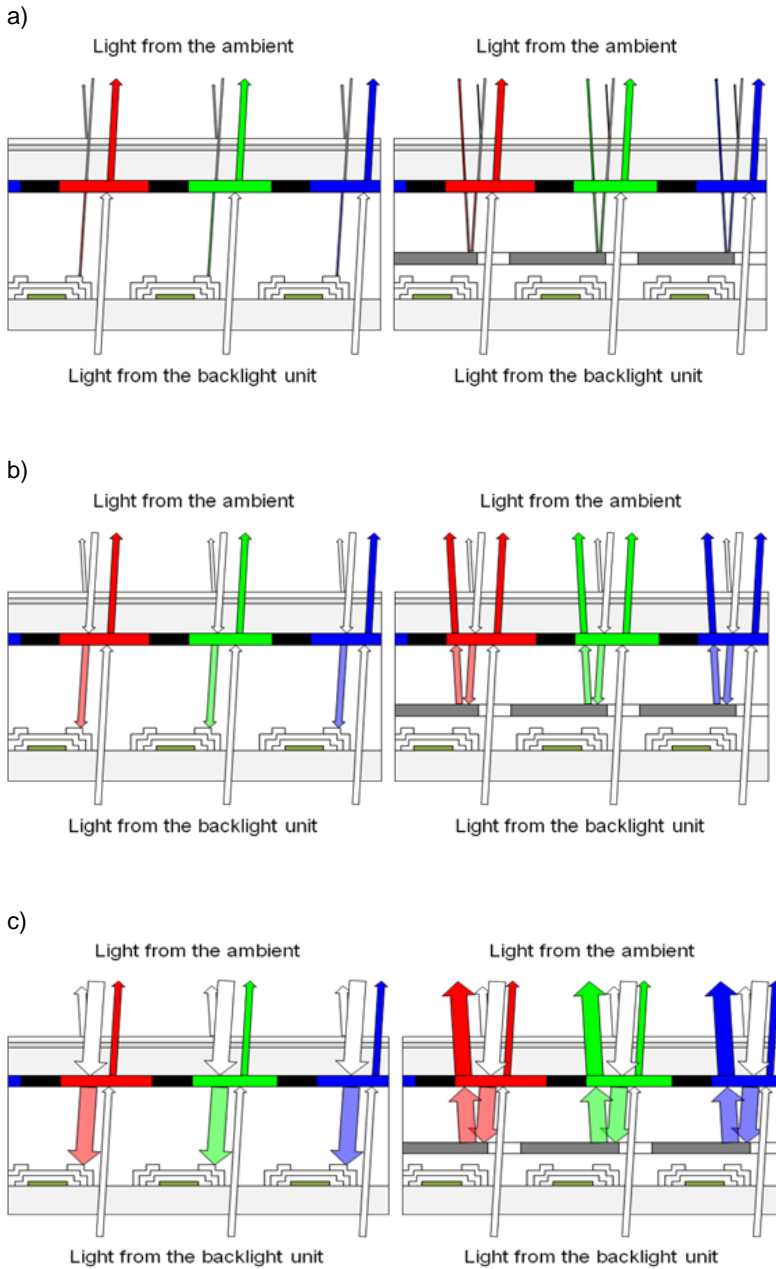


Figure 3. Transmissive (left) and transfective (right) display in varying ambient lighting conditions: a) dark, b) intermediate, c) bright ambient. (Not to scale.) [9] ©Springer Verlag, reprinted with permission.

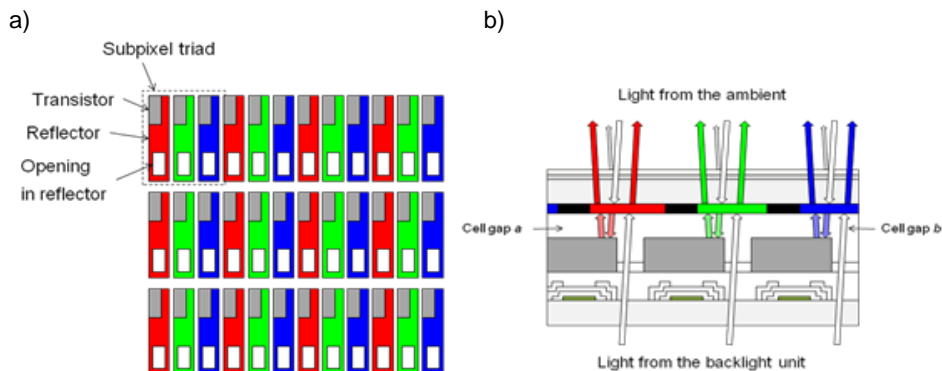


Figure 4. Transflective TFT LCD pixel array layout, a) from the top, b) dual cell gap structure in cross-section. In a) the colors are respective to the color filter array on top of the pixel array (the reflectors are not colored). In b) the cell gap in the transmissive area, b is twice that of in the reflective area, a. (Not to scale.) [9] ©Springer Verlag, reprinted with permission.

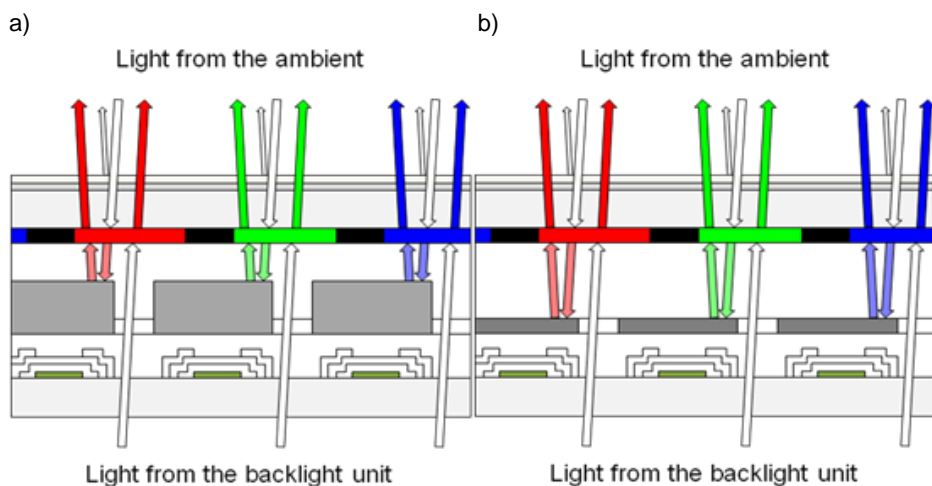


Figure 5. Transflective display variants: a) Dual cell gap structure, b) Single cell gap structure. (Not to scale.) [9] ©Springer Verlag, reprinted with permission.

In addition to the chosen LC mode, the optical film stack of a transflective display plays a major role in the performance. To optimize the front-of-screen performance in the reflective mode, circular polarizers are used on the front surface to hide unwanted reflections. The reflector structure within the transflective subpixel array also needs to be carefully designed to give acceptable viewing characteristics. Very often, “bumpy” reflector surfaces are used to provide the best compromise between specular and diffuse reflective properties. Compensation films are also required to give good contrast outside the immediate normal viewing direction. Polarizers work ideally at normal incidence,

and especially at $\pm 45^\circ$ off the main polarizer axes, viewing artifacts such as contrast reduction and color distortions occur. Uniaxial and biaxial compensation films are therefore used to take care of these artifacts [11, 12].

The backlight of the transfective display needs to be designed to provide a good image quality to the user in transmissive operation. Generally, light from “white” LEDs is launched to the end of a waveguiding transparent polymer slab. This is called the light-guide plate (LGP). Wedge-shaped light guides are also used. Sometimes, dedicated launch structures are used in order to collimate the light before it enters the active area of the LGP. Light within the LGP is guided under total internal reflection (TIR) conditions. For the light to exit the LGP, a distribution of scattering centers, microreflectors, or other means is fabricated to perturb the TIR condition and to scatter the light toward the display panel. The light extractor structure has often features that can be seen by the naked eye, and a film diffuser is often used to mask the macroscopic features of the LGP. Since the light exits the LGP usually in an oblique angle, beam-forming films, often called “brightness-enhancing films” (BEFs), are required to collimate the light. Generally, light can also escape the LGP away from the LC glass direction, below the LGP. A high-efficiency reflector, such as an enhanced specular reflector (ESR) is therefore applied at the bottom of the LGP to direct the light back into the LGP [13].

A modern, conventional mobile display module is therefore a collection of films stacked together with the display panel, to form a dedicated optical structure. The panel includes the top and bottom glass panes, with the color filter array (CFA) usually integrated in the top glass, and the transistor matrix on the bottom glass, and the electro-optic medium (LC) in between. Figure 6 presents this stack in a schematic form, and the optics of the conventional mobile display structure is discussed in the following subsections.

2.2.2 Light Sources

Light-emitting diodes (LEDs) are used in mobile LCDs as light sources [14], although cold-cathode fluorescent lamps (CCFLs) and area light sources such as electroluminescent films and OLED backlights have also been applied or developed for mobile displays. The efficiency of LEDs has, in the last decade, improved remarkably,

and the cost of LED light sources has concurrently decreased to a level where mobile display manufacturers have little incentive to consider other light source alternatives. White or “pseudo-white” LEDs are used in the conventional mobile display module to launch light into a side-lit LGP. These LEDs are based on blue emitters with yellow phosphors embedded in the path of emission. The phosphor then converts a portion of the light to longer wavelength emission. Alternatively to the yellow phosphors, red and green dual phosphors are sometimes used. In television systems, red, (R), green (G), and blue (B) LEDs are used, sometimes also as integrated RGB LED light sources, but in mobile displays these are rare [14].

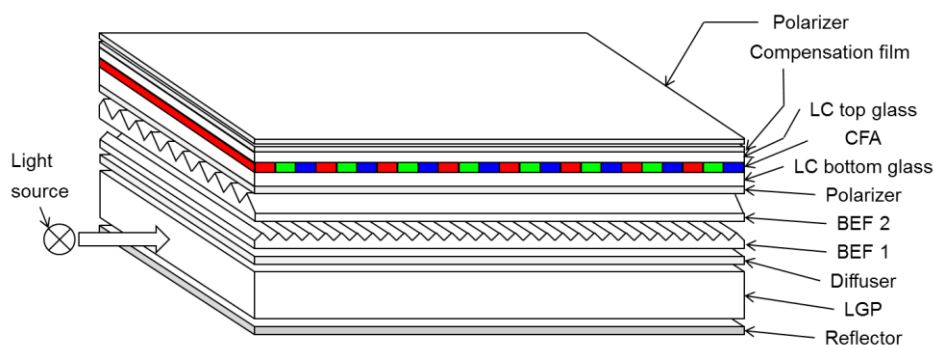


Figure 6. The conventional mobile display structure (not to scale). Brightness-enhancement films BEF 1 and BEF 2 are at right angles to each other. The outcoupling extractors are situated either on the top or on the bottom of the light-guide plate (LGP), or sometimes on both surfaces. (P1)

Mobile display LEDs are very often side-emitting, with sub-millimeter package thickness. The width of the emitting area can be a few millimeters. This form factor provides good compatibility with thin LGPs. The color temperature of “pseudo-white” LEDs can be quite high, e. g. 8000 K. There is usually enough emission at longer wavelengths to produce adequate color reproduction with conventional LCD color filter arrays [15].

LEDs have issues in operating at high temperatures. As the temperature increases, the color of the emission changes, and the degradation of the LED efficiency is accelerated. With the degradation, the white point of the light source can shift, reducing the color rendering capability of the display module in question. For mobile devices this aspect of degradation may not become relevant during the operational lifetime of a mobile phone, for instance, since the LED lifetime figures are in the order of 50 000 hours to half

brightness. The current density in a mobile phone backlight can however be troublesome for thermal management, and it is preferred to use LEDs that have identical specifications and degradation characteristics, in a given display panel design. [14]

2.2.3 Incoupling Structures

The LEDs in a mobile display module are most often mounted on a small section of circuit board that is connected to the display panel by means of a piece of flexible circuit carrier. This “flex” is then bent in place during module assembly so that the emitting edges of the LEDs are in registration with the entrance facet of the LGP. Since the exit characteristics of the LEDs are approximately Lambertian (emitting equally in a hemisphere) [14, 15], light entering the LGP can be wasted at the periphery of the emission cone of the LED if measures are not taken to take this effect into account in LGP design. Incoupling structures, such as tapering sections or microlenses can be molded directly into the entrance facet of the LGP to modify the optics of launching light into the LGP. Sometimes external lenses are also used to collimate the LED light. Quite often the light of the LEDs escapes the LGP toward the display panel directly after entering the LGP, near the LED. This results in the formation of “hot spots” that are seen as bright spots in the display illumination. Metallic reflector shields are often used to counteract this problem, and quite frequently, the launch area after the entrance facet of the LGP is lengthened, and mixing structures are formed in this area to distribute the light from the LEDs into the LGP to achieve uniform illumination for the LCD panel [16, 17].

2.2.4 LGPs and Reflectors

In modern mobile displays, the LGP is a carefully designed and precision-molded piece of transparent polymer that can provide the required uniform illumination to the display panel in an efficient way. Light from the LEDs, when launched into the LGP by means of the incoupling structures, travels inside the LGP by total internal reflection (TIR). Under the active area of the display panel, there are extractor features that break the condition for TIR, and light can escape the LGP. The extractors can be microgrooves, scattering centers, microreflectors, or microprisms (refracting structures) [13, 18]. The extractor features are distributed along the LGP surface by using statistical design

techniques, in order to avoid patterns that could show as Moiré artifacts to the user [13, 18].

The problem with using extractors that are based on geometrical optics is that light also escapes to the opposite side of the LGP, away from the display panel. Therefore, reflectors need to be placed under the LGP to reflect light back toward the LGP. Multilayer polymer/dielectric films, often called enhanced specular reflectors (ESR), have proven very effective, with typical reflectivity of 98.5 % over the visible range of wavelengths [18].

2.2.5 Beam-Forming Optics and Polarizers

With the conventional mobile display structure, there is a preference for light to exit the LGP obliquely, toward the opposite end of the LGP from the light sources. In order to improve the light output and to direct the light toward the display panel preferentially in a normal incidence, beam-forming optical films are used. These are most often thin polymer foils composed of prismatic structures (see Figure 6). Since the effect of using these foils is to improve the brightness of the display module, they are called brightness-enhancing films (BEFs). It is necessary to redirect the light also in the lateral direction, and therefore, two films at right angles to each other are used. The prisms on the foils can either be placed “prism-down” or “prism-up”, with the latter arrangement gaining popularity in modern display modules [13].

A diffuser is often necessary either below or above the BEF films. Its purpose is to mask the macroscopic structures that comprise the LGP light extracting features, and to even out the light distribution before the display panel, to tailor the viewing angle properties of the display panel itself [13, 18].

For the LCD operation, polarized light is required. Light entering the display panel therefore goes through a linear polarizer that can either be an absorbing polarizer film or a reflective polarizer foil. An absorbing polarizer is simple to use but the rejected polarization state of incoming light is in this case completely wasted, reducing the optical efficiency of the panel. In conjunction with a reflective polarizer, a recycling feature is required in the optical stack. This can be for instance a dual BEF (DBEF) film that recycles the reflected polarization state and turns the polarization gradually so that

on further refractions a portion of the light can be admitted through the polarizer. Using DBEF films, an increase of 1.2 to 1.5 can be observed in brightness enhancement compared to using a comparable crossed BEF film structure [18, 19].

At the front surface of the display panel, another polarizer is needed as an analyzer. This is most often an absorbing polarizer. The LCD layer in the display panel acts as a spatial polarization modulator, and the state of polarization of the incoming light is turned, based on the image content to be shown on the display. The analyzer then passes that proportion of the light which remains at the linear state of polarization of the polarization director of the analyzer.

2.2.6 Compensation Films

Modern mobile displays have a defined viewing angle range that depends on the usage parameters of the display module. Usually, in larger mobile displays, the user can be expected to wish to share some of the screen content with other people, and then, a wider viewing angle is required. This creates an added degree of difficulty in LCD design, as the basic principle of operation is designed for viewing the display at the direction normal to the display. Going away from the normal incidence, the light experiences a variable retardation, and the state of polarization changes. Optical compensation films can remedy this problem quite effectively. Uniaxial and biaxial compensation films are often used to improve the viewing angle of mobile transmissive displays [11]. These are manufactured by using LC materials and stretched polymer foils [11].

2.2.7 Integration of Films

Thinness is one of the design goals for mobile displays. In addition to using thinner glass in the display panel itself, and thinner foils in the backlight optical stack, it has become commonplace to integrate several functions of separate films of the display optics into one. This way, remarkable reductions in display thickness can be achieved. For instance, features of the BEF films can be integrated on the top or bottom surface of the LGP [20-22], the diffuser pattern can be imprinted on the first polarizer, and also “unified beam-forming components” can be used that couple light from the LGP directly into the beam-forming foil [23].

2.2.8 Top Coatings and Touch Structures

For outdoor use, it is common in mobile displays to coat the topmost surface of the display panel with an antireflection film. This reduces reflections from the environment. A hard coating is also used at the outermost surface of the display structure, to avoid scratching of the display window or the polarizer. Reflections can occur despite these countermeasures, and especially in display modules with a touch feature, the reflections can become problematic. In-cell touch technology is therefore seen as a useful direction to apply touch features in a mobile device [24].

2.3 Alternative and Emerging Technology

Besides LCDs, several other technology variants aim to claim a stake in the mobile display market. Today, however, no other technology besides the OLED display has made any remarkable effect on the mobile display sales. With the emphasis to curtail power consumption, also LCD technology has available some interesting alternatives. For instance, field-sequential color (FSC) displays aim to improve the power efficiency by removing the CFA and operating the LCD time-sequentially, showing to the users subfields with varying spectral content. Outside the scope of LCD and OLED technologies, emerging technology variants such as electrowetting displays (EWDs), microelectromechanical system (MEMS) displays, and electrophoretic information displays (EPIDs) aim to influence the mobile display market. The following subsections describe the key points of these technologies, especially from the point of view of how they contribute to power savings in a mobile terminal.

2.3.1 OLED Displays

For a very long time, OLED displays aimed to penetrate the mobile display market by simple passive matrix displays [1]. The developers of these displays had major challenges in market entry, as LCDs already were very cheap, and it might have proven impossible for PM OLED technology to produce displays at a comparable cost level to PM LCDs. Moreover, these displays suffered from differential aging characteristics resulting from differing lifetimes of the constituent primary emitter materials, and from defect formation due to insufficient encapsulation of the OLED device. The resulting effects of these degradation mechanisms appeared as white point change, image

sticking, and black spot formation. Since the lifetimes to half luminance of the different primary color OLED emitter materials have different values, with the early materials, the blue and red emitters degraded faster than the green emitter. Over time, the white point changed toward the green. This degradation also resulted in quite noticeable sticking, or burn-in, of static screen content, such as menu icons. Black spots could be seen due to the catastrophic failure of the low work function cathode materials of the devices. These problems have largely been overcome as the lifetimes of the emitter materials have improved to over 50 000 h [25, 26]. Today, OLEDs can be found in many top-tier mobile products. One remaining problem is in the need of OLED displays also to provide enough light for the user to see the information on the display even in bright ambient environments. The display needs to be pushed to a luminance of 300 cd/m^2 or even more, in order to not be washed out in sunlight, and the panel itself has to be driven to twice of that value because there usually is a circular polarizer on top of the panel to reduce reflections [27]. Taking these requirements into account, it can be said that OLEDs have best energy utilization when viewing video content, as for instance web browser screens often have a bright white background. Video, on the other hand, usually is considered to only utilize 10-20 % of total screen brightness, on average [28]. A typical commercial 4" WVGA panel consumes 600 mW at 300 cd/m^2 luminance, at an average of 40 % "on". The ambient contrast ratio of this panel is 70 at 500 lux, and 3 at 10 000 lux [29].

2.3.2 Field-Sequential Color Displays

Field-sequential displays (FSCs) aim to save energy by removing the color filter array in the LCD subpixel structure. Whereas in the common LCD, the primary subpixels are spatially separated, in the FSC, the color information is shown in a temporally separated field, one specific-color subfield at a time [30]. Red, green, and blue LEDs are used as light sources, and these are flashed sequentially, synchronized to the color content of the respective subframe. One problem is that to render the color information this way, fast LC mixtures such as the optically compensated mode (OCB) need to be used. In low temperatures, as may be the case in some usage scenarios of mobile devices, the performance of LCDs in general degrades, and this is why FSC displays have not been available in the mobile case so far [4, 31].

Color breakup (CBU) can also be a problem in FSC displays. Because the subfields are driven one primary color at the time, if the screen moves in relation to the position of the viewer's eye, the eye sees content of the screen separated spatially according to the primary color content. The result is that the image gets blurred and flickering of the screen then causes discomfort [32]. Countermeasures to this problem have been sought by separating the individual color subfields further in time within the frame [32]. Faster rates for switching the content however requires even faster-response LC materials, and therefore, a hybrid solution with dual color filters combined with multiprimary backlights has been demonstrated [33]. Using FSC panels, the projected energy savings in typical mobile panels are around 50 % [31]. This would mean that a typical high-resolution mobile display panel would consume about 200 mW in normal use.

2.3.3 Electrowetting Displays

Electrowetting displays (EWDs) are based on using an electrostatic force to move an interface that occurs between two immiscible liquids, such as between oil and electrolyte [34]. If one of the liquids is transmissive, and the other absorbing, contrast formation can be achieved. Since the layer thickness is in the order of micrometers, it is difficult to find a material with good absorption in such a short distance. In reflective use, light passes the absorbing liquid twice, enhancing the contrast between the absorbing and transmitting state of the pixel. Therefore, although transmissive EWDs have been demonstrated [35], EWD panels are mainly being developed for reflective use. One benefit of EWD technology is that manufacturing of EWDs is compatible with LCD fabrication. Reflector structures can be fabricated readily in a similar way to how transflective mobile displays are made. Since the operation of the EWD is electrostatic, no current flows when the information content shown on the display does not change. The panel power dissipation is otherwise at a similar level to that of LCD technology in general. Therefore, EWDs can be envisaged to be beneficial in terms of energy consumption in low-end devices where the proportion of video content on the display screen is not large, and in reflective reading devices, where the information content stays static for longer periods of time.

2.3.4 Microelectromechanical System Displays

Reflective MEMS displays are now available in small form factors, but also for color EBRs on the Korean market. The main manufacturer is Qualcomm, with the mirasol[®] display [36, 37]. These panels are built on bistable interference-based microelectromechanic structures. The bistable operation means that no current flows when the screen content is static, lending these displays suitable for color EBRs. For enhanced grayscale and color depth, dithering is used in driving the display, and in some cases, this reduces the effective resolution and usability of these displays. Since the operation is based on interference of light, the reflections off the screen are highly specular. Front lights are used in darker ambient conditions, which reduces the power efficiency of this otherwise promising technology [38].

2.3.5 Electrophoretic Information Displays

One of the earliest non-liquid-crystal-based bistable display technologies is the electrophoretic information display (EPID). Originally EPIDs were developed at the MIT Media Lab, and spun out to eInk Corp. [39]. Some other variants, such as the Gyricon rotating ball display [40], and the “microcup” electrophoretic display [41] have appeared on the market. The typical EPID display is based on polymer microparticles that are embedded in a liquid-filled microcapsule. Some of the particles are white, and the others are black. These particles also have opposite surface charge, and in electric field they migrate to the opposite sides of the microcapsule. In a matrix-driven display, content of the screen can then be shown by varying the sign and the magnitude of the driving voltage in each pixel. Since the electrophoretic principle has no threshold, passive matrix driving is not feasible due to crosstalk issues, and either direct segment drive or active matrix driving methods are used. Since the particles stay in place once the drive voltage is removed, the displays can retain the information almost indefinitely with no power dissipation, provided that the information on the screen is not changed. One problem in the EPID display is that very frequently, changing from one screen to the other, there is residual or incomplete migration of the particles and a ghost image from the previous screen can disturb the information to be read. Therefore, the display is often flashed through a white and a black state when changing pages when reading an EBR, which creates a flickering, momentary artifact.

Electronic book reader devices (EBRs) very frequently have an electrophoretic display. There are many EBRs on the market that use one of the varieties of EPID displays. The lack of color limits the use of EPIDs in other products. Although color filter based solutions exist to present colors in EPIDs, the contrast in these is quite poor, and the reflectivity is reduced [42].

From an energy-saving point of view, EPIDs excel in mobile devices where there is a semi-static screen content, and mobile phones (*cf.* Motorola MotoFone [39]) for instance are a marginal market for these displays.

2.4 Energy and Power Savings Considerations

Portable devices are fundamentally different from many other electronic devices in that their energy savings requirements are much more pronounced. Power is not available from a wall outlet in mobile use, and mobile phones are required to be able to make a phone call even when their battery is low, making special demands on power management [4, 43]. In mobile devices, it is possible to design a UI that is optimized for low power consumption, and displays have a major role to play in this. For a mobile product, a display can be used that has intrinsically low power dissipation, for instance a reflective display that will not have a backlight. Another option is to use bistable displays that only expend energy when the information shown changes. One similar solution is to apply panels with a “memory-in-pixel” (MIP) functionality [44, 45], where the screen updates can be slowed to around 0.1 Hz. Thus, for quasi-static screen content with the backlight turned “off”, these user interfaces spend very little energy. For multimedia devices, the story is different, and displays need to be designed in conjunction with the whole electronics system. In display driving, methods can be used that reduce power by optimizing the backlight current based on the screen content. These techniques are generally termed “dynamic backlight driving” [46-48]. In mobile products that are to be used in varied ambient illuminance levels, the effect of ambient illumination can also be taken in account, dimming the screen in lower ambient illuminance situations. An ambient light sensor (ALS) is often used for this purpose [49]. This can either be an external sensor, or integrated in the display panel itself [49]. Using these methods, energy savings in tens of percent can be achieved, but sometimes color distortion and other image artifacts degrade the user experience [48].

The whole mobile device needs a power management strategy, to best make use of the available energy saving possibilities. Power management can be based on power-saving modes and timeouts. These methods are based on either heuristic or adaptive statistical techniques, and the effect on power dissipation of a mobile device can be dramatic [50-52]. The power-saving mode can dim the display, or only drive a part of the display. It is very common to show a screen-saver image that may, for instance, show the time of day on the display. Sometimes, whole functional blocks of a device, including the display, can be turned off when not in use. These power-saving techniques do not retain the best quality of the user experience for the user, especially with mobile multimedia devices. Recently, it has been estimated that only 12 % of smart phone usage is for voice communications purposes [53]. Consequently, the user expects more frequently to be able to interact with the visual content on the screen for prolonged periods of time, and any power-saving method that disrupts viewing the screen is subject to critique. [43]

The user interface (UI) is responsible for roughly one third of a mobile phone power budget [54]. The display backlight is the main reason why the UI functions consume such a large proportion of the available power [13, 14, 18]. Therefore, for future improvements in device energy efficiency, efforts to reduce the display power consumption are important. Since the conventional mobile display is getting “good enough” for the user in terms of image quality, power dissipation remains also the main bottleneck for improvement of the usability of mobile display as a component. In the conventional display structure, the throughput of light is estimated to be less than 10 % [13]. Because the backlight technology, with the associated beam-forming films, is already quite mature, it is difficult to see how energy efficiency can be improved using the conventional display stack-up structure (Figure 6). Thus, redesign of the complete display system is required with more efficient light management, to be able to achieve meaningful energy savings. Color-separating backlights, such as diffractive grating array backlights, have been researched in order to increase the efficiency of mobile display systems (P1-P6).

3 Description of Work

3.1 Conventions and Coordinate Systems in Diffractive Backlight Design

To make the research of Publications 1-6 as presented in this Chapter understandable, it is necessary to define key concepts of light propagation in backlights and associate a system of coordinates with the presentation of the results, as is customary in backlight research literature [55]. Figure 7 presents the embedded light-guide plate (LGP) of a color-separating backlight unit, such as a diffractive, pixelated grating array device of P6. Since light is now entering the LGP from three sides, a main direction needs to be defined. Note that the color-filter array (CFA) in the associated display, if present, need not be in any particular orientation with respect to the propagation directions of individual primary beams of light. In Figure 7, we can choose the main propagation direction of green (G) as the positive x -axis, and the vertical axis, at normal to the LGP surface, as the z -axis. The positive the y -axis is now the axis of the main propagation direction of red (R) light and blue (B) travels in the opposite direction to the R. (In some arrangements, the orientation of B is along the positive y -axis.)

Since there will be a deviation from the vertical in the outcoupling of light, Figure 7 also shows the inclination angle θ and the azimuth angle ϕ that describe the angular separation of light in the following sections describing the results. The inclination angle θ is measured as the angular deviation from the positive z -axis, and the azimuth angle ϕ as the angular deviation from the positive x -axis. It is now possible to use the coordinate system of Figure 7 to describe the light propagation in the designs and experimental demonstrators. Coordinate axes are added to the relevant Figures in this Chapter to help the interpretation of the Figures.

Conoscope measurements, in a similar way to other viewing-angle measurements [56], are often shown either as cross-sections or as polar diagrams, with the inclination angle θ indicated by the concentric circles in the plots, and the value of the azimuth angle ϕ shown at the perimeter of the plots. Figure 8 is illustrates this style of presentation. The

intensity of light is shown to be lighter in grey scale in monochrome polar diagrams, and in false color in multicolor diagrams. Usually a column of shades or these false colors is shown on the right side of the diagram showing the scale for the color coding of the intensity of light emission or outcoupling. In Figure 8, the horizontal axis is associated with the direction of propagation of the green light, and according to the convention presented in Figure 7 it is denoted as the x -axis.

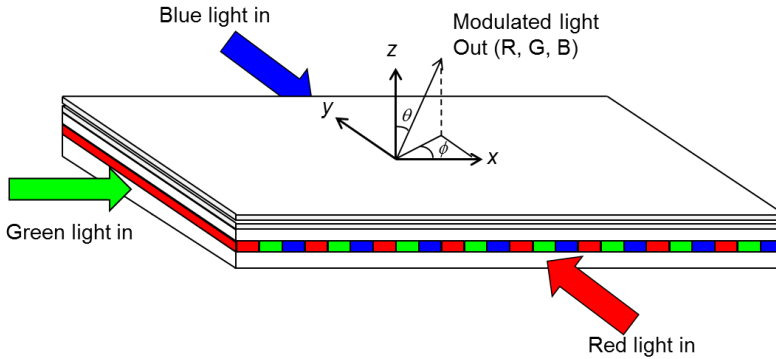


Figure 7. A coordinate system for color-separating backlights. x , y , and z denote the main coordinate axes, at right angles to each other; θ denotes the inclination angle and ϕ the azimuth angle.

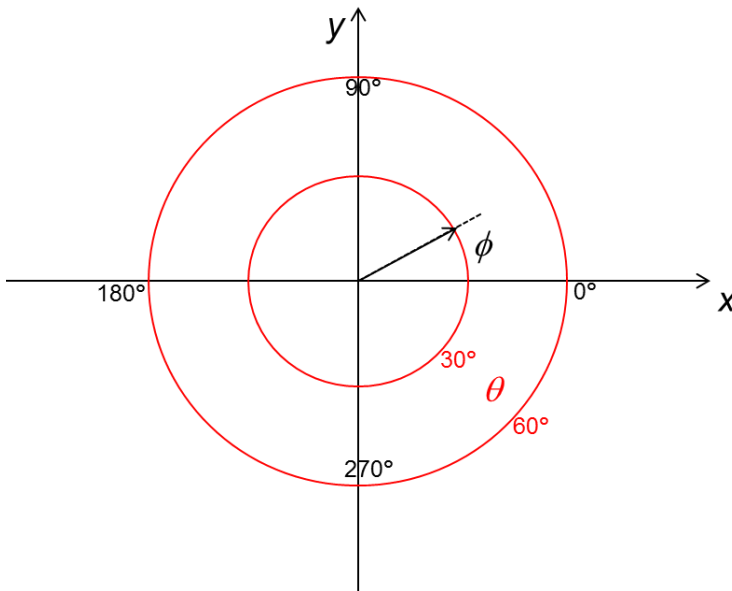


Figure 8. Example of a conoscopic measurement as a polar plot diagram. The inclination angle θ is indicated by the concentric circles (red), and the value of the azimuth angle ϕ is shown at the perimeter of the plots (black).

3.2 Literature on Diffractive Backlight Technologies

The first publication (P1) is a review paper describing the state of the art of diffractive backlight technology variants aimed at improving the efficiency of mobile displays. The review starts by discussing the history and conventional structure of the optical stack in mobile LCDs. The theoretical principles of diffractive backlights are then outlined, and the key studies on polarizing as well as diffractive backlight variants are reviewed. In addition to aiming to improve the system efficiency of LCDs, many research teams also point out that by using diffractive backlights, the CFA can possibly be removed. The review concludes that in order to achieve the efficiency benefits that diffractive, color-separating backlights offer, the display industry needs to adopt a completely new system design paradigm, where diffractive grating arrays are integrated in the back display glass. If light sources can be chosen appropriately, this approach also would make it possible to remove the CFA in the LCD, offsetting the added cost of diffractive optics in the backlight structure. If the diffractive grating arrays are to be integrated into the back substrate of the display panel, cost savings can be expected when the conventional backlight unit is completely removed. Problems to be solved include launching and spreading light at the sides of the grating arrays, as well as the replication technology for the grating arrays.

3.3 Binary and Slanted Small-Area Grating Arrays for Diffractive Backlights

3.3.1 Concept Verification by Binary Striped Grating Array

In the first experimental study (P2), a 1 cm by 1 cm demonstrator grating array with a binary cross-section and a 50 % filling ratio was fabricated by ultraviolet (UV) curing SK-9 resist on a rectangular poly(methyl methacrylate) (PMMA) substrate. In this grating array, one striped grating structure represented each “green” subpixel, and another was used for “blue” and “red” subpixels. The “green” grating lines were perpendicular to the “red and blue” ones, and light was launched into the substrate also orthogonally, green from one side, and red and blue at right angles to the green propagation of light. The grating parameters are summarized in Table 3, and the experimental setup in Figure 9. The grating efficiencies are from a theoretical model

done for the study, and denote the efficiency of diffraction to the first order at each incidence of a given ray of light, for transverse electric (TE) and transverse magnetic (TM) polarization states, at the input inclination angle $\theta_i = 55^\circ$ and the azimuth angle $\varphi_i = 0^\circ$. Originally, the purpose was to launch light into the backlight structure from the corners. Therefore, the gratings are at 45° and 135° orientation with respect to the long axis of each respective stripe. Side-emitting red, green, and blue 0.6 mm thick Osram LEDs were used as light sources, butt-coupled into the LGP [57, 58]. The LED parameters are shown in Table 4. These LEDs were in fact used throughout this work, except in Publication 6. As the orthogonal orientation of the respective light sources makes the light enter the grating arrays perpendicular to the grating lines only for the intended primary band of light, good rejection of outcoupling is expected from the orthogonally oriented array.

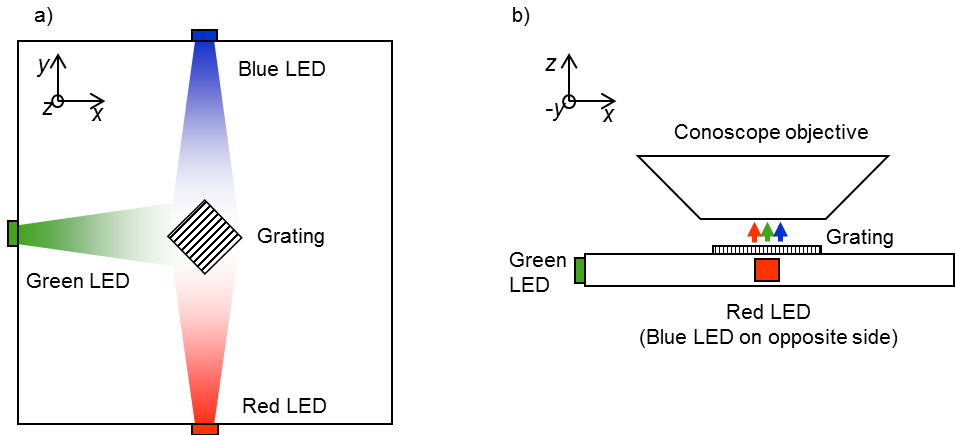


Figure 9. Experimental setup for Publication 2: a) top view; b) side view, with the conoscope objective lens shown. (P2)

Since the grating lines were fabricated at 45° and 135° with respect to the long axis of the array stripe, the LEDs were mounted facing the corners of the square array. The test LGP was placed in front of a conoscope (Eldim EZLite 120 R) and polar light intensity distribution plots were obtained for all individual color bands as well as for the “white” state combining the output of the red, green, and blue LEDs.

It can be seen in the results (Figure 10) that the blue (Fig. 10 a)) and green (Fig. 10 b)) light coupled toward the user, at $\theta = 10.5^\circ$ and $\theta = 15.0^\circ$, respectively, at quite a narrow

distribution. These values follow the design objectives of Publication 2. As expected from the grating design, the red (Fig. 10 c) light coupled out at an angle of about $\theta = 60^\circ$. This is because a compromise was made for the grating that coupled out the blue and red light jointly – it would not have been possible to design a single grating to couple out the light toward the normal of the grating surface for both spectral bands of light. A microscope examination shows that the light was outcoupled separately as green and blue from the respective grating stripes for these primary colors as can be seen in the microscope photographs in Figure 11. The red light could not be photographed since the light was not coupled out within the numerical aperture of the microscope. The results show that it is possible to separate the primary colors using spectrum-specific gratings.

Table 3. Grating parameters and expected efficiency of the gratings for Publication 2. (P2)

Primary	Width (μm)	Depth (nm)	Grating period (nm)	Calculated efficiency of transmitted mode at $\theta_i = 55^\circ, \phi_i = 0^\circ$	
				TE	TM
Red and blue	118	220	450	0.150	0.040
				0.182	0.061
Green	59	220	300	0.204	0.044

Table 4. LED parameters. (P2)

Primary	Dominant wavelength (nm)	FWHM* (nm)	Luminous intensity at 20 mA (mcd)	Luminous efficiency (lm/W) (Typical)
Red	625	19	180...900	43
Green	528	33	560...1800	36
Blue	460	25	90...280	11

*FWHM: Full width at half maximum.

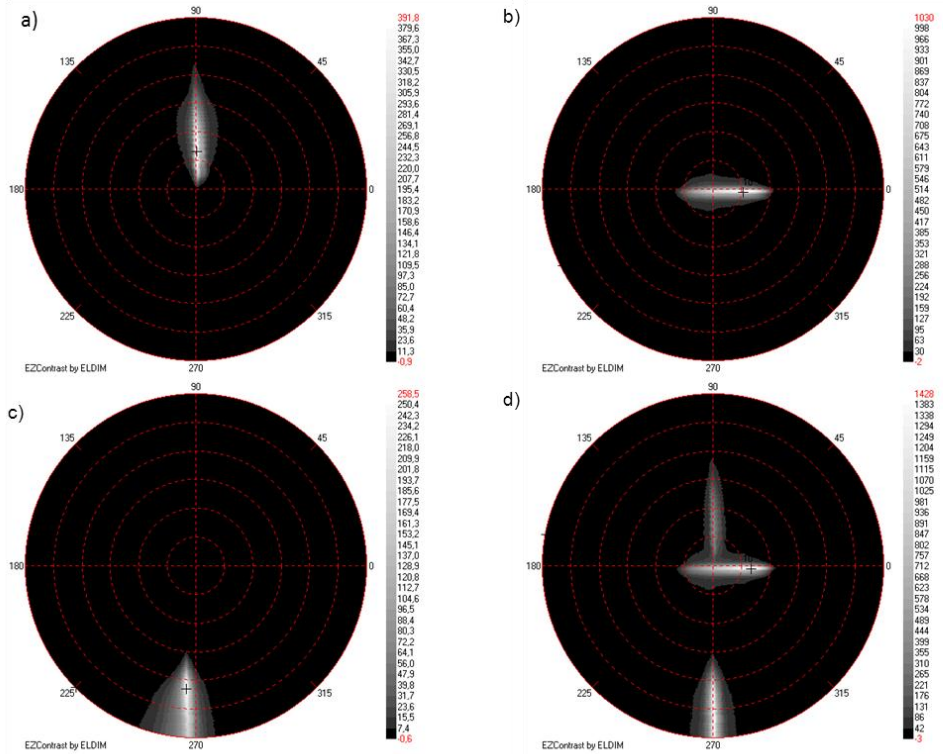


Figure 10. Measurement results from Publication 2: a) blue, b) green, c) red, and d) all combined. The value of the inclination angle θ is indicated by the concentric circles in the plots, and the value of the azimuth angle ϕ is shown at the perimeter of the plots. (P2)

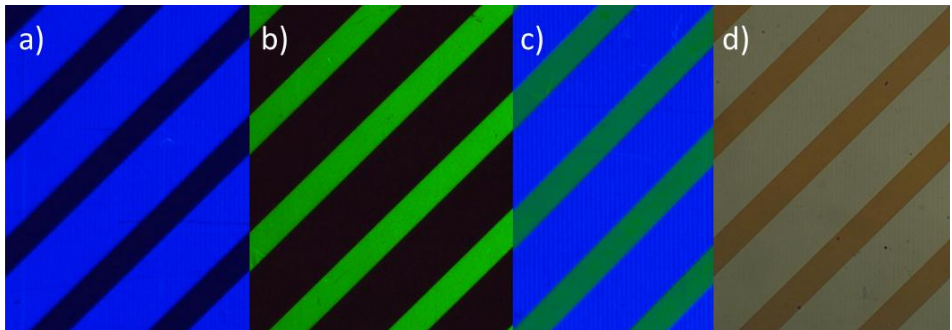


Figure 11. Microscope view of outcoupled light in Publication 2: a) blue, b) green, c) both at the same time, d) view with LEDs off by the microscope illumination. (P2)

3.3.2 Color-Separating Pixelated Slanted Grating Array

In this study (P3), a dedicated grating array was fabricated for each of the three primary colors, within a 1 cm by 1 cm slanted grating array demonstrator. This 56 x 3 by 56 subpixel (1 cm²) model array, with 50 % fill ratio, was designed for verifying the concept of the pixelated diffractive backlight. The grating parameters are shown in Table 5. A similar orthogonal illumination as in Publication 2 was used. The slanted grating array allowed precise control of diffracted orders and rejection of unwanted diffraction of blue light from the “red” grating array, and vice versa. The array was manufactured on a molded substrate of episulfide polymer (refractive index $n=1.717$ at the wavelength $\lambda=525$ nm) by ultraviolet (UV) embossing the same material on the substrate. Using this technique, replication of slanted grating arrays has been demonstrated up to 500 repeats without degradation of the mold or the master [59].

To take into account a possible use in an LCD, it is necessary to couple out the light from all subpixels with the same state of polarization, with respect to the principal lateral axes of a prospective display. Therefore, the “red” and “blue” gratings were designed for TE polarization, and the “green” grating for TM polarized outcoupling.

A fused silica master glass with a 100 nm thick Cr layer was spin coated with a suitable resist, and the master array pattern was exposed on the resist by electron beam lithography, by Nanocomp Oy. A standard development process was used to obtain a resist grating pattern on Cr, which then was developed into a Cr pattern on silica by a dry etching process. The individual primary-specific grating arrays, with the respective slanting directions, were fabricated by directionally patterning the master in a three-step reactive ion beam etching (RIBE) process. In this process, separate resist exposure and development steps are required for each separate grating array, and the master substrate is oriented in the ion beam at the proper angle at each lithography step for final master grating manufacture, and the remaining Cr layer is then removed by a standard wet etching process. The gratings were UV embossed from this master after the master had been coated with a silane-based anti-adhesion layer.

Table 5. Grating parameters for Publication 3. (P3)

Primary	Width (μm)	Depth (nm)	Grating period (nm)	Grating slant direction ($^{\circ}$)
Red (640 nm)	54	340	530	+45
Green (525 nm)	54	340	430	+20
Blue (460 nm)	54	240	375	-45

The UV embossing of the SiO_2 mould was made at Nokia Research Center in Helsinki in a UV Crosslinker (Spectrolinker XL-1500), with a peak ultraviolet wavelength $\lambda_{\text{UV}}=360$ nm, on a hot plate heated to 60 $^{\circ}\text{C}$. Thermally cured episulfide material plates were used as the LGP substrate. The fused silica grating master mould was placed on a metallic plate having uniform temperature of 60 $^{\circ}\text{C}$ and a drop of UV-curable episulfide was dispensed with a pipette on the master. The plastic substrate was then placed on the UV curable episulfide droplet, and the whole assembly was illuminated with UV flux of approximately 120 mJ/cm^2 . The cured replica was subsequently separated with a knife. Perfect separation was observed even though the individual gratings in the mould had slanting angles facing in opposite directions. Figure 12 shows scanning electron microscope (SEM) images of the replicated gratings.

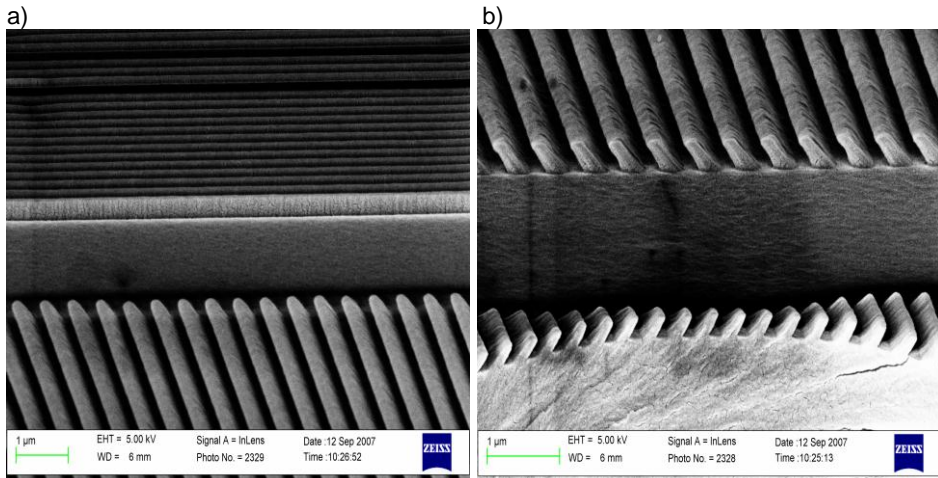


Figure 12. Scanning electron microscope images of the replicated grating array in Publication 3: a) “Green” grating lines at right angles to the “blue” grating lines, b) “Blue” and “red” gratings with opposite slanting directions. (P3)

For the experimental characterization of the grating array, a similar setup as in Publication 2 was used. Single 0.6 mm thick red, green, and blue Osram LEDs [57, 58] were placed at the edges of the display to illuminate the grating array, and 2 mm ball lenses were used to partially collimate the light for incoupling into the grating array. A microscope image was taken to visually examine the output (Figure 13). A conoscope (Eldim EZLite 120 R) was used for measuring the angular distribution of the light output of the array, and measurements were performed for the individual primaries keeping the respective LED “on”, as well as for the “white” output keeping all LEDs “on”. The measurement results show that the individual gratings used in the array performed as expected from the grating design, coupling the light toward the normal of the LGP. From the microscope image (Figure 13) it can be seen that there is some leakage of second-order diffracted blue light coupled out by the red subpixel, and with green illumination there is evidence of some stray light coupling out of the red and blue subpixels. Figure 14 summarizes the conoscope measurements. From these images, it is clear that the individual primaries are coupled toward the viewer quite effectively, at maximum outcoupling angles of 10° to 20° . These angles deviate from the normal, since the light was coupled in from the straight edges of the LGP instead of at the design value of 50° . The stray light evident in Figure 14 is most likely a result of the unpolarized light output of the LEDs scattering out of the grating array.

There is a clear improvement over the results of Publication 2 in the outcoupling of the individual primaries. Especially red is now directed toward the viewer instead of exiting in a very oblique angle. This was expected, since the pixelated design includes an individual grating with a properly oriented slant angle for both red and blue primaries. Furthermore, from examining the microscope images of the grating output, it can be seen that the light output is almost totally confined to the actual active area of each subpixel.

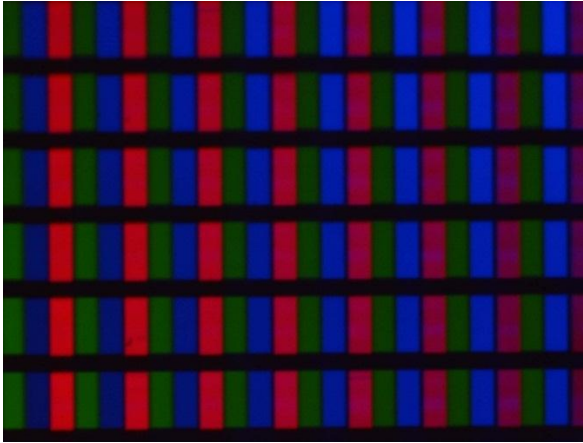


Figure 13. Microscope image of the light output of the grating array LGP of Publication 3. (P3)

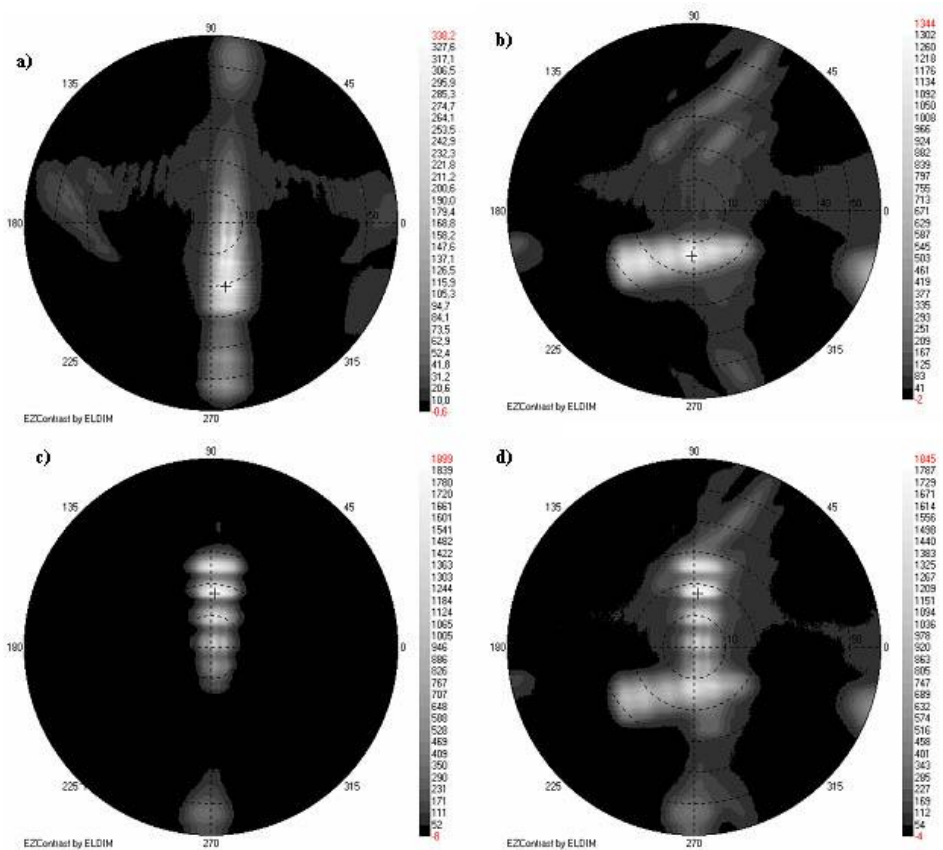


Figure 14. Conoscope measurements of Publication 3: a) blue, b) green, c) red, and d) all combined. The value of the inclination angle θ is indicated by the concentric circles in the plots (the edge of the plot is at 60°), and the value of the azimuth angle ϕ is shown at the perimeter of the plots. (P3)

3.4 Backlight Demonstrator Studies

3.4.1 Diffractive Pixelated Backlight Array

A full display-sized backlight grating array, with a 128 (by 3) by 160 pixel mobile display as the mechanical model, was fabricated in Publication 4 (P4). The prospective display parameters are summarized in Table 6. UV embossed grating arrays on episulfide were manufactured to conform to the mechanical specification of the prospective display. A slanted grating was designed under each display subpixel to diffract light of the corresponding spectral band toward the respective subpixel. An area modulation scheme was implemented to distribute the light outcoupling uniformly across the array, and binary fanout gratings with 50 % fill factor were also designed around the display area to attempt uniform distribution of the light sources laterally. Binary fanout gratings were manufactured on the opposite side of the LGP, to study the lateral spreading of light. The grating parameters are shown in Table 7, and the grating array design is shown in Figure 15 a) and b). The grating array was also used for the following study, Publication 5.

Table 6. Prospective display parameters for the backlight grating array of Publication 4. (P4)

Resolution	128 (x3) by 160
Pixel size	222 μm by 222 μm
Active area	29 mm by 36 mm
Display glass thickness	0.63 mm

The 52 mm by 54 mm LGP for the BLU was fabricated in a clean room at Nanocomp Ltd. in Joensuu area, Finland, from a fused silica master, on a 0.65 mm thick episulfide polymer substrate. The active grating matrix as well as the fanout gratings were manufactured by UV embossing from episulfide on top and bottom of the substrate, respectively, similarly to grating arrays reported in Publication 3. The edges of the LGP were now beveled to 45° to allow efficient coupling of LEDs to the LGP, and for the input coupling distribution of the light to better match the design value of the gratings.

The LGP was mounted on an x - y translation stage, and the Osram LEDs [57, 58] (Table 4) were attached to supports that were cut and ground to a 45° angle, for effective

incoupling of the light into the LGP. Two LEDs, driven at 20 mA nominal current, were used for each of the red, green, and blue primaries (See Figure 15 c). A calibrated conoscope (Eldim EZLite 120 R) was positioned at a location with maximum emission intensity. The conoscope plots for each individual primary color as well as for all RGB LEDs “on” at the same time are shown in Figure 16, and the angles of detected maxima of the angular distribution, as well as the measured full angular width of emission at half maximum intensity (FWHM) of outcoupled light are shown in Table 8.

The measurements were repeated for polarized light, and the outcoupling distributions were similar to those in Figure 30. For these measurements, a thin strip of reflective polarizer was cut to allow the TE polarization to propagate toward the LGP edge from red and green LEDs, and the TM polarization from the green LED. Because only one of the LEDs for each primary color was used, the “side lobes” visible in Figure 16 a) and c) at the 270° region are missing from the measured polar plots for the polarized case.

Table 7. Grating parameters for Publications 4 and 5. (P4, P5)

Primary	Width by length	Depth (nm)	Grating period (nm)	Grating slant direction (°)
Red (640 nm)	111 μm by 59 μm	340	530	+45
Green (525 nm)	59 μm by 111 μm	340	430	+45
Blue (460 nm)	111 μm by 59 μm	240	375	-45
Red fanout (Double bowtie)	10 mm by 36 mm	450	360	0
Green fanout (Double bowtie)	8 mm by 29 mm	370	290	0
Blue fanout (Double bowtie)	10 mm by 36 mm	320	250	0

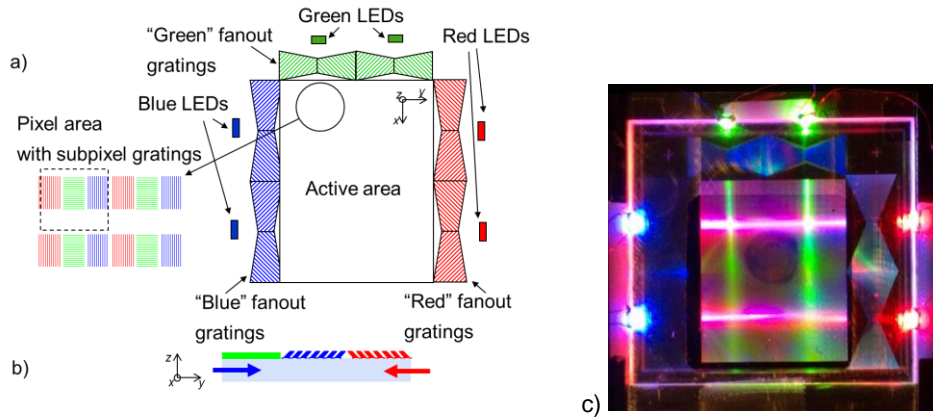


Figure 15. LGP layout for Publication 4. a) Grating arrangement from top, b) Direction of grating slants from the side (“green” slant perpendicular to both “blue” and “red” grating slants)(not to scale); c) Diffractive LGP of Publication 3 with all LEDs on. (P4)

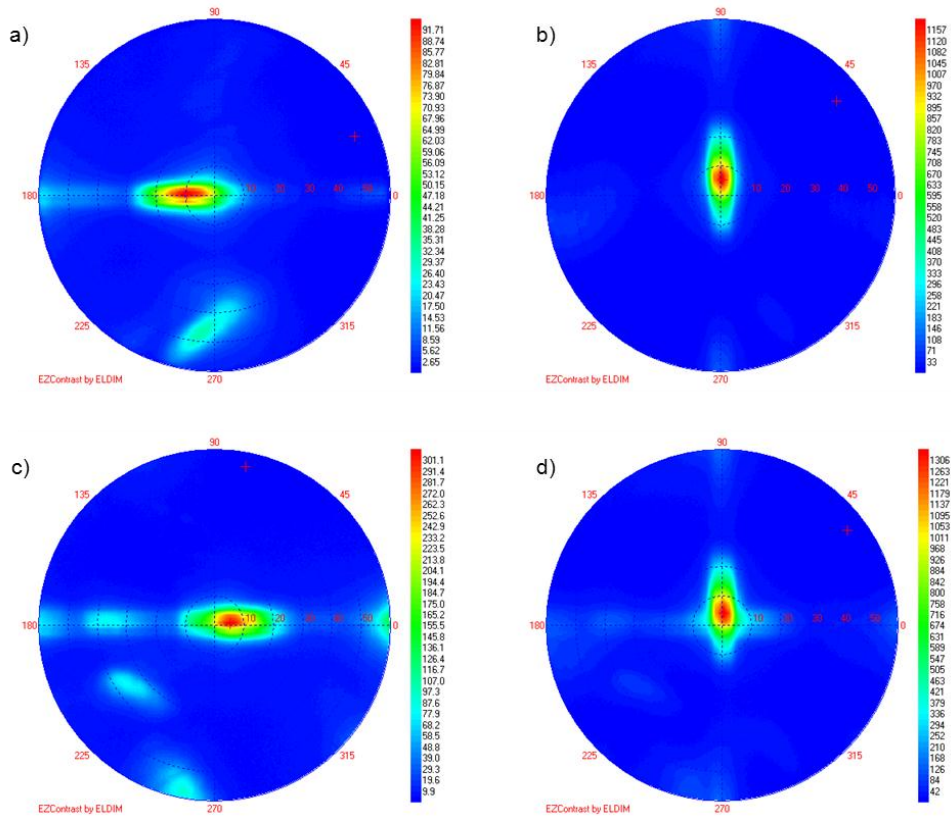


Figure 16. Polar coordinate plots of the light output for Publication 4: a) blue, b) green, c) red, d) all combined. The value of the inclination angle θ is indicated by the concentric circles in the plots, and the value of the azimuth angle ϕ is shown at the perimeter of the plots. (P4)

Table 8. The inclination angle θ of the outcoupling maxima and the FWHM of the emission in the grating experiment of Publication 4. (P4)

Primary	Angle of maximum outcoupling ($^{\circ}$)		Full width at half maximum ($^{\circ}$)	
	Unpolarized	Polarized	Unpolarized	Polarized
Blue	10	6	25	23
Green	5	5	18	18
Red	5	8	23	22

It was clear that the fanout gratings spread out the light only weakly, and streaks of light were prominently visible across the display from the incoupling points of the LEDs (see Figure 15 c)). Scanning electron microscope (SEM) images were taken of surplus molds of the fanout gratings to find out possible reasons for the poor performance of the fanout gratings (see Figure 17). From Figure 17, it can be seen that while the grating period was as expected, the desired binary grating profile had not been realized in the molding of the fanout gratings, and the gratings had a rounded triangular profile with about 15° slope. Moreover, the gratings were somewhat shallower than intended.

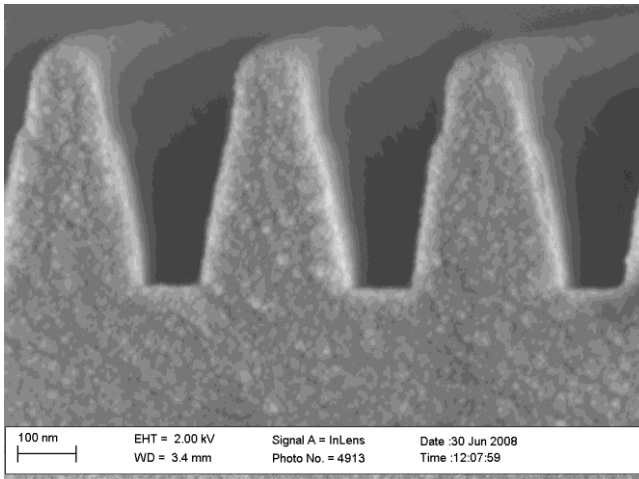


Figure 17. SEM image of the grating profile for the fanout gratings in Publication 4. (P4)

From Table 8, it can be seen that the outcoupled emission is directed quite well toward the user, with the full width at half maximum (FWHM) angular distribution of light

between 18° and 25° , and thus, the results show that a full display sized pixelated diffractive LGP is possible to be manufactured.

3.4.2 Diffractive Pixelated Grating Array in Electrowetting Display Application

The grating array fabricated for the study in Publication 4 was again used for Publication 5 (P5) in conjunction with a Liquavista transmissive electrowetting display (EWD) [35]. A pixelated grating array with a slanted grating for each respective subpixel was placed underneath the EWD. The EWD display characteristics are shown in Table 9, and the grating parameters are shown in Table 5. The binary fanout gratings and the area modulation scheme of the grating array were the same as in Publication 4.

As in Publication 4, the LGP design can be seen in Figure 15 a) and b). In this study, a transmissive EWD panel, without color filters, from Liquavista B. V. with 128 (x3) by 160 pixels was used [35]. The display and the LGP with Osram LEDs [57, 58] (Table 4) mounted at right angles toward the beveled edges of the LGP, were aligned together, by means of a micromanipulator system.

In another experiment, a striped RGB color filter was used in the place of the display to compare color space adjustment. The display was connected in place of the standard LCD on a Nokia 3110 Classic mobile phone. Test screens were stored in the memory of the phone, and the EWD was driven by showing these screens on the display. A calibrated conoscope (Eldim EZLite 120 R) was used to obtain polar plots of the outcoupling characteristics of light throughput. For the display measurement, the LED current was kept at the nominal 20 mA. For the color space adjustment measurement, the drive current of the green LED was kept constant while red and blue LED current was varied. Generally, there is a minor effect to the color space when adjusting the LED current, but in this study, for demonstrating the concept it was adequate to only vary the current.

With the EWD, it was difficult to obtain meaningful results to assess the performance of the combination of the LGP and the display, using the display as the electro-optic shutter. Figure 18 a) shows the conoscopic measurement of the output coupled light with all LEDs driven at 20 mA, and the display turned fully “on”, and the difference to the display “off” state is very small. The ratio of the luminance at the “on” state divided by that at the “off” state (the luminance contrast ratio), measured at one of the

intersecting beams of light propagating in the LGP and taking the average of measurements over the azimuth angle (ϕ) range of -60° to 60° at the conoscope inclination angle $\theta = 0^\circ$, was only 1.6. In Figure 18 a), there is also a periodic structure in the output characteristics that is a result of crosstalk in the EWD subpixel array. Similar results are obtained for the individual primary colors, and the crosstalk in these measurements is also very evident.

Table 9. Display parameters for the experiment. (P5)

Resolution	128 (x3) by 160
Pixel size	222 μm by 222 μm
Active area	29 mm by 36 mm
Display glass thickness	0.63 (x2) mm

3.5 Embedded Solution for Diffractive Backlight

Based on the previous studies (P2-P5), it was deduced that embedding a diffractive backlight to the back substrate of a display would bring the grating array as close as possible to the display subpixel array, in the manner shown in Figure 19. Therefore, in Publication 6 (P6), the pixelated grating array concept with slanted gratings was extended to an integrated one. A small slanted grating array was fabricated on a high refractive index glass substrate with a TiO_2 overlay, with a low-index cladding spin-coated on top of the grating array. The rationale for this investigation was to demonstrate that it is possible to manufacture a grating array that in principle could be embedded in the back substrate of an LCD (Figure 19). Laser light sources were used to characterize the propagation and outcoupling characteristics of the demonstrator assembly.

Using analogous logic to the design of grating arrays fabricated in Publications 3-5, similar slanted gratings were designed for the embedded pixelated LGP structure with red, green, and blue primary subpixels. Again, the green subpixel gratings were oriented at right angles to the red and blue subpixel gratings, and the polarization of the outcoupled light from the green subpixel was designed to be orthogonal (transverse magnetic, TM) to the blue and red subpixel outcoupling (transverse electric, TE). The grating design parameters are shown in Table 10. The rationale was to design the “red”

and “blue” grating period, depth, and slant angle so that mutual rejection of unwanted outcoupling was at the maximum, and the “green” grating characteristics were chosen so that adjusting the efficiency in the design was possible. With the design values of the gratings, light should be coupled out at the normal to the LGP surface.

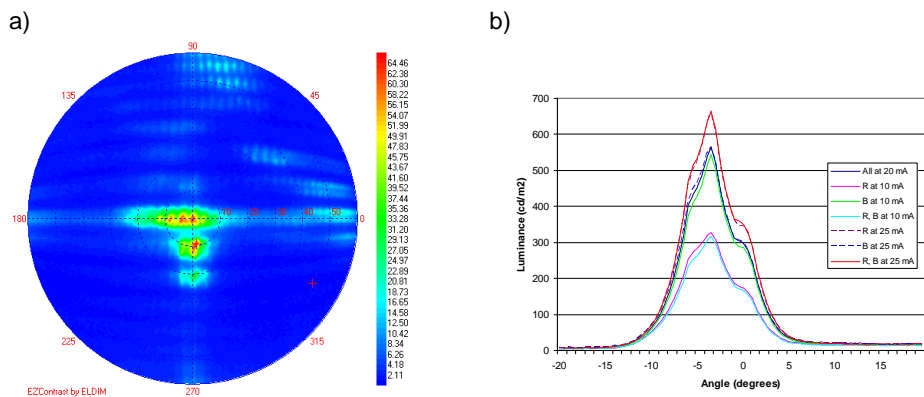


Figure 18. a) Polar coordinate plot of the electrowetting display coupled with the diffractive grating LGP. The value of the inclination angle θ is indicated by the concentric circles in the plot, and the value of the azimuth angle ϕ is shown at the perimeter of the plot. b) The effect of primary LED current to the overall luminance over a range of the inclination angle θ , through the color filter array. The LEDs are driven at 20 mA, unless otherwise mentioned in the legend. (P5)

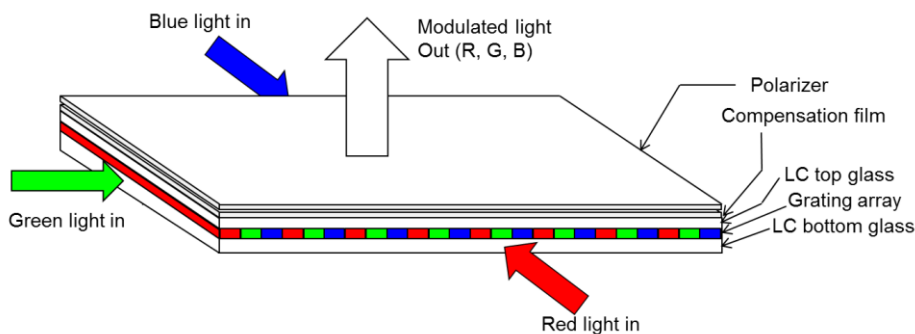


Figure 19. Embedded grating array schematic for an integrated backlight concept of Publication 6 (not to scale). (P1)

A 1.5-mm-thick high refractive index (n) glass (LASFN46A, $n = 1.91$) plate, 10 cm by 10 cm, was processed with a 400 nm thick titanium dioxide overlay fabricated by atomic layer deposition (ALD) at Beneq Oy. A grating array 65 pixels wide (14.43 mm along x -axis) and 81 pixels tall (17.98 mm along y -axis) was fabricated in the center area TiO_2 ($n = 2.2$) layer using reactive ion-beam etching (RIBE), by Nanocomp Oy. A 500 nm thick DuPont AF1600 low-index polymer layer ($n = 1.31$) was spin-coated on

top, as a cladding layer for the whole LGP. Figure 20 presents a SEM image of a model grating, from a cladding deposition trial. Although the cladding polymer lifts off in the preparation process for SEM, the thickness of the cladding layer can be deduced to be on the order of 500 nm.

Table 10. Grating array parameters for Publication 6. (P6)

Parameter / Grating	“Red” subpixel grating	“Green” subpixel grating	“Blue” subpixel grating
Design λ (nm)	640	525	460
Grating period (nm)	450	370	325
Grating depth (nm)	250	240	150
Slant angle ($^{\circ}$)	45	45	-45
Filling ratio (%)	50	50	50
Grating width (μm)	111	59	111
Grating length (μm)	59	111	59
Aperture of grating (%)*	13	13	13

*The aperture refers to the proportion of fabricated grating area of the total pixel area.

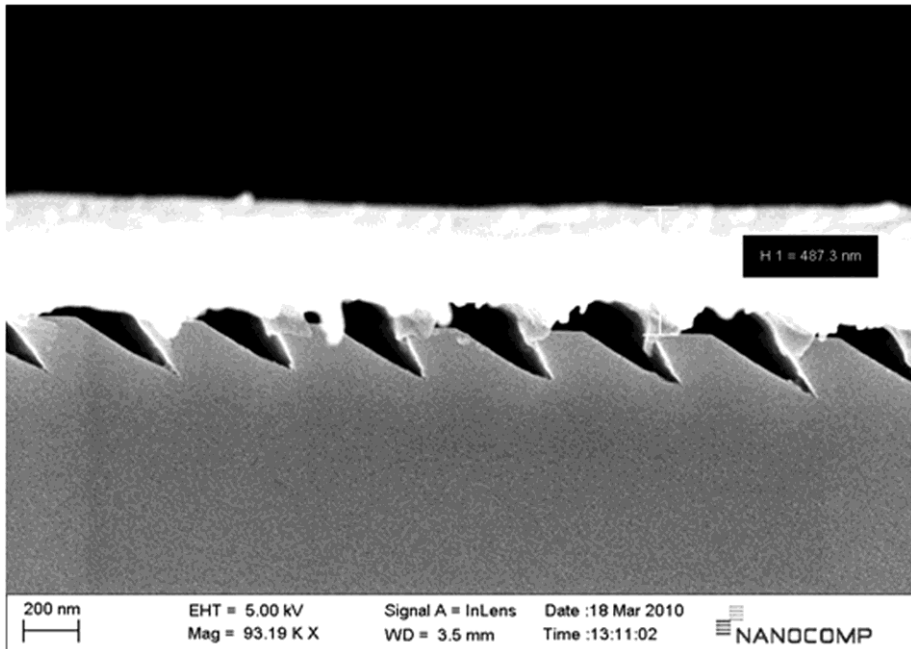


Figure 20. A SEM image of a model grating for the study in Publication 6. The cladding layer is seen above the grating, separated from the grating in the SEM preparation stage. (P6)

Figure 21 shows a schematic drawing of the experimental setup. A 4 mW green frequency-doubled diode laser pointer at 525nm, a 6 mW red helium-neon laser at 632.8 nm, and a 0.4 mW blue frequency-doubled diode laser at 473 nm were used as light sources. An arrangement of apertures, polarizers, and semitransparent mirrors, was used to adjust the path of light, polarization, and light intensity. The light was coupled into the LGP by a BK7 prism adhered to the bottom of the LGP by index matching fluid. A reference detector was used to control the level of illumination at every measurement point in the measurement protocol. The outcoupled TE and TM polarization states of light were measured for each light source. Special care was made to ensure repeatability of the measurements. Since the design for the grating array was done for incident angle of $\theta_i = 50^\circ$, for the plate thickness $h = 1.5$ mm, the expected distance between outcoupled peaks was $l = 3.58$ mm.

Figure 22 presents the measured intensity curves, normalized to the maximum value of outcoupling, after the calculated Fresnel losses [60] in the prism coupling arrangement, of the measurements along the surface of the LGP. The positions of the maxima of these curves show that the average distance l between the outcoupling peaks was 3.6 mm, according to the distance derived from the design incidence angle θ_i of the gratings.

Figure 23 presents the theoretical decay characteristics of the outcoupling peaks together with experimental findings. The intensity of outcoupled light decreases with the distance from the incoupling point except with the green light source, where the decrease starts from the second peak since evidently the incident beam hits the grating only partially, leaving the first outcoupled peak incomplete. This is the expected result in the absence of area modulation in the grating array that would take in account the already outcoupled energy along propagation path of the light. The experimental outcoupled peaks decay more rapidly than the theoretical calculations predict, indicating that there is more scattering-based loss than what has been taken into account by the calculations.

Although the gratings were designed for color separation, the polarization sensitivity of outcoupling was also studied, and a variance in polarization sensitivity of outcoupling was found. The green TE outcoupling was 7 % higher than the TM outcoupling; red TE coupling out 206 % stronger than TM; and blue TE 78 % over the respective TM

polarization state. The differences could be attributed to differences in final manufactured grating depths from the calculated designs and the possible effect of the finite thickness of the cladding layer that was not fully taken into account in the design of the gratings.

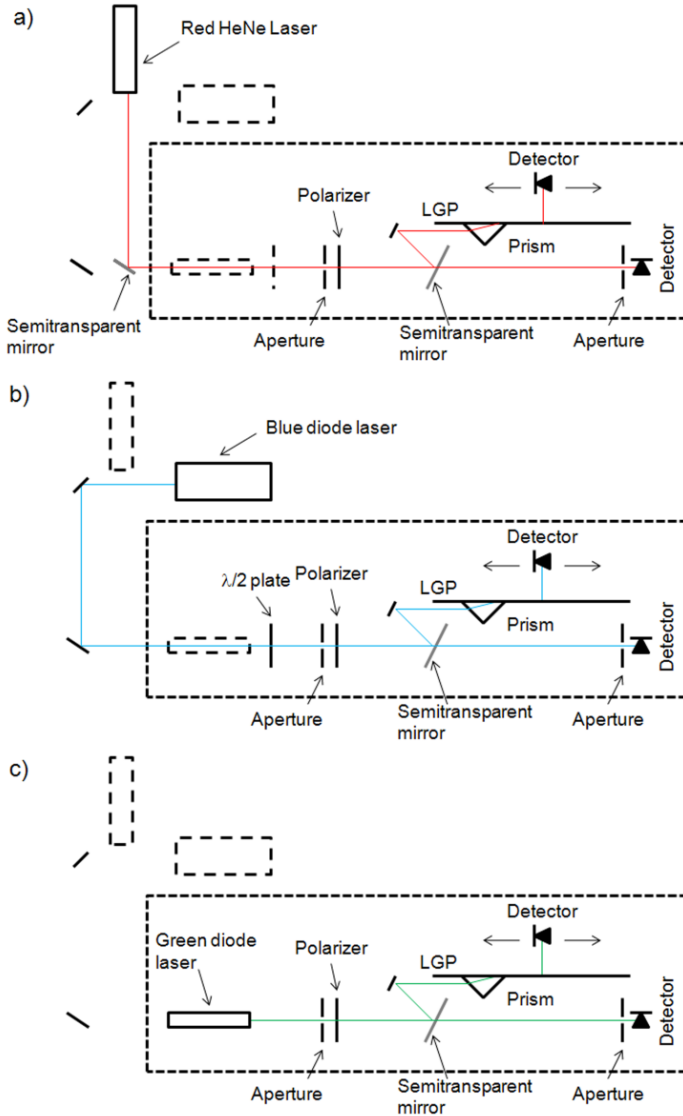


Figure 21. Experimental setup for Publication 6. The apertures in the path of light are used for experiment alignment, and the reference detector at the end of the experiment is used to compensate for any variation in input light intensity. The light sources in a)-c) are used each in turn, with the green removed when not in use. (P6)

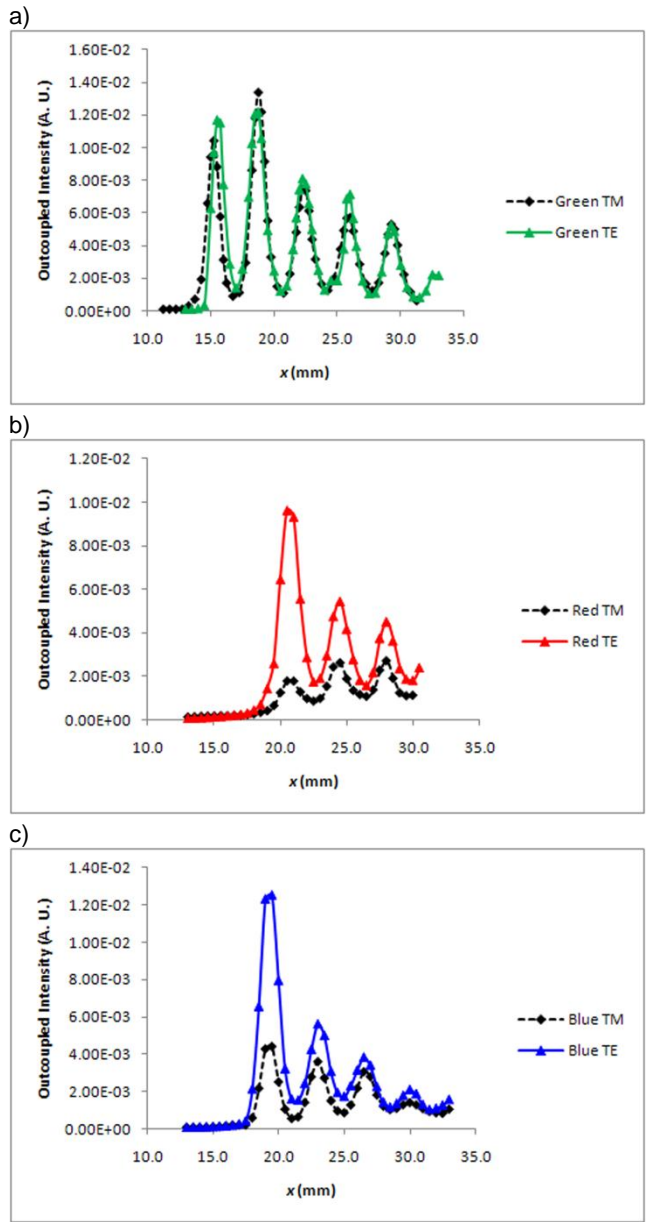


Figure 22. Normalized intensity in a) green, b) red, c) blue outcoupling in Publication 6. (P6)

The results show sharply directed outcoupling of the laser light, with the FWHM of the outcoupling in the order of 3°. The results show that the polarization contrast in outcoupling is remarkable, but not adequate for a LCD without a back polarizer for all colors. Based on this study, the grating arrays etched in high refractive index glass

could in principle be used as the back substrate of an LCD, placing the grating arrays as close as possible to the subpixel array, thus eliminating crosstalk (see Figure 19).

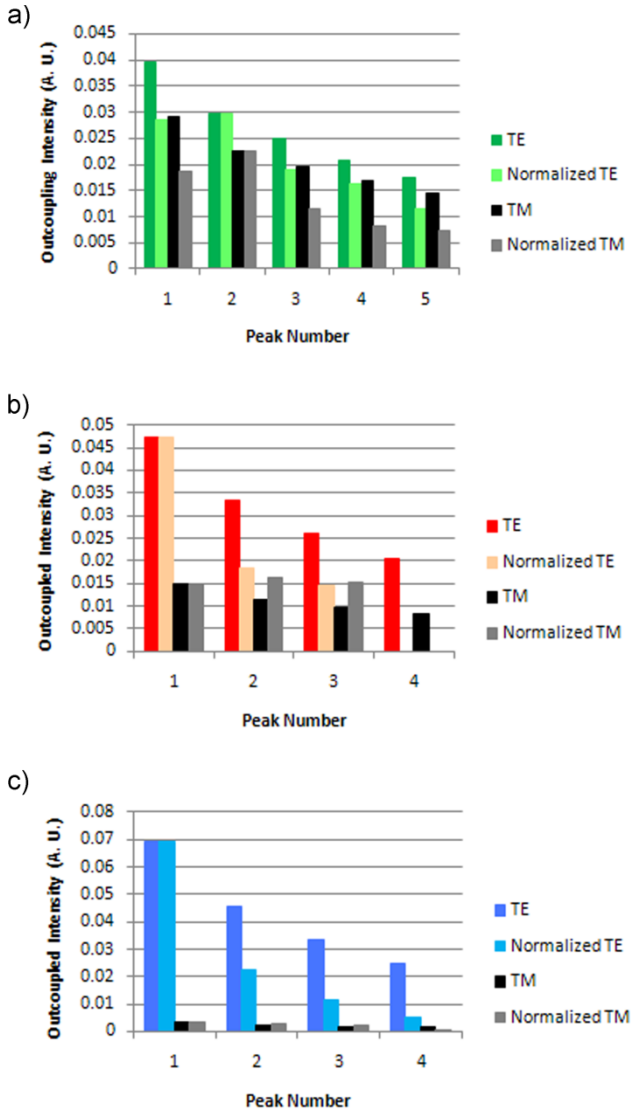


Figure 23. Comparison of theoretical decay (“TE” and “TM”) and experimental results (“Normalized TE” and “Normalized TM”) for the outcoupled peak intensities in Publication 6: a) green outcoupling, b) red outcoupling, c) blue outcoupling. (P6)

4 Discussion and Conclusions

Displays in mobile devices have developed in the last fifteen years from simple monochrome alphanumeric components that provided the user the basic interface to access information on voice-based communication, to high-quality visual interface elements to access the mobile internet, imaging functions, navigation features, games, *etc.* The display is today a strategic component that should not be compromised in high-end mobile devices. Since the image quality in mobile displays today is high, energy consumption has become a bottleneck issue. This thesis addresses technology to lower the power dissipation of a mobile display by diffractive optics. In contrast to the conventional display module design using a backlight unit with white light sources and a color filter array (CFA) in the LC cell, the method in this thesis aims to select the emission of the red, green, and blue primary LEDs and guide each of these through the respective subpixels in the LCD. The color-separating approach could potentially bring about a 4.5 to 6 times enhancement of efficiency of the LCD module (P1), and both geometrical optics based [61, 62] and diffractive optics based solutions to separate colors in a display BLU [63-73] have been reported. The mobile device integrator could apply these energy-saving display modules to make products that allow longer “multimedia time” to the user, allow the integration of smaller batteries in the device, or have a slimmer form factor in the product.

The conventional LCD module in mobile devices today is optically a complicated stack of transparent polymer parts, reflectors, beam-guiding and shaping films and polarizers, with the LC glass having the electro-optic modulator medium and the CFA at its central layer. Attempts to reduce the number of films have led to the development of advanced light-guide plates in backlights, and color-separating backlights have also been developed to make the CFA an unnecessary item in the display. The diffractive approach for color separation also attempts to achieve these two goals with one and the same new display paradigm, while reducing the power dissipation of the display system to a fraction of that of the conventional mobile LCD.

Currently, there are other, emerging technology variants on the market aiming to take their niche of the mobile display market, but so far, only the OLED and EPID displays have had any success. The OLED user experience can be very compelling in live video use, but the applications can be limited due to the high power consumption when the majority of the pixels are fully on, and due to the poor sunlight readability of OLED displays. These problems limit the application of OLEDs somewhat. EPIDs on the other hand excel in bright ambient conditions, but they cannot be regarded as full-function multimedia displays, as their use is best suited in reading devices, where the information content on the screen is quasi-static. Advanced dynamic backlight driving algorithms for the LCD also have achieved power savings, but often the penalty paid by the user is in the delivered “quality of service” in that the algorithms may cause distortion in the color space and image quality therefore can be reduced.

The research on diffractive backlights (P1) has always addressed the immediate need of the mobile device integrators. Starting from studies to reduce the number of films in monochrome display modules [74], the arc of research has progressed through stages where a broad spectrum of light was guided through the CFA and the LCD subpixel array [67-70 and 75-79], via polarizing backlights [80-88], and finally, to color-separating backlights where the main purpose was to dispense with the absorbing CFA to markedly improve the energy efficiency of the display module [70-73 and 89-92]. Taking these results as the starting point, the research into the central theme of this thesis examines ways to realize a diffractive backlight where the backlight function is in the end integrated into the back substrate of the display glass itself (P2-P6) [94-98].

Most research centers working on diffractive backlights have access to commercial software solutions such as ASAP® and GSOLVER® for designing the waveguides and related optical structures [63, 66, 70, and 77]. With these software modeling packages, usually only sinusoidal or binary grating profiles can be used. This limits the grating design capability in research, since with this approach the light distribution in the various diffracted grating orders cannot readily be optimized. Also, many times only a single grating or a single-type grating array has been applied in the design, which results in cumbersome optical structures, and also sometimes requires special array arrangements for the display [66, 70]. T. Levola’s dissertation [99] includes a starting point of a software solution that can take in account arbitrary periodic structures. While

this software has mostly been used in designing near-to-eye optics for virtual display applications [100-103], it also has been an asset in designing pixelated multi-grating arrays (P2-P6), [94-98]. The software can model the behavior of light in gratings with arbitrary periodic shapes very accurately, and for this work, it has presented solutions that otherwise could not have been possible to design.

Previous studies indicate that the pixelated grating array needs to be in close contact to the actual LCD subpixel array in order to eliminate crosstalk [66, 96]. In Publication 5, an embedded structure is proposed as the back substrate of the display, bringing the outcoupling grating array effectively in contact with the bottom of the LCD subpixel array. Then, the backlight unit could be manufactured as an integral part of the back substrate of an LCD.

The research during the course of this thesis has given answers to some of the questions while raising more to be answered later. It has been shown, first of all, that light can be separated by binary and preferably by slanted gratings into the primary spectral bands; secondly, that the grating arrays can be manufactured to conform to a prospective display on top and that the light can be directed toward the user quite effectively; and finally, that it is possible to integrate the diffractive backlight into the back substrate of the LCD.

The results also suggest the possibility to remove the CFA in panel design. This statement is only qualitative, as color measurements using the grating array structures developed for the purpose of this thesis have not been performed. These are only in the planning phase, for future work. Since the outcoupling distributions of red, green, and blue light differ from each other within each grating array component studied in this Thesis, the color performance also differs greatly when viewing the demonstrator samples from different angles. This effect can be inferred from the conoscope plots shown in Figures 10, 14, and 16, for instance. Even at the normal direction, R, G, and B luminance values differ greatly, making it hard to achieve a “white” signal at any specific viewing angle, and observing the LGPs will result in a strong spectral dependence on the viewing direction. In all studies (P2-P5), the LEDs were driven at their nominal 20 mA current, and there was no intention of attempting to select the drive current otherwise, except in the color filter measurements of P5. In the microscope

observation, light is collected within the numerical aperture of the microscope objective, and on individual subpixel grating level, the primary color performance can be observed, as is seen in Figure 13. Outcoupling of the second order diffraction from the “red” grating can be visually observed by turning “on” only the B light source. The grating design has to be very accurate to counteract this effect in a color-filterless design.

The remaining problems in diffractive BLU design relate to the incoupling of LEDs directly into the substrate glass, fanning out the light at the sides of the display, and finding a suitable technique for replication instead of directly etching the backlight grating array into the glass substrate. For best operation of the gratings, the light source ought to be as collimated as possible, either by using an external collimator or manufacturing the collimating structure on the incoupling area of the display glass. Geometrical optics based collimating means can produce FWHM of $\pm 10^\circ$ [55], which already is an improvement. The light from the LEDs outside the active area of the display does not need to be fanned out in a diffractive fashion, as color separation is not necessary in this region. Diffractive optical fanout can, however, yield to the same manufacturing technique as the actual grating array, so this solution should still be kept in mind. A suitable replication technique needs to be found for the grating array; it must be compatible with stepwise replication on a large substrate and the resulting grating structure should withstand the process steps of LCD manufacturing. It would also be preferable if the waveguiding properties of the whole integrated backlight structure could be realized, retaining the high efficiency of the gratings, with lower refractive index glass than what was used in Publication 6, making the process compatible with current LCD production. Finally, the output characteristics of the resulting display need to be tuned with a possible diffuser [89, 91]. Since in the pixelated approach, green output is spread at right angles to the red and blue output, a color-anisotropic solution would be preferable.

This new concept of an integrated backlight (P6) could not only create savings in eliminating films in the beam-shaping section of the backlight, but it would also remove the separate backlight unit from the display manufacturing process. In addition, the color filter array is not required if the grating array can be designed in a proper way. This manufacturing paradigm would require the LCD industry to start experimenting

with, and finally, adopting into use a totally new manufacturing philosophy. It remains to be seen whether ever-increasing demands on energy savings in all forms of electronic appliances can bring about incentives to guide the industry through such a change. This will only be possible through collaboration between academic and industrial sectors, and with a proper research framework and funding.

References

1. J. Kimmel, J. Hautanen, and T. Levola, "Display Technologies for Portable Communication Devices," *Proceedings of the IEEE*, Vol. 90, pp. 581-590, 2002.
2. J. Kimmel, "Mobile Multimedia Displays," *SID Symposium 2010 Application Tutorial Notes*, 2010.
3. J. Kimmel, "Overview of Mobile Displays," Chapter 10.1.1 in: Janglin (John) Chen, Wayne Cranton, Mark Fihn (Eds.), *Handbook of Visual Display Technology*, Springer-SBM, Heidelberg, pp. 1983-1992, 2012.
4. J. Kimmel, "Displays Enabling Mobile Multimedia," *Proceedings of the SPIE*, Vol. 6507, p. 650705-1 - 650705-11, 2007.
5. "Industry Outlook 2012," *Informa Telecom & Media*, 2011.
6. R. Akins, "Displays for Hand-held Portable Electronic Products," *JSID*, Vol. 7, No. 4, p. 273-276, 1999.
7. E. Lueder, "Liquid Crystal Displays. Addressing Schemes and Electro-Optical Effects," 2nd Edition, Wiley, Chichester, pp. 80-82, 2010
8. Z. Li, A. K. Bhowmik, and P. J. Bos, "Introduction to Mobile Displays," Ch. 1 in: "Mobile Displays – Technology and Applications," Bhowmik, A. K., Li, Z, and Bos, P. J. (Eds.), Wiley, Chichester, pp. 1-22, 2008.
9. J. Kimmel, "Transflective Displays for Mobile Devices," Chapter 10.1.2 in: Janglin (John) Chen, Wayne Cranton, Mark Fihn (Eds.), *Handbook of Visual Display Technology*, Springer-SBM, Heidelberg, pp. 1993-2002, 2012.
10. J. J. Romero, "The Take-Anywhere, Do-Anything Display," *IEEE Spectrum*, January 2010, pp. 46-51, 2010.

11. Z. Ge, and S.-T. Wu, "Device Concept of Transflective Liquid Crystal Displays," Ch. 1 in "Transflective Liquid Crystal Displays," Wiley, Chichester, pp. 1-58, 2010.
12. X. Zhu, Z. Ge, T. X. Wu, and S.-T. Wu, "Transflective Liquid Crystal Displays," IEEE/OSA Journal of Display Technology, Vol. 1, No. 1, pp. 15-29, 2005.
13. G. Boyd, "LCD Backlights," Chapter 7.5.1 in: Janglin (John) Chen, Wayne Cranton, Mark Fihn (Eds.), Handbook of Visual Display Technology, Springer-SBM, Heidelberg, pp. 1609-1624, 2012.
14. M. Anandan, "Progress of LED backlights for LCDs," JSID, Vol. 16, No. 2, pp. 287-310, 2008.
15. "Micro SIDELED 0.8mm Long Life, Enhanced Optical Power LED, Lead (Pb) Free Product – RoHS Compliant LW Y1SG," Osram datasheet, 2009.
16. W. J. Cassarly, "Backlight Pattern Optimization," Proceedings of the SPIE, Vol. 6834, pp. 683407-1 - 683407-12, 2007.
17. T. Murata and I. Fujieda, "Input Couplers for Thin Light-Guides and Light-Emitting Diodes," Optical Engineering, Vol. 47, No. 2, pp. 027001-1 - 027001-7, 2008.
18. P. Watson, and G. T. Boyd, "Backlighting of Mobile Displays," "Ch. 7 in: "Mobile Displays – Technology and Applications," Bhowmik, A. K., Li, Z, and Bos, P. J. (Eds.), Wiley, Chichester, pp. 211-225, 2008.
19. M. Suzuki, "Two Approaches to the Luminance Enhancement of Backlighting Units for LCDs," JSID, Vol. 7, No. 3, pp. 157-161, 1999.
20. A. Funamoto, Y. Kawabata, M. Ohira, and S. Aoyama, "Prism-sheetless High Bright Backlight System for Mobile Phone," Proceedings of the International Display Workshops 2004, pp. 687-690, 2004.

21. D. Feng, X. Yang, G. Jin, Y. Yan, and S. Fan, "Integrated Light-Guide Plates that Can Control the Illumination Angle for Liquid Crystal Display Backlight System," *Proceedings of the SPIE*, Vol. 6034, pp. 603406-1 - 603406-8, 2006.
22. C. H. Chien and Z. P. Chen, "Fabrication of Integrated Light Guiding Plate for Backlight System," *Proceedings of the SPIE*, Vol. 6109, pp. 610909-1 - 610909-8, 2006.
23. A. Nagasawa, T. Eguchi, Y. Sanai, and K. Fujisawa, "A Novel Backlight System with the Unified Component," *Proceedings of the International Display Workshops/Asia Display, IDW/AD '05*, pp. 1285-1288, 2005.
24. J. Kimmel, "Liquid Crystal Optics for Mobile Displays," Chapter 10.1.4 in: Janglin (John) Chen, Wayne Cranton, Mark Fihn (Eds.), *Handbook of Visual Display Technology*, Springer-SBM, Heidelberg, pp. 2013-2022, 2012.
25. A. Lääperi, I. Hyytiäinen, T. Mustonen, and S. Kallio, "OLED Lifetime Issues in Mobile Phone Industry," *SID International Symposium Digest of Technical Papers*, Vol. XXXVIII, pp. 1183-1187, 2007.
26. A. Lääperi, "OLED lifetime issues from a mobile-phone-industry point of view," *JSID*, Vol. 16, No. 11, p. 1125-1130, 2008.
27. J. Kimmel, "Alternative Technologies for Mobile Direct-View Displays," Chapter 10.1.3 in: Janglin (John) Chen, Wayne Cranton, Mark Fihn (Eds.), *Handbook of Visual Display Technology*, Springer-SBM, Heidelberg, pp. 2003-2012, 2012.
28. F. P. M. Budzelaar, C. N. Cordes, J. J. L. Hoppenbrouwers, N. C. van der Vaart, W. H. M. van Beek, F. J. Vossen, A. A. M. Hoevenaars, and R. G. H. Boom, "Video Processing for Active-Matrix Polymer OLED TV," *JSID*, Vol. 14, No. 5, pp. 461-466, 2006.
29. "On-Cell Touch AMOLED (OCTA)," *Technical Documentation*, Samsung Mobile Display, 2011.

30. Z. Ge and S.-T. Wu, "Color Sequential Mobile LCDs," Chapter 5 in Ge, Z., and Wu, S-T (Eds.), "Transflective Liquid Crystal Displays," Wiley, Chichester, pp. 189-211, 2010.
31. F. Yamada, H. Nakamura, Y. Sakaguchi, and Y. Taira, "Sequential-color LCD based on OCB with an LED backlight," JSID, vol. 10, No. 1, pp. 81-85, 2002.
32. K. Sekiya, "Technologies Related to Field Sequential Color LCDs," IMID/IDMC/Asia Display 2010 Digest, pp. 239-240, 2010.
33. S. J. Roosendaal, E. van der Tol, E. H. A. Langendijk, J. R. Hector, J. R. Hughes, M. Inoue, H. Fujimoto, H. Watanabe, K. Nasu, T. Inada, M. Yoshiga, S. Naitoh, M. Shibazaki, S. Kawata, and N. Sumi, "A Wide Gamut, High Aperture Mobile Spectrum Sequential Liquid Crystal Display," SID International Symposium Digest of Technical Papers, Vol. XXXVI, pp. 1116-1119, 2005.
34. R. A. Hayes and B. J. Feenstra, "Video-speed Electronic Paper Based on Electrowetting," Nature, Vol. 425, No. 25, pp. 383-385, 2003.
35. A. Giraldo, J. Aubert, N. Bergeron, E. Derckx, B. J. Feenstra, R. Massard, J. Mans, A. Slack, and P. Vermeulen, "Transmissive Electrowetting-based Displays for Portable Multimedia Devices," JSID, Vol. 18, No. 4, pp. 317-325, 2010.
36. B. Gally and B. Young, "Reflective Displays: Enabling Mobile Devices of the Future," SID Business Conference, pp. BC8/1-8, Los Angeles, 2008.
37. I. Bitá, "mirasolTM Displays: Technology and Manufacturing of Interferometric MEMS on Large Area Glass Substrates," Proceedings of the International Display Workshops 2008, pp. 89-92, 2008.
38. I. Bitá, I. H. Tavakoli, E. Poliakov, K. Li, T. Fiske, J. Gille, and R. A. Martin, "Tailoring Reflective Display Brightness for Mobile Device Applications," SID International Symposium Digest of Technical Papers, Vol. XLII, pp. 261-263, 2011.
39. K. Amundson, "Electrophoretic Displays," Chapter 8.1.1 in: Janglin (John) Chen, Wayne Cranton, Mark Fihn (Eds.), Handbook of Visual Display Technology, Springer-SBM, Heidelberg, pp. 1700-1713, 2012.

-
40. N. K. Sheridan, E. A. Richley, J. C. Mikkelsen, D. Tsuda, J. M. Crowley, K. A. Oraha, M. E. Howard, M. A. Rodkin, R. Swidler, and R. Sprague, "The Gyricon Rotating Ball Display," *JSID*, Vol. 7, No. 2, pp. 141-144, 1999.
 41. R. C. Liang, J. Hou, H. Zang, J. Chung, and S. Tseng, "Microcup® Displays: Electronic Paper Roll-to-Roll Manufacturing Processes," *JSID*, Vol. 11, No. 4, pp. 621-628, 2003.
 42. "EInk Triton Imaging Film™," Technical Document, E Ink Corp., 2010.
 43. J. Kimmel, "Energy Aspects of Mobile Display Technology," Chapter 10.1.5 in: Janglin (John) Chen, Wayne Cranton, Mark Fihn (Eds.), *Handbook of Visual Display Technology*, Springer-SBM, Heidelberg, pp. 2023-2032, 2012.
 44. "New Memory LCD Adds to Sharp's© Extended Use Mobile Display Suite, Delivers Ultra Low-Power Graphic Display Options," Press Release, Sharp Inc., 2009.
 45. N. Ueda, Y. Ogawa, K. Tanaka, K. Yamamoto, and Y. Yamauchi, "A Novel Multi-level Memory in Pixel Technology for Ultra Low Power LTPS TFT-LCD," *SID International Symposium Digest of Technical Papers*, Vol. XXXXI, pp. 616-618, 2010.
 46. N. Chang, I. Choi, and H. Shim, "DLS: Dynamic Backlight Luminance Scaling of Liquid Crystal Display," *IEEE Transactions on VLSI Systems*, Vol. 12, No. 8, pp. 837-846, 2004.
 47. N. Raman and G. Hekstra, "Content Based Contrast Enhancement for Liquid Crystal Displays with Backlight Modulation," *IEEE Transactions on Consumer Electronics*, Vol. 51, No. 1, pp. 18-21, 2005.
 48. A. Iranli, W. Lee, and M. Pedram, "HVS-Aware Dynamic Backlight Scaling in TFT-LCDs," *IEEE Transactions on VLSI Systems*, Vol. 14, No. 10, pp. 1103-1116, 2006.
 49. S. Koide, S. Fujita, T. Ito, S. Fujikawa, and T. Matsumoto, "LTPS Ambient Light Sensor with Temperature Compensation," *Proceedings of the International Display Workshops 2006*, pp. 689-690, 2006.

50. C. H. Hwang and A. Wu, "A Predictive System Shutdown Method for Energy Saving of Event-Driven Computation," International Conference on Computer Aided Design, pp. 28–32, 1997.
51. T. Simunic, L. Benini, P. Glynn, and G. De Micheli, "Event-Driven Power Management," IEEE Transactions on Computer-Aided Design of Integrated Circuits and Systems, Vol. 20, No. 7, pp. 840-857, 2001.
52. Q. Qiu, Q. Wu, and M. Pedram, "Stochastic Modeling of a Power-managed System - Construction and Optimization," IEEE Transactions on Computer-Aided Design of Integrated Circuits and Systems, Vol. 20, No. 10, pp. 1200-1217, 2001.
53. K. Kulojärvi, "Window to Mobile Internet," Keynote presentation at the 29th International Display Conference, Eurodisplay'09, Rome, Italy, September, 2009.
54. Y. Neuvo, "Cellular Phones as Embedded Systems," IEEE Solid-State Circuits Conference, 2004. Digest of Technical Papers, ISSCC, Vol.1, pp. 32-37, 2004.
55. K. Kälantär, "A Directional Backlight with Narrow Angular Luminance Distribution for Widening the Viewing Angle for an LCD with a Front-surface Light-Scattering Film," JSID, Vol. 20, No. 3, pp. 133-142, 2012.
56. "Flat Panel Measurement Standard. Version 2.0," Video Electronics Standards Association, Display Metrology Committee, 2001.
57. "Micro SideLED® Enhanced Optical Power LED (Thin GaAN®), Blue/True Green," Osram datasheet, 2006.
58. "Micro SideLED® Enhanced Thin Film LED, Red," Osram datasheet, 2006.
59. T. Levola and P. Laakkonen, "Replicated Slanted Gratings with a High Refractive Index Material for In and Outcoupling of Light," Optics Express, Vol. 15, No. 5, pp. 2067-2074, 2007.
60. M. Born and E. Wolf, "Principles of Optics," 7th Edition (corrected), Cambridge University Press, Cambridge, 2002.

61. A. Travis, T. Large, N. Emerton, and S. Bathiche, "Collimated Light from a Waveguide for a Display Backlight," *Optics Express*, Vol. 17, No. 22, pp. 19715-19719, 2009.
62. P.-C. Chen, H.-H. Lin, C.-H. Chen, C.-H. Lee, and M.-H. Lu, "Color Separation System with Angularly Positioned Light Source Module for Pixelized Backlighting," *Optics Express*, Vol. 18, No. 2, pp. 645-655, 2010.
63. D.R. Selviah and K. Wang, "Modeling of a Color-Separating Backlight with Internal Mirrors," *SID International Symposium Digest of Technical Papers*, Vol. XXXV, pp. 487-489, 2004.
64. D. K. G. de Boer, and H. J. Cornelissen, "Colour-separating Backlight Based on Surface-relief Grating," *Proceedings of Eurodisplay 2005*, pp. 236-239, 2005.
65. D. K. G. deBoer, R. Caputo, H. J. Cornelissen, C. M. van Heesch, E. J. Hornix, and M. J. J. Jak, "Diffractive Grating Structures for Colour-separating Backlights," *Proceedings of the SPIE Vol. 6196*, pp. 61960R-1 - 61960R-8, 2006.
66. R. Caputo, L. de Sio, M. J. J. Jak, E. J. Hornix, D. K. G. deBoer, and H. J. Cornelissen, "Short Period Holographic Structures for Backlight Display Applications," *Optics Express*, Vol. 15, No. 17, pp. 10540-10522, 2007.
67. E. Miyamoto, S. Maruyama, A. Nagano, L. M. Murillo-Mora, T. Toda, and F. Iwata, "Novel diffraction grating light guide for LED backlight," *Proceedings of the SPIE Vol. 6488*, p. 64880H-1-64880H-8, 2007.
68. S. R. Park, O. J. Kwon, D. Shin, S-H. Song, H-S. Lee, and H. Y. Choi, "Grating Micro-dot Patterned Light Guide Plates for LED Backlights," *Optics Express*, Vol. 15, no. 6, pp. 2888-2899, 2007.
69. K. Niu, Q. Tan, J. Zhu, Y. Zhang, and G. Jin, "Holographic Light-guide Plate for LCD Backlight System," *Proceedings of the SPIE Vol. 6832*, p. 683228-1 - 683228-8, 2007.
70. Y. Zhang, Q. Tan, Y. Yan, and G. Jin, "Talbot Grating for Color Separation in Color Liquid Crystal Display," *Proceedings of the SPIE Vol. 6832*, pp. 68320P-1 - 68320P-8, 2007.

71. M. J. J. Jak, R. Caputo, E. J. Hornix, L. de Sio, D. K. G. deBoer, and H. J. Cornelissen, "Color-separating Backlight for Improved LCD Efficiency," *JSID*, Vol. 16, No. 8, pp. 803-810, 2008.
72. Y. D. Yao, D. H. Wei, K. W. Chang, S. Y. Hsu, P. K. Wei, T. P. Lin, and C. N. Mo, "Light Plate with Metallic Nanostructures for Color Filterless Display," *Proceedings of the International Display Workshop 2008*, pp. 1695-1698, 2008.
73. J. Orava, T. Jääskeläinen, and J. Parkkinen, "Large Gamut Backlight for an LCD with Four Primaries," *Journal of Display Technology*, Vol. 6, No. 5, p. 170-177, 2010.
74. M. Parikka, T. Kaikuranta, P. Laakkonen, J. Lautanen, J. Tervo, M. Honkanen, and J. Turunen, "Deterministic Diffractive Diffusers for Displays," *Applied Optics*, Vol. 40, No. 14, pp. 2239-2246, 2001.
75. H. Y. Choi, M. G. Lee, J. H. Min, and J. S. Choi, "Hologram Based Light-Guide Plate for LCD-Backlights," *Proceedings of Asia Display/ International Display Workshop 2001*, pp. 521-524, 2001.
76. M. G. Lee, H. W. Choi, J. H. Min, J. S. Choi, J. H. Kim, and S. M. Lee, "Optical Characteristics of Holographic Light-guide Plate for LCD," *Proceedings of Eurodisplay 2002*, pp. 343-346, 2002.
77. J. H. Min, H. Y. Choi, M. G. Lee, J. S. Choi, J. H. Kim, and S. M. Lee, "Holographic Backlight Unit for Mobile LCD Devices," *JSID* Vol. 11, No. 4, pp. 653-657, 2003.
78. A. K. Aristov, V. V. Novosel'skii, G. B. Semenov, and T. V. Shchedrunova, "Holographic Diffraction Grating for Side Lighting of Liquid-crystal Displays," *J. Opt. Technol.* Vol. 70, No. 7, pp. 480-484, 2003.
79. D. Nesterenko, J. H. Min, and H. Y. Choi, "Design and Analysis of Tapered Waveguides as Collimators for LED Backlighting," *SID International Symposium Digest of Technical Papers*, Vol. XXXVI, pp. 1388-1391, 2005.

80. S.M. P. Blom, H. P. M. Huck, and H. J. Cornelissen, "Towards Polarised Light Emitting Back Lights: Micro-structured Anisotropic Layers," Proceedings of Asia Display/International Display Workshop 2001, pp. 525-528, 2001.
81. H. J. B. Jagt, H. J. Cornelissen, D. J. Broer, and C. W. M. Bastiaansen, "Linearly Polarized Light-emitting Backlight," JSID, Vol. 10, No. 1, pp. 107-112, 2002.
82. S. M. P. Blom, H. P. M. Huck, H. J. Cornelissen, and H. Greiner, "Towards a Polarized Light-emitting Backlight: Micro-structured Anisotropic Layers," JSID, Vol. 10, No. 3, pp. 209-213, 2002.
83. H. J. B. Jagt, H. J. Cornelissen, and D. J. Broer, "Micro-structured Polymeric Linearly Polarized Light Emitting Lightguide for LCD Illumination," SID International Symposium Digest of Technical Papers, Vol. XXXIII, pp. 1236-1239, 2002.
84. H. J. Cornelissen, H. P. M. Huck, D. J. Broer, S. J. Picken, C. W. M. Bastiaansen, E. Erdhuisen, and N. Maaskant, "Polarized Light LCD Backlight Based on Liquid Crystalline Polymer Film: A New Manufacturing Process," SID International Symposium Digest of Technical Papers, Vol. XXXV, pp. 1178-1180, 2004.
85. K.-W. Chien, H.-P. D. Shieh, and H. Cornelissen, "Polarized Backlight Based on Selective Total Internal Reflection at Microgrooves," Applied Optics, Vol. 43, No. 24, pp. 4672-4676, 2004.
86. K.-W. Chien and H.-P. D. Shieh, "Design and Fabrication of an Integrated Polarized Light Guide for Liquid-crystal-display Illumination," Applied Optics, Vol. 43, No. 9, pp. 1830-1834, 2004.
87. X. Yang, Y. Yan, and G. Jin, "Polarized Light-guide Plate for Liquid Crystal Display," Optics Express, Vol. 13, No. 21, pp. 8349-8356, 2005.
88. S. Hwang, Y.-T. Kim, S. Nam, and S.-D. Lee, "Highly efficient backlight unit with a Polarization-separating Anisotropic Layer," SID International Symposium Digest of Technical Papers, Vol. XXXVIII, pp. 476-479, 2007.

89. Y. Taira, D. Nakano, H. Numata, A. Nishikai, S. Ono, F. Yamada, M. Suzuki, M. Noguchi, R. Singh, and E. G. Colgan, "Low-power LCD Using a Novel Optical System," SID International Symposium Digest of Technical Papers, Vol. XXXIII, pp.1313-1315, 2002.
90. Y. Taira, D. Nakano, H. Numata, A. Nishikai, K. Sueoka, F. Yamada, M. Suzuki, M. Noguchi, R. Singh, and E. G. Colgan, "Illumination System for Color Filterless Liquid Crystal Display," Proceedings of Eurodisplay 2002, pp. 585-588, 2002.
91. F. Yamada, S. Ono, and Y. Taira, "Optical Components Directly Molded on the LCD Glass Substrate," SID International Symposium Digest of Technical Papers, pp.1042-1045, 2002.
92. F. Yamada, S. Ono, and Y. Taira, "Dual Layered Very Thin Flat Surface Micro Prism Array Directly Molded in an LCD cell," Proceedings of Eurodisplay 2002, pp. 339-342, 2002.
93. F. Yamada, H. Numata, and Y. Taira, "Multi-layered Flat-surface Micro-optical Components Directly Molded on an LCD panel," JSID, Vol. 11, No. 3, pp. 525-531, 2003.
94. J. Kimmel, T. Levola, P. Saarikko, and J. Bergquist, "A Novel Diffractive Backlight Concept for Mobile Displays," SID International Symposium Digest of Technical Papers, Vol. XXXVIII, pp. 42-45, 2007.
95. J. Kimmel, T. Levola, and P. Laakkonen, "Diffractive Backlight Grating Array for Mobile Displays," Digest of Eurodisplay 2007 (27th International Display Research Conference), pp. 171-174, 2007.
96. J. Kimmel and T. Levola, "Backlights in Mobile Display Power Management," SID International Symposium Digest of Technical Papers, Vol. XXXIX, pp. 1594-1597, 2008.
97. J. Kimmel and T. Levola, "Mobile Display Backlight Light Guide Plates Based on Slanted Grating Arrays," Proceedings of the SPIE, vol. 8065, pp. 806538-1 - 806538-9, 2011.

98. J. Kimmel and T. Levola, "Embedded Diffractive Backlight Light Guide Plates in Mobile Display Applications," Proceedings of Eurodisplay '11 (31st International Display Research Conference), Bordeaux, Paper 1-6, 2011.
99. T. Levola, "Diffractive Optics for Virtual Reality Displays," University of Joensuu, Department of Physics, Dissertations 47, 2005.
100. T. Levola, "Diffractive Optics for Virtual Reality Displays," Proceedings of Eurodisplay 2005, pp. 542-545, 2005.
101. T. Levola, "Diffractive Optics for Virtual Reality Displays," JSID, Vol. 14, No. 5, pp. 467-475, 2006.
102. T. Levola, "Novel Diffractive Optical Components for Near to Eye Displays," SID International Symposium Digest of Technical Papers, Vol. XXXVII, pp. 64-67, 2006.
103. T. Levola, "Compact See-through Near to Eye Display with Diffractive Optical Elements," Proc. IMID '07, paper 53-2, 2007.

Publications

Publication [P1]

J. Kimmel, "Diffractive Backlight Technologies for Mobile Applications," JSID, Vol. 20, No. 5, pp. 245-258, 2012.

Copyright © 2012 Society for Information Display.
Reprinted with permission.

Review Paper: Diffractive backlight technologies for mobile applications

Jyrki Kimmel (SID Senior Member)

Abstract — Liquid-crystal-display backlight units have developed in their conventional configuration into very efficient and uniform components that allow the display to present a high-quality image to the user. Developing the backlight unit itself further faces a challenge of diminishing returns to the investment in innovation. A system-level redesign is required for the entire display module, and diffractive alternatives to the backlight design can allow a more-energy-efficient design for the display. This review concentrates on small-to-medium displays because diffractive backlight studies have also centered in this class of displays. The state of the art of backlight design is summarized and the motivation for energy-efficient system design is outlined. The theoretical basis of diffractive backlights is given, and key research studies in the area of diffractive backlights are reviewed. Finally, a discussion on the performance and future outlook of diffractive backlights completes the paper.

Keywords — Active-matrix liquid-crystal display (AMLCD), mobile display, backlight unit (BLU), diffractive optics, diffractive backlight.

DOI # 10.1889/JSID20.5.245

1 Introduction

High-quality multimedia is becoming one of the main use cases for mobile communication devices. As the capability of mobile and broadband networks to deliver data into the terminal increases, the demand for display resolution, contrast, brightness, and color gamut approaches that of a personal-computer monitor or a flat-panel television, in terms of the user experience.¹ Recent simulated tests on mobile-display color-space acceptance show that the test subjects rated the saturation of red and green primaries optimal at 90% of the European Broadcasting Union (EBU) specification and blue at 70% of the EBU gamut. There is room for improvement, especially in reflective mobile designs, to be acceptable to the general public.² In another study it was found that test subjects preferred higher color gamuts to increased luminance in images rendered on mobile displays³ (in general, light sources and displays with higher chroma, *i.e.*, colorfulness, appear brighter due to the Helmholtz–Kohlrausch effect⁴). These results clearly indicate that the image-quality issues in mobile devices are important to consumers. Taking into account the ambient lighting environment where the device is used adds another level of difficulty in mobile-display design. Other demands with regard to mobile terminals constrain the mechanical design of the display, as the mobile device stays small in its outer dimensions to remain “pocketable.”⁵

Current mobile-phone displays are most often liquid-crystal displays (LCDs). The LCD backlight plays an important role in generating and delivering the light of the display to the user. All LCDs in mobile phones use a backlight, as the displays are either transmissive or transreflective. The need to save energy has become an important aspect in mobile-device design. It has been estimated that the user interface is responsible for about a third of the power dissipation

on a mobile phone,⁶ and of the user interface (UI) components, the display backlight unit (BLU) consumes the most of the available power in portable devices.^{7,8} Similarly, in notebook computers, it is estimated that the display subsystem consumes about 30% of the power,⁹ and generally in portable devices, the LCD module is responsible for more than 50% of the total energy consumption.⁸ It is therefore important to attempt to reduce the power dissipation of the display by designing efficient BLUs and LCD systems. Other approaches to realize energy-saving mobile displays are in developing field-sequential LCDs (FSLCDs), where instead of using color filters, color-primary light-emitting diodes (LEDs) are flashed individually within each video frame to form an image that is temporally integrated by the visual system.^{10,11} FSLCDs require fast LCD mixtures, and the temperature sensitivity of the LCD can be a problem when driving the display at fast frame rates in low ambient temperature.

Recently, steps have been taken to radically redesign the BLU to direct the appropriate band of the visible spectrum through the LCD subpixel matrix by using diffractive optics.¹⁰ In addition to the energy-saving aspect of this design approach, developers of diffractive backlights foresee the elimination of currently integral LCD color-filter arrays as well as beam-shaping films to offset the added cost of using diffractive optics instead of conventional scattering and reflecting light-guide-plate (LGP) structures in novel mobile display systems.

Backlights based on diffractive optics could be developed with the goal of extending the technology to large, mainstream flat-panel displays as well, but thus far the demonstrated size range of diffractive backlights has remained appropriate only for mobile or portable displays. The reason for this may be that manufacturing large diffractive grating

Received 11-27-11; accepted 3-20-12.

The author is with Nokia Research Center, Media Technologies Laboratory, P.O. Box 1000, Visiokatu 1, Tampere, 33721 Finland; telephone +358-504-835-484, e-mail: jyrki.kimmel@nokia.com.

© Copyright 2012 Society for Information Display 1071-0922/12/2005-0245\$1.00.

masters is expensive and time consuming. Thus, the scope of this review is limited to diffractive backlights for mobile and portable displays.

This paper gives an overview of backlight technology used in mobile devices, discusses the theory of diffractive BLUs, and gives a review of work done in the advancement of diffractive optics for BLUs. Further, the state of the art and future directions in diffractive backlights are discussed, and conclusions are given on the work performed thus far and on what direction the research in this field should take.

2 State of the art in mobile-display backlights

The development of mobile backlights began from the need to illuminate the LCD for the user of a mobile telephone to see the dialed number, as the mobile phone was starting to be used in various levels of ambient illumination.^{1,12} This function could be realized with light-emitting-diode (LED) displays and simple monochrome LCDs.^{12,13} Backlights for these LCDs frequently used electroluminescent foils and LEDs.¹³ The earliest LCD-backlight light-guide plates (LGP) were edge-lit roughened pieces of transparent polymer that scattered the light from LEDs placed on the sides of the LGP.^{14,15} As the legibility of the display suffered outdoors from the specular glare from the sun, holographic films were developed to divert the glare from the direction of the user, especially in reflective mobile displays.¹⁶

With the advent of mobile color supertwist-nematic (CSTN) LCDs in around 1998, and with the emergence of active-matrix LCDs (AMLCDs) a few years later, a need arose for more advanced backlights in mobile displays.⁵ White (or pseudo-white) LEDs were necessary and LGP structures aimed at providing an efficient and uniform out-coupling of light from the white LEDs that were used as light sources to replace the previously applied green or amber LEDs. Concurrently, brightness-enhancing film (BEF) stacks such as prism sheets and reflecting polarizer films were being developed to control the output angular distribution and polarization of light in mobile displays.¹⁷ In the conventional display structure shown in Fig. 1, light is

launched into a LGP that confines the light by total internal reflection (TIR). The TIR condition is perturbed by the out-coupling structure, and light escapes the LGP. The diffuser distributes the light so that the outward appearance of the outcoupling structure on the LGP is masked, and the BEF films collimate the light through the LC glass. An LCD has its optimal response at the normal viewing direction, and away from this direction there usually can be found viewing artifacts that are a result of non-ideal electrooptic polarization response at oblique viewing angles. The polarizers and the compensation films account for tailoring the LC electrooptical response so that the user ideally sees a uniform image with acceptable color gamut, contrast, and viewing angle.

The LGP structures began to employ V-groove patterns or printed scattering dot patterns on one side of the LGP.^{13,18} Very good uniformity has been achieved by applying these design principles in scattering-based LGPs, but thick diffuser sheets are required to hide the macroscopic scattering centers from causing visible artifacts in the displayed image. Highly scattering polymer LGPs were proposed as an alternative design by A. Tagaya *et al.*,⁸ with twice the brightness of a conventional scattering-based backlight, and at the same time, in a thinner LGP with a smaller number of light-management films. In a similar fashion, microreflector structures have been employed in LGP design, which gives a more controlled output distribution for the light as well as better system efficiency due to the application of thin diffuser sheets in conjunction with microreflector-based LGPs.^{18–22} These structures have also been distributed throughout the LGP by designs that apply statistical means for the distribution of these structures throughout the LGP.²³

With the demand for thinner display modules, many of the separate functions of the optical films in mobile display modules have been integrated as hybrid films with combined functionality.^{24,25} This development has led to demonstrated mobile-display modules below 1 mm in total thickness.²⁶ Concurrently with eliminating the prism sheets and diffusers, highly efficient structures for LGPs have been realized by S. Aoyama, A. Funamoto, and co-workers, who have demonstrated designs for small displays with only one

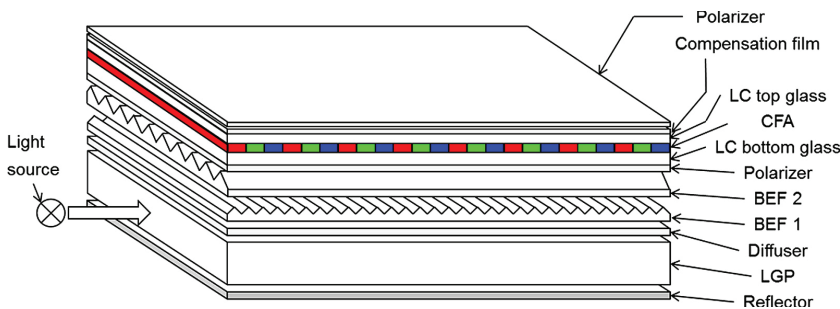


FIGURE 1 — Standard mobile-display structure (not to scale). The outcoupling extractors are situated either on the top or on the bottom of the LGP (or on both surfaces).

white LED light source consisting of one or two bare LED chips.^{27–29} These designs use small “normal-reverse prism structures” or hybrid prism couplers (HPCs)²⁸ with height and width in tens of micrometers to direct the light from the one light source toward the LCD. The diffuser sheet could also be eliminated in their design because the extractor features and their separation were below human visual acuity limit for a normal display viewing distance.

Mobile-display backlights today are thus thin, efficient, uniform, and provide good image quality to the user at least in office and home lighting conditions and are simple to manufacture and to integrate in a display module by stacking the appropriate films together with the LGP and display glass. Coupled with current LCD designs, however, the system-level efficiency leaves room for improvement in the way that light is coupled through the LCD matrix. Currently, it is estimated that using white LEDs as light sources, less than 10% of the light from the LEDs is available to the user to provide the image on the display.²⁶ Therefore, to improve the system efficiency, system level issues must be addressed in light management. One possible solution is to direct the appropriate primary bands of light to the respective subpixels instead of using color filters. Diffractive optics thus presents an alternative way to approach the light management in the displays, due to the inherent color-separation function in diffraction. Previously, holographically recorded films and diffractive components have been used in or proposed for transmissive and reflective LCDs, for instance, as holographic diffusers,^{30–33} antireflection coatings,³¹ and input couplers.^{34,35} Holographic polymer-dispersed LCDs can also be regarded as diffractive.³⁶ The newest developments offer a way to use diffraction gratings to directly couple out the light from the LGP through the display matrix to the user.

3 Principles of diffractive backlight units

Diffractive outcoupling in backlights serves many purposes, and the use of diffractive structures presents several advantages over conventional backlights.¹⁵ An expected increase in system efficiency is combined with ease of fabrication of a replicated subwavelength structure, and as the features of the outcoupling structure are very small, diffusers are not required below the LCD. The precisely controlled outcoupling efficiency with a continuous or modulated diffraction pattern means that a highly uniform backlight can be designed. In addition, the high directivity of outcoupling removes the need of redirecting films.¹⁵ The ultimate goal is to separate the individual primary spectral bands of light spatially, in order to direct these bands through the primary-specific subpixels in the color LCD array. H. Dammann separated color bands, for imaging applications, with a sandwich grating structure.³⁷ In displays, such separation of color bands means that there is potential to remove the color-filter array from the LCD structure altogether, allowing for higher system efficiency. In addition, due to the highly directive

nature of diffracted orders of light from the diffraction grating, additional collimating films may not be required. There are drawbacks in diffractive grating designs that are based on one single grating that spans the entire extent of the LGP. First, a lenticular lens or a microlens array is mandatory to direct the light through the subpixel array. Secondly, also mirrors are required to redirect the reflected diffraction orders toward the display glass. Recently, solutions have been demonstrated to overcome these issues by making a wholly pixelated array of gratings, resulting in a subpixel-specific grating array precisely aligned with the overlaying display. These studies have been reviewed in Sec. 4.

The analysis of diffractive grating backlights involves the entire path of light, starting from the light sources and ending with the perception and synthesis of the information as compiled by the human visual system. The essential physics of the diffractive backlights is centered on the analysis of the grating structures. The gratings are generally situated on an interface of two materials, where light enters from material 1 with refractive index n_1 and is transmitted toward material 2 with refractive index n_2 . Let us call this interface the grating surface. If θ_i is the angle of incidence and θ_m is the diffracted angle of diffraction order m , with respect to the surface normal of the grating surface, and φ_i is the incident and φ_m is the diffracted azimuthal angle of the light with wavelength λ , the conical diffraction equations for a grating with a period between the grooves d are³⁸

$$\begin{cases} n_2 \sin \theta_m \sin \varphi_m = n_1 \sin \theta_i \sin \varphi_i \\ n_2 \sin \theta_m \cos \varphi_m = n_1 \sin \theta_i \cos \varphi_i + m\lambda/d \end{cases} \quad (1)$$

The geometry of the conical diffraction problem is shown in Fig. 2. From Eq. (1), it can be seen that light entering the grating surface exits the surface in different directions, depending on the wavelength λ of the light source and the grating period d .

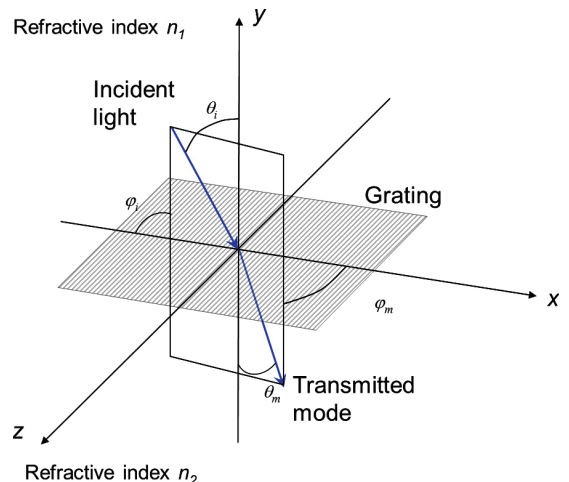


FIGURE 2 — Geometry of the conical diffraction problem (after Ref. 44).

Diffractive backlights usually have a LGP made of transparent polymer, with light sources outside the LGP. Using conventional terminology of waveguide optics, the input angles of the LGP are determined by the TIR condition of the LGP material ($n_1 > 1$) and its surrounding medium, usually air ($n_2 = 1$). The TIR condition arises from the definition of the critical angle of refraction of light $\theta_c = \theta_i = \arcsin(n_2/n_1)$. The range of angles of incidence of the incoming light to the grating is in this case determined by the acceptance angle at the input surface of the LGP and by the total internal reflection condition (critical angle) at the grating surface:

$$\arcsin(n_2/n_1) < \theta_i \leq 90^\circ. \quad (2)$$

Usually, the LGP material is a transparent polymer such as poly(methyl) methacrylate (PMMA, $n_1 = 1.49$), polycarbonate (PC, $n_1 = 1.58$), or in some cases, glass or a high-refractive-index polymer (n_1 ranges approximately from 1.5 to 2.2). The range of angles of incidence is therefore usually from about 40 to 90°, and by using Eq. (1) we obtain the outcoupled angles of diffraction:

$$\begin{cases} \tan \phi_m = \frac{\sin \theta_i \sin \phi_i}{\sin \theta_i \cos \phi_i + m\lambda/nd} \\ \sin \theta_m = \sqrt{n^2 \sin^2 \theta_i \sin^2 \phi_i + (n \sin \theta_i \cos \phi_i + m\lambda/d)^2} \end{cases}, \quad (3)$$

where n_1 is now denoted with n and material 2 is now air, with refractive index 1. In the general case, the intensity distribution of light among the diffracted orders depends on the actual geometry of the grating lines.

Commonly, in LGP design, the desired state is to direct the outcoupled light toward the normal of the surface ($\theta_m = 90^\circ$) in order to obtain the best efficiency of the display system and also the best user experience. The first approximation to start the design is to only use the classical grating equation,

$$d(\sin \theta_m + \sin \theta_i) = m\lambda, \quad (4)$$

and to limit the diffracted orders to $m = 1$ and $m = -1$. The remaining design question is to select the optimum wavelength, which obviously is in the visible range ($400 < \lambda < 700$ nm). Taking these constraints in account, the grating period should be in the range of 200–426 nm (for instance, by using Eq. (4), for $\theta_i = 60^\circ$ and $\lambda = 500$ nm, the design value for the grating period $d = 268$ nm).

Practical light sources for displays, such as LEDs today, are not collimated. Rather, they frequently exhibit Lambertian emission characteristics. This means that the conical grating equation [Eq. (1)] must be used together with the output distribution of the light source, at every point on the grating surface, to be able to accurately model the properties of the backlight LGP.

T. Levola has analyzed grating systems in planar incoupling and outcoupling for several optical systems, including near-to-eye displays (NEDs)^{39–43} and, with co-workers, backlight LGPs.^{44–48} For general grating profiles, he has

developed a simulation tool based on the coordinate transformation method (C-method, or Chandezon method) based on rigorous diffraction theory.^{49,50} The studies of planar waveguiding NED optics^{41,42} show that for a diffractive system it is advantageous to use a high-refractive-index waveguide material with n approaching 2. More importantly, it has been shown that slanted gratings can produce a high coupling efficiency for a single transmitted order, up to 98%.⁴³ Therefore, in diffractive backlights, solutions that combine both a high-refractive-index substrate and slanted gratings can result in high-quality systems that have a great potential in achieving the design goal of accurately delivered spectrally separated light toward the LCD. T. Levola and P. Laakkonen, in fact, present an ultraviolet (UV)-embossing technique where slanted gratings can be repeatedly replicated from a fused silica master on episulfide polymer waveguides.⁵¹ This approach has been extended to diffractive backlights as well.^{47,48}

The application of rigorous diffraction theory is a demanding task, and numerical methods are often used to calculate fields that have complex boundary conditions. M. Xu *et al.* have used finite-element modeling (FEM) in simulation studies of polarizing color-separating backlights,⁵² and found good agreement with experiments. The conical diffraction case has been analyzed for a diffraction grating with an anisotropic material overlay to separate polarization as well as the primary colors. The advantage of using FEM in this case is in that the anisotropy of the birefringent layer can relatively easily be incorporated in the material mesh model of the problem at hand. The $m = -1$ diffraction order is coupled out and the polarization contrast is evaluated. The s -polarization is transmitted, and the almost negligible contribution of the p -polarization is attributed to the refractive-index mismatch between the modeled substrate and the ordinary axis of the LC polymer.⁵²

In summary, a diffractive backlight should be manufactured on a high-refractive-index material. Also, the grating period should be subwavelength, and the grating profile asymmetric, in order to couple out only one desired diffraction order and to suppress all other but the zeroth (reflected) diffraction order. Since it has been found that subwavelength gratings can be polarization sensitive,⁵³ an added benefit for diffractive LCD backlights would be to design the system in such a way that the gratings only diffract out one polarized state. These design principles would allow for improved system efficiency for an LCD, as the light would be directed to the subpixels where they actually are required, with the desired polarization state and outcoupled spectral band. Compared to the conventional LCD system, the efficiency improvement would in principle be threefold because the spatial arrangement of the color-filter array (CFA) blocks two-thirds of the incoming light. Furthermore, if a pixelated approach could be used where the light only enters the active aperture of each subpixel, another factor of 1.5–2 improvement would be expected since the transmissive aperture in mobile displays is only about

30–50% of the total area of a given subpixel. Total efficiency improvement in employing a pixelated diffractive array approach could be therefore 4.5–6 times over the conventional LCD system approach, not even taking into account the material losses commonly associated with the LCD color-filter array.

4 State of the art of diffractive backlights

Diffractive backlight designs have been demonstrated in the last few years by many research groups both in the academia and in the industry. This section reviews the state of the art in diffractive-backlight research literature. It is organized in subsections that focus on developments that can be categorized in advances in polarizing backlights, uniform and modulated grating-based solutions, constant-pitch grating array solutions, and fully pixelated grating array designs with variable pitch.

4.1 Polarizing backlights based on grooved and diffractive structures

The purpose of polarizing backlights is to extract only the preferred polarization of the light to be utilized by the LCD. The unwanted polarization inside the LGP is recycled, converting the polarization state of the recycled light in the process to become the desired state of polarization for the LCD.^{54,55} Potentially, a gain of two over a non-polarized LGP could be achieved by using a polarized backlight, and if the polarization contrast is high enough, the back polarizer

could be left off the LCD design.⁵⁶ Figure 3(a) presents the general principle of a display with a polarizing backlight. In the figure, *s*-polarization is coupled out, but some designs couple out the *p*-polarization instead. The aim is to completely reflect the unwanted polarization back into the LGP, and to progressively recycle the light into the desired polarization for outcoupling. Recycling has been achieved or proposed by retardation layers on one face of the LGP and by using depolarizing end reflectors as well as a combination of quarter-wave plates and specular reflectors.⁵⁵ The result of using polarization extraction and recycling is that the system efficiency of the LCD module is improved by the degree of polarization recycling efficiency. A pre-aligned liquid-crystal layer has been applied on a microgroove-patterned LGP, with birefringent outcoupling of the *s*-polarization by S. M. P. Blom *et al.*⁵⁴ and H. J. B. Jagt *et al.*⁵⁵ at Philips Research. A local polarization contrast of 15 has been achieved. The imperfect uniformity of this approach⁵⁵ has been improved by the same group by filling LGP microgroove structures with an anisotropic LC polymer, and a polarization contrast of above 100 has been achieved by this approach.^{56,57} In this approach, simulations show that with proper groove shape and extended material anisotropy, light could be directed effectively toward the user. The experimental result shows that the light is directed approximately 30° off the normal of the LGP.⁵⁶ By using efficient polarizing backlights, the back polarizer and light-shaping films of an LCD module can be removed, leading to the construction of a thinner display module, as depicted in Fig. 3(b).⁵⁸ Continuing the work in Refs. 56 and 57, an improved structure was made by using a periodic relief on the LGP instead of a groove structure. A

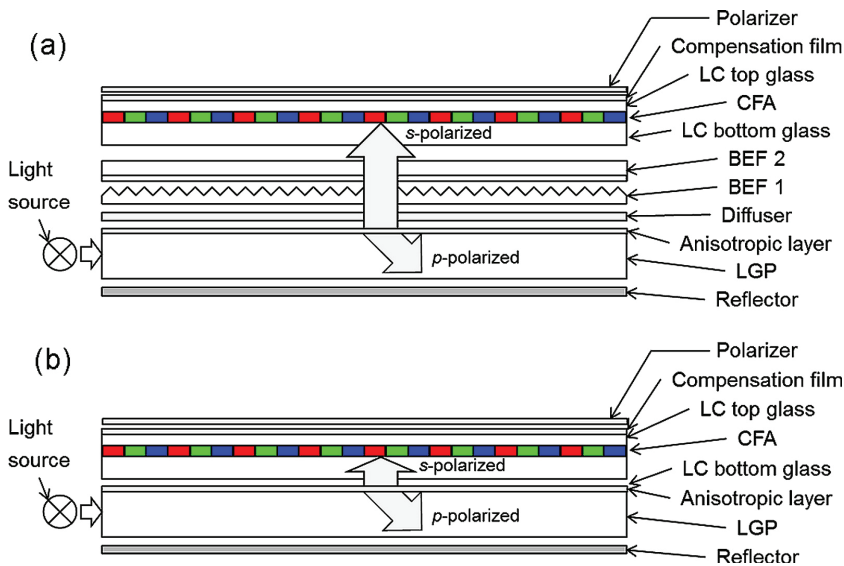


FIGURE 3 — (a) General principle of a display with a polarizing backlight (not to scale). Instead of the back polarizer, an anisotropic layer has been added to the top of the LGP; (b) polarizing backlight without brightness-enhancing films.

gain (increase of desired polarization state over the non-polarized case) of 1.78 was measured over a non-polarized LGP.⁵⁸ Using stretched polyethylene naphthalate (PEN) films as the anisotropic medium adhered to PMMA foil, a polarization gain factor of 1.6 was achieved by K.-W. Chien and co-workers in a similar experiment.⁵⁹ S. Hwang *et al.* used an asymmetric dual prism microstructure made by hot embossing on a uniaxially stretched polyethylene terephthalate (PET) layer.⁶⁰ They report a 30% increase in efficiency over a reflective polarizer backlight, but from the results it is evident that the total polarization contrast (ratio of the outcoupled *s*-polarized light over the outcoupled *p*-polarized light) could be improved by using a more advanced outcoupling structure.

A grating-based approach for polarizing backlights was demonstrated by K.-W. Chien and H.-P. D. Shieh.⁶¹ A microstructured LGP was equipped with a subwavelength binary grating on the top substrate. The slot structure was modulated by a gradient in the density of slots to achieve good uniformity across the LGP. The subwavelength grating operated as a form birefringent layer which presents a different effective refractive index for the *s*-polarized and *p*-polarized components of incident light. A multilayered structure was implemented in order to broaden the wavelength response, which in a non-layered design was poor for the blue end of the visible spectrum. A polarization gain factor of 1.7 was achieved.⁶¹ Another subwavelength grating approach was proposed by X. Yang *et al.*⁶² In this theoretical simulation, a stress-induced birefringence LGP was used as the polarization converter, and a subwavelength Al grating with a 140-nm period was to be fabricated on the top surface. Further control of incident angles was to be achieved by

a microgroove pattern on the bottom surface. As expected, this theoretical study showed a twofold improvement in out-coupling efficiency over a conventional backlight.

4.2 Diffractive backlights based on constant or variable pitch gratings

Before color displays became popular in mobile displays, already monochrome diffractive solutions to the LGP were being sought, as evidenced by the pioneering work by M. Parikka *et al.*¹⁵ This research was done in order to get rid of scattering-based LGPs and the associated beam-shaping foils. Uniform outcoupling (attenuation of the illumination was 20% longitudinally, and “nearly perfect” in transverse direction) was achieved by utilizing a grating pattern that spreads the light from the light sources using a distribution of gratings in conical incidence. Light was coupled out from the gratings that were oriented at a normal to the incoming beam of light. The gratings were manufactured on a master by electron-beam lithography and then replicated by hot embossing on a PMMA substrate, with a period of 2 μm. Chromatic dispersion of outcoupled light was seen to be a potential problem when light sources with additional spectral peaks, such as pseudo-white LEDs, were to be used. Figure 4(a) presents the general principle of a display with a diffractive backlight, where the purpose of the diffractive structure is only to direct the light out without regard to color separation. Figure 4(b) shows a display with a diffractive color-separating backlight. A lenticular lens array is now added to redirect the color-separated light beams into the respective subpixels.

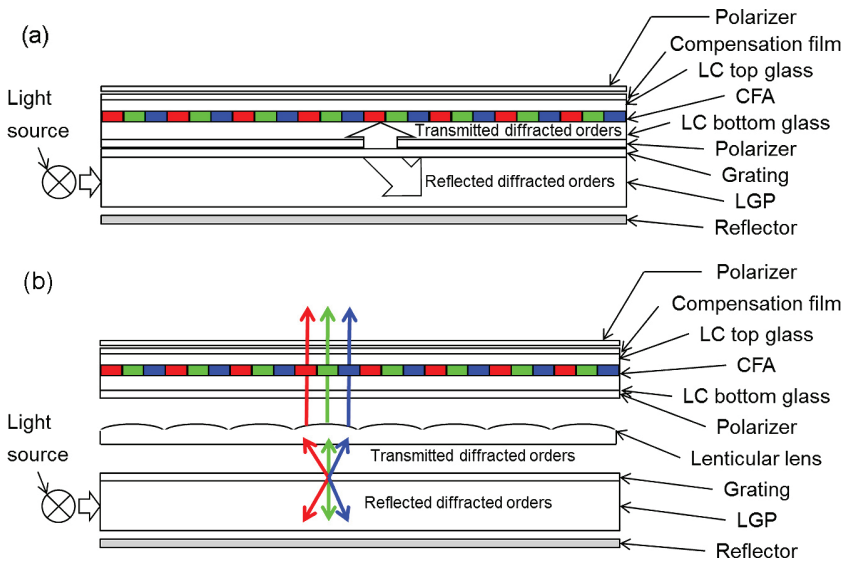


FIGURE 4 — (a) General principle of a display with a non-color separating diffractive backlight; (b) color-separating diffractive backlight display. Not to scale.

H. Y. Choi and co-workers proposed a backlight light-guide with a holographic grating at the bottom to diffractively couple the light out toward the top.⁶³ They suggest that by this arrangement, several optical films can be left out of conventional backlight modules, including prism sheets and a diffuser. They utilize a grating with a difference in the outcoupling polarization state to enhance the proportion of the desired state of polarization in the outcoupled light. The grating periods used in the experimentally manufactured sinusoidal gratings were 360 and 450 nm, and it was found that the light distribution in outcoupling was directed at normal to the LGP using the 450-nm grating period. A cold-cathode fluorescent lamp (CCFL) light source was used, but no mention is given on the color performance of this backlight design. The theoretical analysis was expanded and a mirror was added to the end of the waveguide.⁶⁴ The use of this inclined mirror enhanced the outcoupled intensity by 50%. Another similar structure, with the grating now at the top of the LGP, was later shown.⁶⁵ Here, an integrated collimation structure was fabricated near the light sources on the LGP itself. Improved outcoupling was observed. The results were averaged over the relevant wavelength bands, but no comment was given regarding the color performance of the backlight. An improved collimation structure based on a waveguiding section was reported in Ref. 66. The output luminance was improved by roughly a third.

K. Aristov *et al.* reported a similar idea but with a wedge light guide and a holographic grating on the bottom side.⁶⁷ Special emphasis was expended on ensuring good uniformity of illumination. A scattering foil was used on top of the LGP to achieve adequate color mixing. Contact replication was used in manufacturing a 55×45 mm test piece from the holographically manufactured master. Grating period and reflectance were varied along the wedge to achieve the desired degree of uniformity. The uniformity for green light was 83% but worse for blue and red. The experimental results show narrower illumination cones and less overall light flux than for a conventional display system. The authors comment that a slab LGP might be better to increase the efficiency of the system. As a solution to the observed spectral dependence, the authors suggest placing the light sources at both ends of the LGP and modulating the outcoupling efficiency of the gratings so that the center of the LGP has maximum outcoupling efficiency.

Y. Taira and co-workers were the first to demonstrate a color-filterless display using a diffractive color-separating array on a backlight wedge.⁶⁸ The grating was a uniform blazed grating with 530-nm pitch, directing the green band of a CCFL light source toward the normal of the wedge top surface. A 13.3-in. XGA display without color filters was used as the demonstrator display, with a 264- μ m pixel pitch (88 μ m between subpixel centers). The authors suggest that using LEDs as light sources would provide better color purity. Light-source collimation is regarded as a possible improvement in the design, although the collimation for a CCFL was achieved by a separate illuminator design.⁶⁸ A

diffuser on top of the display completed the design, allowing for a viewing angle up to 20° in both horizontal and vertical directions. LEDs in place of the CCFL light source were demonstrated in a similar display demonstrator in Ref. 69; however, the effect of this improvement is not quantified in the paper. The viewing-angle dependence of the diffractive color separation was compensated in a test structure by molding a prism array on a black-matrix glass substrate using the photopolymer (2P) molding technique^{70–72} on top of the bottom polarizer. This array directed the subpixel-specific bands of primary components of the CCFL spectrum orthogonally through the subpixel array.⁷¹

A surface-relief grating combined with a birefringent coating was demonstrated as a color-separating polarizing backlight LGP by D. K. G. de Boer and H. Cornelissen.⁷³ This structure employed both the polarizing and color-separating properties of a uniform grating in a single component. A sinusoidal grating with a period of 400 nm and groove depth of 140 nm was fabricated on polycarbonate (PC). This grating was applied on a PMMA LGP. A liquid-crystal mixture and LC polymer were used as the birefringent material, and the achieved polarization contrast was 23 at the maximum. The authors believe that with this arrangement a color filter is still necessary in the display matrix, and that an additional mirror can be used to redirect the reflected diffraction orders toward the viewer. In a related work, de Boer and co-workers state that the masters for grating structures can be manufactured by electron-beam lithography or by laser interferometric techniques. The gratings can then be replicated on the LGPs by embossing or by direct laser interferometry by using a suitable photosensitive material.⁷⁴ Small samples (laser interferometrically exposed area was 20 mm²) up to 300 nm deep were characterized optically and found to conform to outcoupling characteristics obtained by software simulations quite well.

A new pixel structure, based on the earlier work,^{73–75} was adopted by M. J. J. Jak *et al.*⁷⁶ Since the light output of a diffractive backlight can be improved by illuminating the LGP from both ends of the waveguide in the uniform grating arrangement, the subpixel array needs to be symmetric with respect to the output spectra of the diffracted orders of the primary-color bands of light. If, instead of directing the green light out normally to the face of the LGP, blue is coupled out at the zero inclination angle, green and red bands of light can be symmetrically coupled out from both sides of the blue emission. This requires a repeating RGBG array for the subpixels, as is shown in Fig. 5. The grating is shorter in period (320 nm) compared to the previous work.^{73,74} Again, a lenticular lens array is proposed to couple the light out to the subpixel array retaining similar viewing characteristics for all colors. R. Caputo and co-workers from the same group earlier presented a grating structure with a short grating period, <500 nm, stating that the near or subwavelength regime is a requirement for a single diffraction order to exist in the transmissive and reflective first-order modes.⁷⁵ For the reflected first order, a mirror at the back face of the LGP

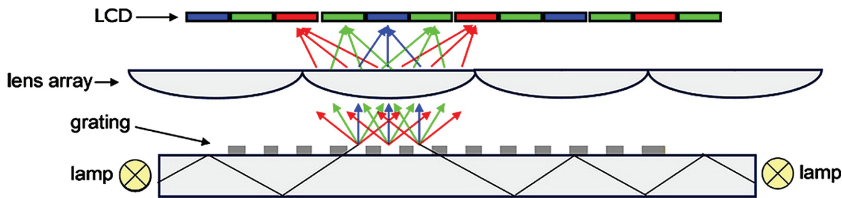


FIGURE 5 — The RGB subpixel structure of a symmetrically illuminated diffractive backlight.⁷⁶

was suggested to recycle the light back toward the LGP. The recycled light would, by the reciprocity principle, couple back into the original propagation direction of the light under TIR conditions, and on a further diffraction be available for outcoupling in the transmitted first-order diffraction. The RGB pixel array and lenticular lens arrays again were required for verification of the theoretical calculations. The color space obtained in this study lacked in gamut as some of the red and green spectra overlapped. The study by Jak *et al.*⁷⁶ improved the situation in this respect. RGB LEDs were used instead of a CCFL. The gratings were 210 nm deep with a 320-nm pitch. The authors state that deeper gratings would give better outcoupling efficiency, but they would be more difficult to fabricate. They also mention that further optimization is required and that a gain of three in efficiency is then expected.

Another direction in research is to design grating arrays that do not separate the colors, as the gratings are only used to redirect the light.^{77–79} In this sense, the grating arrays replace the function of the scattering centers or microreflectors of conventional backlight LGPs. The advantages of this approach relate to the reduction of components in the backlight module. Miyamoto *et al.* have designed a 2.4-in. mobile-phone display LGP that has on its bottom face a distribution of gratings that has a number of different grating periods in order to achieve a thin LGP with good uniformity and small spectral dependence.⁷⁷ Electron-beam patterning was used in making the master of the grating pattern. The uniformity of the LGP was optimized by distributing the gratings in a statistically simulated pattern and by using a “directional diffuser” structure that occupies the space in between the individual gratings. A prism sheet was required for equivalent illumination efficiency as with a conventional LGP. S. R. Park and co-workers presented a similar idea with depth modulation in the grating pattern instead of area modulation.⁷⁸ Only one LED was required to illuminate a 30 × 40 mm test LGP. UV-embossed sinusoidal 394-nm-period gratings from holographic microdot masters were used in this study on a PC LGP that was fabricated by ultraviolet (UV) embossing from a master. The sidewalls of the LGP were reflection-coated by aluminum sheets, giving rise to “virtual light sources” that were effectively used with suitably oriented grating microdots so that efficient directional outcoupling with about 62% uniformity (85% simulated; differences were attributed to various manufacturing issues of the prototype) could be achieved.

K. Niu *et al.* proposed a holographic LGP that used a distribution of light sources and rather steep-angle wedges.⁷⁹ A holographic pattern of an optical component was recorded on the bottom of each constituent wedge, and as the hologram was reconstructed the reference beam was directed toward the prospective LCD. The study was done for a 632-nm wavelength, and the authors do not comment on the use of this backlight for a full-color display.

4.3 Diffractive color-separating backlights based on single-type array gratings

The uniform grating approach does not accurately position the outcoupling grating with respect to the subpixel array, requiring a high numerical aperture of the lenticular lens array to confine the spectrally separated color bands to the appropriate subpixels in the LCD glass.^{75,76} Therefore, better registration between the backlight and the LCD matrices is required, and this can be achieved by making grating arrays that correspond exactly to the LCD that is intended to be used in conjunction with the designed LGP. These are termed single-type array gratings.

D. R. Selviah and K. Wang from the University College London proposed a pixel array in place of a uniform grating.⁸⁰ The modeling study incorporated also a micro-mirror array beneath the array of outcoupling gratings, at a 10- μm depth, right below the grating array. Figure 6 shows a schematic of the simulated model. The micromirrors were 160 μm wide, based on the modeling optimization. A cylindrical lenticular array was designed to direct the light toward the LCD subpixel array. All the constituent components were assumed to be registered with each other, making this study the first of the kind where the pixel grating array was subpixel-specific. Prospective display properties were not modeled in the study, and no experimental results are available.

Y. Zhang and co-workers propose, in another simulation study, a three-level Talbot grating for LCD color separation.⁸¹ The simulation achieves 85% system efficiency, and the authors remark that compared to the conventional LCD system efficiency of 5%, the improvement could be dramatic. The simulation still shows color mixing at the subpixel level, and the authors suggest leaving the color-filter array in place in the LCD if this type of diffractive LGP is applied in a real LCD.

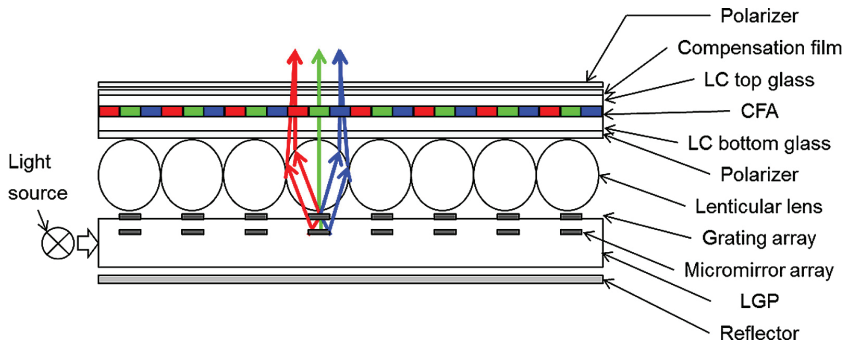


FIGURE 6 — Principal view of the simulated pixelated diffractive backlight display system (after Ref. 80). Not to scale.

J. Orava and co-workers present a four-primary diffractive backlight prototype⁸² where a distribution of gratings was fabricated on a 1-mm-thick PMMA plate and the gratings with a blazed profile were ultraviolet embossed on a 20- μ m plastic layer on the bottom of the LGP. The dimensions of the gratings were large with an 8- μ m period and 5- μ m height, and the authors comment that they could be considered as microprisms as well. In this 50 \times 50 pixel array, an area modulation scheme was implemented to improve uniformity, and each subpixel grating was therefore of different size except in the very center of the LGP. White balance in the center was good, but toward each of the light sources, color differences were observed.

4.4 Pixelated diffractive grating arrays for backlights

Both the uniform grating design and the single-type grating-based approach require complicated microstructures to be fabricated both on top, and sometimes, within the waveguide. In addition, if a reflector is applied at the end of the LGP, or light sources are applied at both ends of the LGP, a complicated, non-standard subpixel structure is necessary for good color separation. Bearing these difficulties in mind, Kimmel *et al.* have demonstrated diffractive grating arrays based on a new pixelated concept.^{44–48,83–87} The basic principle of the concept is shown schematically in Fig. 7. The all-diffractive approach is based on individual red, green, and blue LEDs as light sources, and uniform spreading of light from the LEDs through fanout structures on the sides of the LGP along the main grating array. The light is then coupled out of the LGP toward the active area of the display.

In the first study,^{44,45} a 1 \times 1-cm demonstrator grating array was fabricated by UV-curing SK-9 on a PMMA substrate. The grating array was a binary one, with one striped grating structure for each “green” subpixel, and another for “blue” and “red” subpixels. The “green” grating lines were perpendicular to the “red and blue” ones, and light was launched into the substrate also orthogonally, green from one side, and red and blue at right angles to the green

propagation of light. Side-emitting Osram LEDs were used as light sources. As the orthogonal coupling makes the light enter the grating arrays perpendicular to the grating lines only for the intended spectral band of light, the light is not affected by the orthogonal, unwanted array. The results were shown in the form of polar contrast plots, as the light outcoupling was analyzed by using an Eldim conoscope. It was clearly visible in the results that the green and blue light outcoupling was directed toward the user. As expected, the red outcoupling occurred at an angle of 60°, which was the limit of detection for the conoscope. By examining the outcoupling under a microscope, it was seen that the light was outcoupled separately as green and blue from the respective grating areas for these primary colors. In this experiment, it was therefore demonstrated that it is possible to separate the primary colors using spectrum-specific gratings.

In the following verification study,^{46,47} Kimmel and co-workers again used a 1 \times 1-cm grating array. This time, however, a dedicated grating array was fabricated for each of the three primary colors. Green light was coupled into the LGP orthogonally to red and blue light, and these latter two

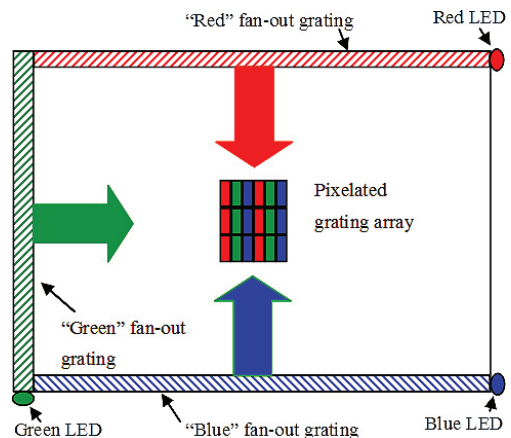


FIGURE 7 — Pixelated-diffractive-grating-array concept (not to scale).⁴⁴

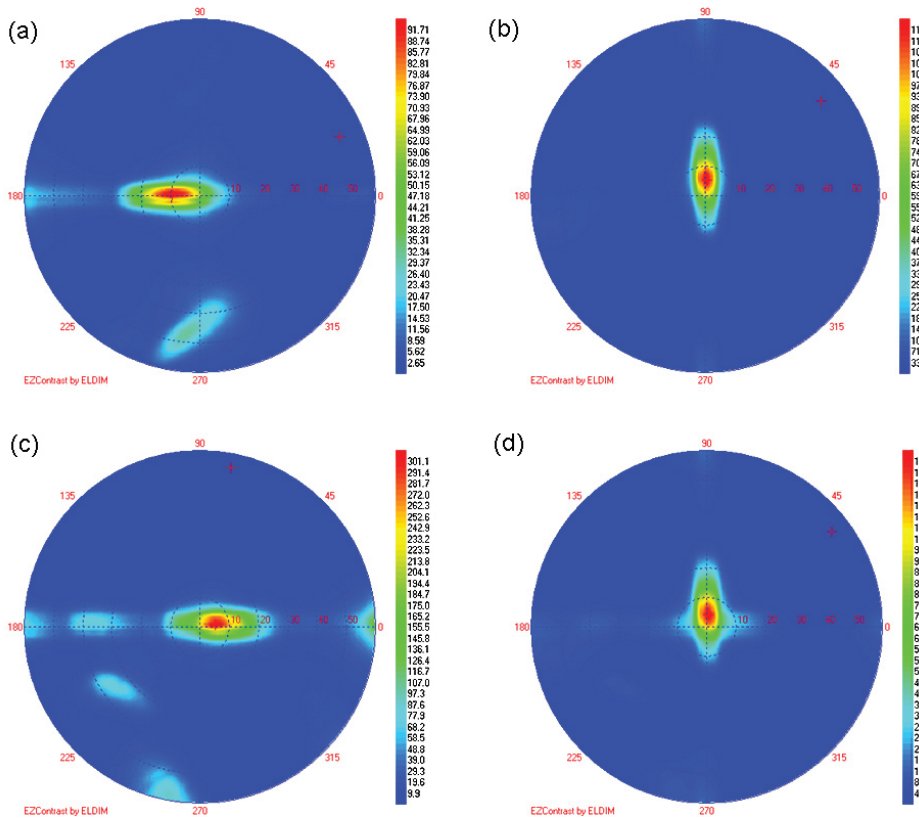


FIGURE 8 — Polar-coordinate plots of the light output in Ref. 48: (a) blue, (b) green, (c) red, (d) all combined. The value of the inclination angle θ is indicated by the concentric circles in the plots, and the value of the azimuth angle ϕ is shown at the perimeter of the plots.

light sources were again facing each other for incoupling from the opposite edges of the LGP. The grating array was now a slanted array with slant directions facing each light source. This allowed precise control of diffracted orders and rejection of unwanted diffraction of blue light from the “red” grating array, and vice versa. The gratings were manufactured on a molded substrate of episulfide polymer by UV embossing the same material on the substrate. This technique has been proven to be repeatable, and replication of slanted grating arrays has been demonstrated up to 500 repeats without degradation of the mold or the master.⁵¹ In this study, all three primary colors were coupled preferentially toward the user, as evidenced by the polar coscope plots of outcoupled light distribution.

Kimmel *et al.* continued the diffractive pixelated-grating-array concept onwards and produced a full display-sized array.⁴⁵ Again, UV-embossed grating arrays on episulfide were used in the study. The outcoupled emission shows very direct outcoupling toward the user, with the full width at half maximum (FWHM) angular distribution of light at 18–25°. In this study, the lateral spreading of light was attempted by the use of fanout gratings. These binary gratings, however,

did not work as intended. The reasons for this relate to poor collimation of the light sources and inadequate profiles of the fanout gratings. Figure 8 shows the outcoupling properties of the grating array in the form of polar plots as characterized by a coscope.

The grating array fabricated for the study in Ref. 48 was again used by Kimmel *et al.* in conjunction with a Liquavista transmissive electrowetting display (EWD).^{55,88} An electrowetting display is based on pixel structures that use electrostatic driving of a liquid-liquid interface, where one liquid is clear and the other is absorbing.⁵⁹ This experiment applying diffractive pixelated grating arrays on EWDs was inconclusive as to how the diffractive pixelated grating arrays could be used together with a display, primarily because the transmissive electrowetting display was fabricated on too thick a substrate to effectively confine the light within the subpixel array in a subpixel-specific fashion. In the study, a color-filter array was placed next to the LGP and results showed a possibility to tune the white point of a display by varying the intensity of the individual red, green, and blue LEDs.

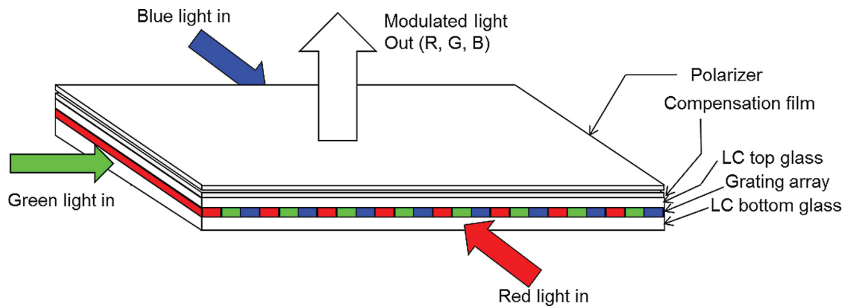


FIGURE 9 — Embedded-grating-array schematic for an integrated backlight concept (not to scale) (after Ref. 86).

Kimmel *et al.* performed a final study, extending their pixelated grating array concept to an integrated one.^{84,86} In this study, a demonstrator grating array was fabricated on a high-refractive-index glass substrate with a TiO₂ overlay. A low-index cladding was spin-coated on top of the slanted grating array. Diode and He-Ne lasers were used to characterize the demonstrator component. The results show very sharply directed outcoupling of the laser light. The polarization state of outcoupling was designed to be transverse electric for the outcoupled red and blue bands of light, and transverse magnetic for the green, in order to achieve the same resulting output state of polarization for all color bands. The results show that there is a clear difference in the state of polarization in outcoupling in the red [206% stronger in transverse electric (TE) than in transverse magnetic (TM) outcoupling] and in the blue (78% stronger TE than TM), but this is not quite good enough for a LCD without a back polarizer. The green TE outcoupling was only 7% stronger than the TM polarization. The authors state that the study presents a starting point to design a new paradigm in LCD manufacturing, as the grating arrays etched in glass could be used as the back substrate of an LCD. In this way, the grating arrays would inherently be placed as close as possible to the subpixel array and cross-talk would thus be eliminated. Figure 9 presents this concept in a schematic form. The same demonstrator sample was also used to study the LGP in LED illumination.⁸⁷ Prism-coupled red, green, and blue LEDs were directed to the central area of the grating array and conoscope measurements showed good directivity of the light toward the user. There was some leakage of blue light through the “red” grating array. The authors state that later simulation studies showed that by taking in account the exact cladding layer thickness, and by better control of the etching process, a more precise agreement with the simulation goals could be achieved, and thus a color-filterless display without a back polarizer could possibly be produced by using an embedded diffractive grating array.

Y. D. Yao *et al.* have presented a pixelated array of Ag nanowires that have been fabricated with a selected periodicity for each primary-color band. A color-filterless display can then be manufactured by using white-light sources. The authors mention the need to use an array of micromir-

rors in the device. Test structures have been characterized that confirm the expectations of the design, but no complete display system has been shown.⁹⁰

5 Discussion

The motivation for diffractive backlight research has shifted from early attempts to optimize mobile-display viewing characteristics¹⁵ to the need to radically redesign the display-manufacturing paradigm in order to achieve energy savings.^{44–48,83–87,90} Since especially mobile displays are becoming otherwise satisfactory for the users, especially with regard to their image-quality characteristics, their power dissipation in multimedia use is often excessive, requiring the user to charge the mobile device battery more frequently than what is desired. The uniform grating designs as well as the single-grating approach for this dilemma results in cumbersome optical structures, and also sometimes requires special array arrangements for the display.^{76,80}

Most groups working with diffractive backlights have used commercial software solutions such as ASAPTM and GSOLVERTM for designing the waveguides and related optical structures.^{65,73,76,80} These programs have limitations as to what kinds of grating characteristics can be modeled. Most often the gratings designed using these software packages are either binary, or consisting of grating profile approximations based on layered binary profiles, or sinusoidal. Without precise simulation of non-sinusoidal or non-binary grating profiles, such as blazed, slanted, or overhanging gratings, the precise control of the amount of outcoupled light entering each of the transmitted and reflected diffraction orders is not possible. The single-type or uniform grating solutions therefore become complicated, especially since the reflected orders need to be directed back toward the waveguide by means of a separate mirror, or sometimes, an array of mirrors.⁸⁰ T. Levola has developed, as a part of his dissertation,⁴² a software solution that can take in account arbitrary periodic structures. This software has mostly been used in designing near-to-eye optics for virtual-display applications,^{39–41,43} but it also has been an asset in designing pixelated multi-grating arrays.^{44–48,83–87} Slanted gratings

designed with the aid of this modeling software have performed as expected, and it has been possible to design precise grating arrays that couple out light effectively to the respective subpixels in the prospective display subpixel arrays.

A similar rationale to directing spectrally separated light toward the LCD subpixel array in a registered fashion has been adapted by A. Travis *et al.* in their wedge waveguide that is used as a flat imaging component.⁹¹ Instead of diffractive components, geometric light guides are used in this study to image red, green, and blue LEDs as stripes on top of the waveguide. A 3-in. prototype based on a similar geometric principle was demonstrated by P.-C. Chen *et al.*⁹² In contrast to the previous approach, an external cylindrical lens and dedicated LED housings were used to achieve a high degree of collimation of the light sources. An RGBG repeating pattern was proposed for the pixel layout in a display; 85% of the National Television System Committee (NTSC) color space was achieved by this system.

It has been already noted that the pixelated-grating-array approach requires the gratings to be in close proximity to the modulating subpixel array and that thin displays are required.^{76,83} Kimmel *et al.* have approached this problem by proposing an embedded structure to be used as the back substrate of the display, bringing the outcoupling grating array effectively on the bottom of the LCD subpixel array.^{84,86,87} Using normal LCD manufacturing processes, the backlight would then be integrated in the glass-manufacturing stage instead of at the “back end” of module fabrication. The remaining issues with this approach are tied to the incoupling of LEDs directly into the substrate glass, distributing the light toward the sides of the display, and most of all, finding a suitable technique to use replication instead of directly etching the backlight grating array into the glass substrate. In the incoupling, there should be a degree of collimation in order for the output gratings to direct the light through the subpixel structure with the best efficiency. Therefore, either an external collimator or an integrated collimator at the injection area of the LCD back substrate should be used. In the fanout section, it is not required to use a grating-based approach, as the respective primary colors are already separated at the light source, and, thus, the diffractive property of the gratings is not required here. However, a diffractive approach might be useful even in this area since the fabrication could be done at the same process step as for the grating array itself. For the replication of the grating arrays on a large glass substrate, prior to the display processing, a solution needs to be found that allows for embossing, nanoimprint lithography, or some other analogous technique, preferably in a stepwise fashion from a single master. These technologies are not available today.

Any display with an ideally collimated backlight needs a diffuser on top of the display to control the viewing angle.^{68,69} The diffuser should be designed in such a way that the color purity of the display remains after the outcoupling of light takes place. Especially in the designs where LEDs are cou-

pled in from different directions, the outcoupled distribution of the primary color bands may vary according to the grating orientation. The polarization of the incoupled light needs also to be designed so that output polarization is uniform, despite the orthogonal direction of polarization in one of the incoupled spectral bands of light. This is important especially when LCDs are used as the electrooptically modulating display medium. The overlay structures should therefore be in some cases either patterned or otherwise spectrally and polarizationwise anisotropic, in order to provide the least amount of variation in the chromaticity and state of polarization of outcoupled light.

6 Conclusions

Ideally, a diffractive backlight will direct the light from LEDs, via the diffractive outcoupling structure, into the LCD subpixel array in such a way that the light of the appropriate primary spectral band only enters the actual active area of each respective subpixel, without cross-talk, in a normal angle to the display surface. The research so far has approached this goal from several points of view, and while remarkable progress has been achieved, display modules with diffractive backlights have not yet been manufactured. The potential benefit of increasing the energy efficiency of a diffractive backlight display system by 4.5–6 times compared to conventional display solutions (see Sec. 3) is only partially realized in the research reviewed in this paper. In the mean time, advanced backlighting solutions have emerged, enabling more efficient LCD systems on the market for mobile devices.

The most advanced pixelated-grating-array approach requires a new display-manufacturing paradigm. The LCD industry should adopt a new manufacturing approach in order to achieve the proposed benefits of diffractive backlight design. This involves either accurate registration of the backlight unit with the LCD panel or incorporating the diffractive backlight into the back substrate of the display itself. There are many challenges involved with moving to this kind of manufacturing, and it remains to be seen whether the demands for energy-efficient display systems will reach the stage where the LCD industry needs to adopt this new manufacturing paradigm.

Organic LEDs (OLEDs) are another potential alternative in energy savings, and these are increasingly being adopted as mobile displays. The early disinterest of mobile-display integrators toward using OLEDs was founded on the unfavorable differential aging characteristics and the short lifetimes of the OLED materials. OLEDs have recently been developed to provide acceptable degradation characteristics for a lifetime of a mobile phone, and simulation studies have supported the adoption of OLEDs in mobile phones.⁹³ The power dissipation of OLEDs is dependent on image content, and if the UI style of the device relies on bright icons on a white background, it suits poorly to applying OLEDs as the display module. Recently, OLEDs have

found use in advanced smart-phone models, as the lifetime-related issues and the user-interface design problems have been solved by the industry.⁹³

Regardless of what happens in the display industry, the research has shown that it is possible to challenge an incumbent paradigm in display manufacturing by utilizing basic principles of optics, and that by doing so, science and technology of displays can be further advanced. This requires access to advanced design tools which are not available in optics design software packages. Especially the application of advanced diffractive structures, such as the slanted grating arrays reviewed in Subsection 4.4, could not have been designed without a dedicated software package developed just for this purpose.

The design of diffractive backlights requires interaction with the display manufacturer at the advanced research and development stage. Demonstrator gratings are expensive to manufacture, and the design should match the intended display-module structure exactly. Industry collaboration with academic researchers seems to be the only way to achieve actual results that end up in manufacturing diffractive backlight displays on a product line.

Acknowledgments

The author would like to thank the Editor, Dr. Andras Lakatos, for his patience and helpful comments during the preparation of this manuscript, Dr. Tapani Levola for his helpful comments with regard to the revision of the manuscript, and Dr. Jyri Huopaniemi as well as Ms. Marja Salmi-maa of Nokia Research Center for their support.

References

- J. Kimmel, "Introduction to mobile displays," *Handbook of Visual Display Technology*, Chap. 10.1.1, Janglin (John) Chen, Wayne Cranton, and Mark Fihn, eds. (Springer-SBM, Heidelberg, 2012), pp. 1982–1992.
- E. H. A. Langendijk and I. Heynderickx, "Optimal and acceptable color ranges of display primaries for mobile applications," *J. Soc. Info. Display* **11**, No. 2, 379–385 (2003).
- J. Xia *et al.*, "Preferred balance between luminance and color gamut in mobile displays," *J. Soc. Info. Display* **14**, No. 10, 873–881 (2006).
- R. L. Donofrio, "Review paper: The Helmholtz–Kohlrausch effect," *J. Soc. Info. Display* **19**, No. 10, 658–664 (2011).
- J. Kimmel, "Displays enabling mobile multimedia," *Proc. SPIE* **6507**, 650705-1–650705-11 (2007).
- Y. Neuvo, "Cellular phones as embedded systems," *IEEE Solid-State Circuits Conference. Digest of Technical Papers. ISSCC* **1**, 32–37 (2004).
- A. Iranli *et al.*, "HVS-aware dynamic backlight scaling in TFT-LCDs," *IEEE Trans. VLSI Systems* **14**, 1103–1116 (2006).
- A. Tagaya *et al.*, "Thin liquid-crystal display backlight system with highly scattering optical transmission polymers," *Appl. Opt.* **40**, No. 34, 6274–6280 (2001).
- J. Hüttner *et al.*, "LED backlighting of LCDs in mobile appliances," *Mobile Displays – Technology and Applications*, Chap. 8, A. K. Bhowmik, Z. Li, and P. J. Bos, (eds.) (Wiley, Chichester, 2008).
- E. Lueder, *Liquid Crystal Displays. Addressing Schemes and Electro-Optical Effects* (Wiley, Chichester, 2010).
- F. Yamada *et al.*, "Sequential-color LCD based on OCB with an LED backlight," *J. Soc. Info. Display* **10**, No. 2, 81–85 (2002).
- R. Akins, "Displays for hand-held portable electronic products," *J. Soc. Info. Display* **7**, No. 4, 273–276 (1999).
- M. Anandan, "Progress of LED backlights for LCDs," *J. Soc. Info. Display* **16**, No. 2, 287–310 (2008).
- G. Hooker and D. Smith, "Illuminated LCD apparatus," U.S. Patent 5,477,422 (1995).
- M. Parikka *et al.*, "Deterministic diffractive diffusers for displays," *Appl. Opt.* **40**, No. 14, 2239–2246 (2001).
- A. G. Chen *et al.*, "Holographic reflective liquid-crystal display," *J. Soc. Info. Display* **3**, No. 4, 159–268 (1995).
- M. Suzuki, "Two approaches to the luminance enhancement of backlighting units for LCDs," *J. Soc. Info. Display* **7**, No. 3, 157–161 (1999).
- P. Watson and G. T. Boyd, "Backlighting of mobile displays," *Mobile Displays – Technology and Applications*, Chap. 7, A. K. Bhowmik, Z. Li, and P. J. Bos, (eds.) (Wiley, Chichester, 2008), pp. 211–225.
- K. Kälantär, "Functional light-guide plate for backlight unit," *SID Symposium Digest* **30**, 764–767 (1999).
- K. Kälantär *et al.*, "Optical micro deflector based functional light-guide plate for backlight unit," *SID Symposium Digest* **31**, 1029–1031 (2000).
- S. Matsumoto *et al.*, "Functional light-guide plate characterized by optical micro-structures for LCD backlight unit," *Proc. IDW '00*, 463–465 (2000).
- K. Kälantär *et al.*, "Micro-structured light-guide plate for efficient backlighting transmissive LCDs used in mobile phones and PDAs," *Proc. Asia Display/IDW '01*, 645–647 (2001).
- W. J. Cassarly, "Backlight pattern optimization," *Proc. SPIE* **6834**, 683407-1–683407-12 (2007).
- A. Nagasawa *et al.*, "A novel backlight system with the unified component," *Proc. IDW/Asia Display '05*, 1285–1288 (2005).
- P. H. Yao *et al.*, "Micro-structure optical film with hybrid functions for LCD backlight," *SID Symposium Digest* **37**, 851–853 (2006).
- G. Boyd, "LCD backlights," *Handbook of Visual Display Technology*, J. Chen, W. Cranton, and M. Fihn (eds.) (Springer-SBM, Heidelberg, 2012), pp. 1609–1623.
- A. Funamoto *et al.*, "Prism-sheetless high bright backlight system for mobile phone," *Proc. IDW '04*, 687–690 (2004).
- S. Aoyama *et al.*, "Hybrid normal-reverse prism coupler for light-emitting diode backlight systems," *Appl. Opt.* **45**, No. 28, 7273–7278 (2006).
- A. Funamoto and S. Aoyama, "LED backlight system with double-prism pattern," *J. Soc. Info. Display* **14**, No. 11, 1045–1051 (2006).
- S. I. Kim *et al.*, "Holographic diffuser by use of a silver halide sensitized gelatin process," *Appl. Opt.* **42**, No. 14, 2482–2491 (2003).
- D. G. Pelka *et al.*, "Replication of microstructured display films," *SID Symposium Digest* **34**, 72–75 (2003).
- J. Qi *et al.*, "Tailored holographic micro-diffusers for display applications," *SID Symposium Digest* **35**, 314–317 (2004).
- J. Qi *et al.*, "Tailored elliptical holographic diffusers for LCD applications," *J. Soc. Info. Display* **13**, No. 9, 781–786 (2005).
- S. Siitonen *et al.*, "A double-sided grating coupler for thin light guides," *Opt. Express* **15**, No. 5, 2008–2018 (2007).
- B. Bai *et al.*, "High-efficiency broadband grating coupler for light guides," *Proc. 29th Intl. Display Research Conf., EuroDisplay '09*, Paper 22.5 (2009).
- M. L. Ermold and A. K. Fontecchio, "Viewing-angle enhancement in holographic reflective displays by nanoscale holographic patterning," *J. Soc. Info. Display* **13**, No. 9, 787–792 (2005).
- H. Dammann, "Color separation gratings," *Appl. Opt.* **17**, No. 15, 2273–2279 (1978).
- M. Born and E. Wolf, *Principles of Optics*, 7th ed. (corrected) (Cambridge University Press, Cambridge, 2002).
- T. Levola, "Diffractive optics for virtual reality displays," *Proc. Eurodisplay 2005 (International Display Research Conference)*, 542–545 (2005).
- T. Levola, "Diffractive optics for virtual reality displays," *J. Soc. Info. Display* **14**, No. 5, 467–475 (2006).
- T. Levola, "Novel diffractive optical components for near to eye displays," *SID Symposium Digest* **37**, 64–67 (2006).
- T. Levola, "Diffractive optics for virtual reality displays," University of Joensuu, Department of Physics, Dissertations 47 (2005).
- T. Levola, "Compact see-through near to eye display with diffractive optical elements," *Proc. IMID '07*, Paper 53-2 (2007).
- J. Kimmel *et al.*, "A novel diffractive backlight concept for mobile displays," *J. Soc. Info. Display* **16**, No. 2, 351–357 (2008).
- J. Kimmel *et al.*, "A novel diffractive backlight concept for mobile displays," *SID Symposium Digest* **39**, 42–45 (2007).

- 46 J. Kimmel *et al.*, "Diffractive backlight grating array for mobile displays," *Digest of Eurodisplay 2007 (International Display Research Conference)*, 171–174 (2007).
- 47 J. Kimmel *et al.*, "Diffractive backlight grating array for mobile displays," *J. Soc. Info. Display* **16**, No. 8, 863–870 (2008).
- 48 J. Kimmel *et al.*, "A new diffractive backlight for mobile displays," *Proc. IDRC 2008*, 290–293 (2008).
- 49 L. Li *et al.*, "Rigorous and efficient grating-analysis method made easy for optical engineers," *Appl. Opt.* **38**, No. 2, 304–313 (1999).
- 50 J.-P. Plumey and G. Granet, "Generalization of the coordinate transformation method with application to surface-relief gratings," *JOSA* **16**, No. 3, 508–516 (1999).
- 51 T. Levola and P. Laakkonen, "Replicated slanted gratings with a high refractive index material for in and outcoupling of light," *Opt. Express* **15**, No. 5, 2067–2074 (2007).
- 52 M. Xu *et al.*, "Simulations of birefringent gratings as polarizing color separator in backlight for flat-panel displays," *Opt. Express* **15**, No. 9, 5789–5800 (2007).
- 53 R. Petit (ed.), *Electromagnetic Theory of Gratings* (Springer, Heidelberg, 1980).
- 54 S. M. P. Blom *et al.*, "Towards polarised light emitting back lights: Micro-structured anisotropic layers," *Proc. Asia Display/IDW '01*, 525–528 (2001).
- 55 H. J. B. Jagt *et al.*, "Linearly polarized light-emitting backlight," *J. Soc. Info. Display* **10**, No. 1, 107–112 (2002).
- 56 S. M. P. Blom *et al.*, "Towards a polarized light-emitting backlight: Micro-structured anisotropic layers," *J. Soc. Info. Display* **10**, No. 3, 209–213 (2002).
- 57 H. J. B. Jagt *et al.*, "Micro-structured polymeric linearly polarized light emitting lightguide for LCD illumination," *SID Symposium Digest* **33**, 1236–1239 (2002).
- 58 H. J. Cornelissen *et al.*, "Polarized light LCD backlight based on liquid crystalline polymer film: A new manufacturing process," *SID Symposium Digest* **35**, 1178–1180 (2004).
- 59 K.-W. Chien *et al.*, "Polarized backlight based on selective total internal reflection at microgrooves," *Appl. Opt.* **43**, No. 24, 4672–4676 (2004).
- 60 S. Hwang *et al.*, "Highly efficient backlight unit with a polarization-separating anisotropic layer," *SID Symposium Digest* **38**, 476–479 (2007).
- 61 K.-W. Chien and H.-P. D. Shieh, "Design and fabrication of an integrated polarized light guide for liquid-crystal-display illumination," *Appl. Opt.* **43**, No. 9, 1830–1834 (2004).
- 62 X. Yang *et al.*, "Polarized light-guide plate for liquid crystal display," *Opt. Express* **13**, No. 21, 8349–8356 (2005).
- 63 H. Y. Choi *et al.*, "Hologram based light-guide plate for LCD-backlights," *Proc. Asia Display/IDW '01*, 521–524 (2001).
- 64 M. G. Lee *et al.*, "Optical characteristics of holographic light-guide plate for LCD," *Proc. Eurodisplay 2002*, 343–346 (2002).
- 65 J. H. Min *et al.*, "Holographic backlight unit for mobile LCD devices," *J. Soc. Info. Display* **11**, No. 4, 653–657 (2003).
- 66 D. Nesterenko *et al.*, "Design and analysis of tapered waveguides as collimators for LED backlighting," *SID Symposium Digest* **36**, 1388–1391 (2005).
- 67 A. K. Aristov *et al.*, "Holographic diffraction grating for side lighting of liquid-crystal displays," *J. Opt. Technol.* **70**, No. 7, 480–484 (2003).
- 68 Y. Taira *et al.*, "Low-power LCD using a novel optical system," *SID Symposium Digest* **33**, 1313–1315 (2002).
- 69 Y. Taira *et al.*, "Illumination system for color filterless liquid crystal display," *Proc. Eurodisplay 2002*, 585–588 (2002).
- 70 F. Yamada *et al.*, "Optical components directly molded on the LCD glass substrate," *SID Symposium Digest* **33**, 1042–1045 (2002).
- 71 F. Yamada *et al.*, "Dual layered very thin flat surface micro prism array directly molded in and LCD cell," *Proc. Eurodisplay 2002*, 339–342 (2002).
- 72 F. Yamada *et al.*, "Multi-layered flat-surface micro-optical components directly molded on an LCD panel," *J. Soc. Info. Display* **11**, No. 3, 525–531 (2003).
- 73 D. K. G. de Boer and H. J. Cornelissen, "Colour-separating backlight based on surface-relief grating," *Proc. Eurodisplay 2005 (International Display Research Conference)*, 236–239 (2005).
- 74 D. K. G. de Boer *et al.*, "Diffractive grating structures for colour-separating backlights," *Proc. SPIE* **6196**, 61960R-1–61960R-8 (2006).
- 75 R. Caputo *et al.*, "Short period holographic structures for backlight display applications," *Opt. Express* **15**, No. 17, 10540–10522 (2007).
- 76 M. J. J. Jak *et al.*, "Color-separating backlight for improved LCD efficiency," *J. Soc. Info. Display* **16**, No. 8, 803–810 (2008).
- 77 E. Miyamoto *et al.*, "Novel diffraction grating light guide for LED backlight," *Proc. SPIE* **6488**, 64880H-1–64880H-8 (2007).
- 78 S. R. Park *et al.*, "Grating micro-dot patterned light guide plates for LED backlights," *Opt. Express* **15**, No. 6, 2888–2899 (2007).
- 79 K. Niu *et al.*, "Holographic light-guide plate for LCD backlight system," *Proc. SPIE* **6832**, 68322S-1–68322S-8 (2007).
- 80 D. R. Selviah and K. Wang, "Modeling of a color-separating backlight with internal mirrors," *SID Symposium Digest* **35**, 487–489 (2004).
- 81 Y. Zhang *et al.*, "Talbot grating for color separation in color liquid crystal display," *Proc. SPIE* **6832**, 68320P-1–68320P-8 (2007).
- 82 J. Orava *et al.*, "Large gamut backlight for an LCD with four primaries," *J. Display Technol.* **6**, No. 5, 170–177 (2010).
- 83 J. Kimmel and T. Levola, "Backlights in mobile display power management," *SID Symposium Digest* **39**, 1594–1597 (2008).
- 84 J. Kimmel and T. Levola, "Mobile display backlight light guide plates based on slanted grating arrays," *Proc. SPIE* **8065**, 80653S-1–80653S-9 (2011).
- 85 J. Kimmel *et al.*, "Diffractive backlight light guide plates in mobile electrowetting display applications," *SID Symposium Digest* **15**, 826–829 (2009).
- 86 J. Kimmel and T. Levola, "Mobile display backlight light guide plates based on slanted grating arrays," *SPIE J. Photonics Energy* **2**, 024501-1–024501-11 (2012).
- 87 J. Kimmel and T. Levola, "Embedded diffractive backlight light guide plates in mobile display applications," Paper Presented at Eurodisplay '11 (31st International Display Research Conference), Bordeaux (2011).
- 88 A. Giraldo *et al.*, "Transmissive electrowetting-based displays for portable multimedia devices," *J. Soc. Info. Display* **18**, No. 4, 317–325 (2010).
- 89 R. A. Hayes and B. J. Feenstra, "Video-speed electronic paper based on electrowetting," *Nature* **425**, 383–385 (2003).
- 90 Y. D. Yao *et al.*, "Light plate with metallic nanostructures for color filterless display," *Proc. IDW '08*, 1695–1698 (2008).
- 91 A. Travis *et al.*, "Collimated light from a waveguide for a display backlight," *Opt. Express* **17**, No. 22, 9715–9719 (2009).
- 92 P.-C. Chen *et al.*, "Color separation system with angularly positioned light source module for pixelized backlighting," *Opt. Express* **18**, No. 2, 645–655 (2010).
- 93 A. Lääperi, "OLED lifetime issues from a mobile-phone-industry point of view," *J. Soc. Info. Display* **16**, No. 11, 1125–1130 (2008).



Jyrki Kimmel received his M.Sc. and Licentiate of Technology degrees in electrical engineering from the Tampere University of Technology in 1986 and 1992, respectively. He is currently Distinguished Researcher at Nokia Research Center in Tampere, Finland. He also lectures on display-related topics at Tampere University of Technology. Before joining Nokia in 1996, he was with the Technical Research Centre of Finland and was a Fulbright Scholar at the University of Utah. His current research interests relate to mobile displays, especially backlights.

Publication [P2]

J. Kimmel, T. Levola, P. Saarikko, and J. Bergquist, "A Novel Diffractive Backlight Concept for Mobile Displays," JSID, Vol. 16, No. 2, pp. 351-357, 2008.

Copyright © 2008 Society for Information Display.
Reprinted with permission.

A novel diffractive backlight concept for mobile displays

Jyrki Kimmel
Tapani Levola
Pasi Saarikko
Johan Bergquist

Abstract — Power-efficiency demands on mobile communications device displays have become severe with the emergence of full-video-capable cellular phones and mobile telephony services such as third-generation (3G) networks. The display is the main culprit for power consumption in the mobile-phone user interface and the backlight unit (BLU) of commonly used active-matrix liquid-crystal displays (AMLCDs) is the main power drain in the display. One way of reducing the power dissipation of a mobile liquid-crystal display is to efficiently distribute and outcouple the light available in the backlight unit to direct the primary wavelength bands in a spectrum-specific fashion through the respective color subpixels. This paper describes a diffractive-optics approach for a novel backlight unit to realize this goal. A model grating structure was fabricated and the distribution of outcoupled light was studied. The results verify that the new BLU concept based on an array of spectrum-specific gratings is feasible.

Keywords — Active-matrix liquid-crystal display (AMLCD), backlight unit (BLU), diffractive optics.

1 Introduction

Recent developments in mobile communications terminals and networks have led to increased demands on the power efficiency of handheld communications devices such as mobile phones. With the rapid adoption of third-generation (3G) networks and mobile digital television broadcasts, the mobile terminal is becoming a major multimedia appliance for everyday use. The mobile-phone user interface (UI) has been shown to dissipate roughly one third of the electrical power of a mobile phone.¹ Displays especially are a drain on the current shared by other functions of the mobile terminal, and developments in the display power efficiency are sought after.²

The backlight is the dominating component in the display-module power consumption, particularly in the case of transmissive liquid-crystal displays (LCDs) for multimedia applications which require higher color saturation and perceived brightness. Current backlight designs are based on creating a uniform distribution of white light throughout the display pixel matrix, which in the majority of cases is an active-matrix liquid-crystal display (AMLCD). Although this design results in a relatively compact and simple structure with moderate needs for lateral alignment of the optical films in the display, a large fraction of light generated in the light-emitting diodes (LEDs) of the backlight module is wasted in the absorption of unwanted spectral content in color-filter arrays, as well as in the opaque areas of the AMLCD matrix thin-film transistor (TFT) and reflector arrays. One way to improve the light throughput is to use field-sequential color (FSC), where instead of separating the color primaries spatially by arranging them in subpixels,

color is separated in a temporal fashion and modulated by a monochrome matrix.³ The problem in this approach is the duty cycle, reducing the effective light throughput in time to less than one-third of the available frame sequence and the need for faster and thus more expensive liquid-crystal materials, TFTs, and driver components.³

Directing the emitted light only to the active pixel areas where its spectral content matches the respective primaries of the color-filter array would help in curtailing the power drain of the display module and thus enabling an increased overall power efficiency in a mobile-phone user interface.

This paper presents a new diffractive optics concept for spatially modulated display backlights, such as LCDs, with color-selective extraction of light matching the respective primaries of the color-filter pixel matrix. An experimental study was performed with a striped model grating array representing a 1 cm by 1 cm area of a prospective 2.8-in. QVGA (320 × 240 pixels) display in order to verify the concept.

2 State of the art of backlight units and the diffractive backlight concept

2.1 State of the art of backlight units

Early mobile phone backlight units (BLUs) were simply roughened pieces of transparent polymer, molded to fit the frame of the display module. In the back of the BLU there was a reflector film. Hotspots from LEDs could be a problem, and they were taken care of by darkening the reflector area near the illuminating LEDs, if at all.⁴ Later on, with

Extended revised version of a paper presented at the 2007 SID Symposium, Seminar & Exhibition (SID '07) held in Long Beach, California, May 20–25, 2007.

J. S. Kimmel and Tapani Levola are with Nokia Research Center, P.O. Box 1000, Visiokatu 1, Tampere, N.A. 33721, Finland; telephone +358-504-835-484, fax +358-7180-35; e-mail: jyrki.kimmel@nokia.com.

P. Saarikko is with Nokia Research Center, Helsinki, Finland.

J. Bergquist, Nokia Technology Platforms, Tokyo, Japan.

© Copyright 2008 Society for Information Display 1071-0922/08/1602-0351\$1.00

increasing legibility demands, glare from the display was reduced by directing the specular reflections of the ambient light out of the viewing direction.⁵ While these approaches were adequate for monochrome displays, it became apparent with the emergence of color LCDs in mobile phones that a high contrast and good color gamut with an adequate viewing angle was to be required of mobile displays.⁶ The focus of development was shifted to adding collimating films in mobile and laptop LCDs to control the propagation of light through the pixel array.⁷ Concurrently, white (or “pseudo-white”) LEDs appeared as light sources in color LCDs, since the previously used green LEDs obviously could not provide the desired spectral characteristics for the new full-color UIs.²

Most notably, the BLU light-guide structure evolved, from the molded polymer component with a roughened surface to precisely engineered plates with efficient incoupling lens areas^{8,9} and statistically distributed scattering centers made by screen printing on the back of the BLU light guide. The main improvement, however, came about when the scattering centers were replaced by microreflectors.^{10–13} These structures can, in principle, be very efficient directing most of the light emitted by the LEDs into the AMLCD color-filter array with better than 80% uniformity.¹³ Thus, the state-of-the-art mobile BLU today is a stack of optical films, with a reflector structure as the bottom-most surface. The emitted light from LEDs is coupled into the light guide, and the microreflector structure directs the light toward the display itself. Two brightness-enhancing films (BEFs) are typically used, perpendicularly to each other, to collimate the light through the LCD and to provide a degree of polarization recycling. The optics stack is completed by adding the LCD with polarizers on both sides to modulate the light emerging from the BLU by the AMLCD matrix, which typically consists of an array of red, green, and blue subpixels. The main drawback of this structure is that the light emitted by the white or pseudo-white LEDs is not separated to the primary-color bands of the subpixels in the AMLCD matrix. Therefore, in the ideal case, only one-third of the light in a typical LCD can pass through each pixel. Furthermore, since the active-matrix TFT array has an active aperture that is limited by the transistor structure and in the case of transmissive LCDs, also by the reflector area, the throughput of light is further reduced to roughly two-thirds of the available illumination through each subpixel. The LCD polarizer further reduces the throughput to one-half or less of the light emerging from the BLU. Thus, the efficiency of the whole array, not accounting for the transmissivity losses in the LCD color filter and the material losses in the optics stack of the display, is on the order of 10%.

To increase the efficiency and to decrease the thickness, polarizing backlights have been proposed.^{14–19} Also, several of the functions traditionally incorporated in single and separate films have been combined as hybrid films.²⁰ This development has led to thin mobile-display structures,

in conjunction with engineering efforts to reduce the overall thickness of mobile displays and mobile LCD modules less than 1 mm thick have been reported.²¹

Diffraction components have been previously proposed for color-imaging applications.²² These early diffractive-grating-based systems employed relative coarse groove periods on the order of several micrometers, and spectral separation was only possible with an adequate back distance from the imaged scene.²² In the area of display technology, holographic films have been developed for mobile LCD panels to be employed in various functions.^{8,9,23–25} These films use surface-relief holograms to diffract a desired polarization state of light into the LCD panel^{8,9} or to diffuse the emitted light in a precise way to control the viewing angle of the display.^{23–25} These applications of holographic films in mobile LCD development are examples of using diffraction in BLU design, and in the polarizing holographic BLU, the hologram is essentially a submicrometer period diffraction grating.^{8,9} Diffractive backlights have also been proposed with a pixelated single-period grating pattern.²⁶ Ray-tracing models showed that the backlight using the pixelated single-period gratings requires both microlenses to direct the light onto the respective pixels and thin micromirrors inside the grating structure to reflect the negative diffraction orders back into the desired direction.²⁶ The uniform-sheet approach in diffractive backlights also would require a lenticular lens sheet to direct the spectrally spread emission from the light sources to enter the desired subpixels in the TFT array, as the spectral divergence is large.^{8,9}

2.2 Diffractive backlight concept

Previous studies indicate that high-efficiency gratings can be manufactured on polymers, in a replicable fashion, for example, for personal-display exit-pupil expanders (EPEs).^{27–30} The gratings are made by optical or electron-beam lithography on fused silica masters and then replicated by molding. Thermal or ultra-violet (UV) curing and sometimes embossing can be used to replicate these gratings multiple times.³⁰ It is possible to achieve high efficiency, experimentally verified up to 80%, in outcoupling of light by these gratings by controlling the light distribution into selected diffraction orders, and the gratings can be made wavelength-selective so that only determined color bands of light are coupled out of the grating structure.³⁰ The EPE studies also indicate that it is possible to manufacture efficient fan-out gratings for the distribution of light uniformly along the EPE plate. It has been shown that the EPE gratings can be replicated repeatedly, up to hundreds of times from a single master, by UV embossing.³⁰

Figure 1 shows a schematic outline of the new pixelated diffractive backlight concept. Incoming light is fanned out by a grating that is selective for each primary color, and respective red, green, and blue LEDs are used for the color primaries. The light is then distributed throughout the active area of the display by total internal reflection

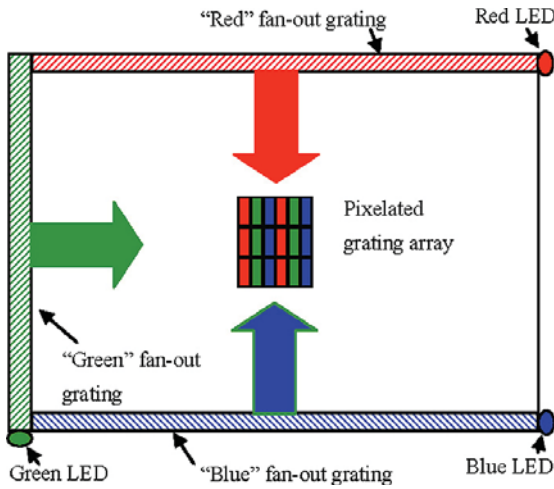


FIGURE 1 — Pixelated backlight concept (not to scale).

(TIR). In the active area, an array of gratings couples out the light into the active aperture of the display pixel matrix. The separation of color primaries at the pixel level is achieved by color-specific gratings, and by orienting the green-primary light propagation inside the TIR light guide perpendicularly to the red and blue primaries.

3 Model grating design and experiment

3.1 Model grating design

The conical grating equations [Eq. (1)]³¹ for the light coming from the material 1 to material 2, represented by refractive indices n_1 and n_2 , respectively, through a grating interphase are

$$\begin{aligned} n_2 \sin \theta_m \sin \varphi_m &= n_1 \sin \theta_i \sin \varphi_i, \\ n_2 \sin \theta_m \cos \theta_m &= n_1 \sin \theta_i \cos \varphi_i + m\lambda/d, \end{aligned} \quad (1)$$

where d is the period of the grooves in the grating, θ_i is the angle of incidence, θ_m is the diffracted angle with respect to the surface normal of the plate, φ_i is the incident, and φ_m is the diffracted azimuthal angle of the light, m is the diffracted order, and λ is the wavelength of light incident on the grating (see Fig. 2). Light that is trapped inside a light guide due to total internal reflection (TIR) has an angular intensity distribution that depends on the light source and on how the light is coupled into the light guide. Because the diffraction efficiency of surface-relief gratings typically depends strongly on the incidence angles, a unidirectional light field traveling close to the TIR limit would provide the optimum case for controlling the properties of the outcoupled light. In practice, the incoupling angles in the range of $\theta_i = 45\text{--}65^\circ$ and $\varphi_i = -10^\circ$ to $+10^\circ$ are sufficient for most cases. The diffraction angles for the outcoupled light of the

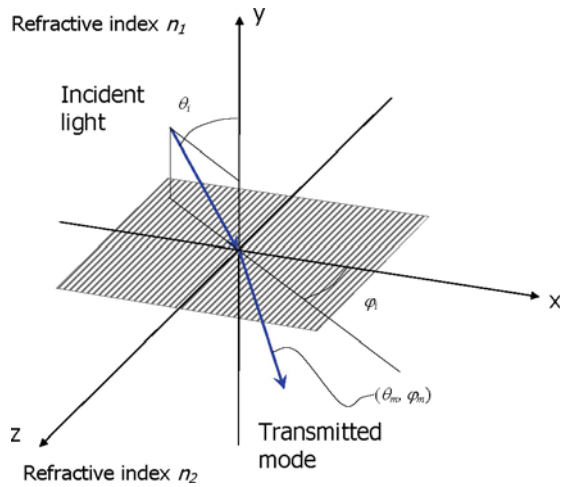


FIGURE 2 — The coordinate system used in grating design.

mode m in the case of $n_1 = n$ and $n_2 = 1$ (air) can be written as

$$\begin{aligned} \tan \varphi_m &= \frac{\sin \theta_i \sin \varphi_i}{\sin \theta_i \cos \varphi_i + m\lambda/nd}, \\ \sin \theta_m &= \sqrt{n^2 \sin^2 \theta_i \sin^2 \varphi_i + (n \sin \theta_i \cos \varphi_i + m\lambda/d)^2}. \end{aligned} \quad (2)$$

Equation (2) shows that the diffraction angles of the maxima of the diffracted orders of light follow the incident angle of the corresponding light and are strongly dependent on the wavelength. The gratings should be constructed so that they are selective for wavelengths and so that the distribution of outcoupled light can be controlled spatially. If the grating period is sufficiently small, only the first-order diffractions ($m = \pm 1$) are present at small azimuthal angles ($\varphi_i \sim 0^\circ$). Moreover, it can be seen from Eq. (2) that only the zeroth-order diffraction exists at large azimuthal angles. This means that the outcoupling of two different wavelength bands can be decoupled by using gratings with perpendicular groove directions. This enables color-selective outcoupling for two primaries, but leaves the third one mixed with either one of the first two. Because of the large spectral separation between red and blue wavelength bands, it appears attractive to decouple the outcoupling of green from red and blue with the aid of the perpendicular gratings. For blue–red separation, we need gratings that are either strongly wavelength or incidence-angle dependent, *e.g.*, the illumination direction for the red and blue primaries can be from opposite directions.

The condition for light outcoupling along the normal direction can be obtained from Eq. (2) by setting $\varphi_i = 0$, $\theta_m = 0$, and $m = 1$

$$d = \lambda/n \sin \theta_i. \quad (3)$$

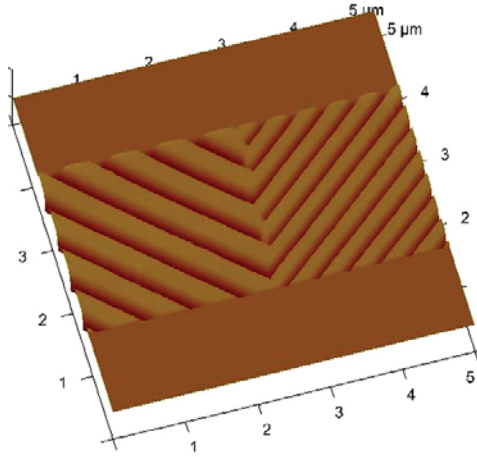


FIGURE 3 — Atomic force microscope (AFM) image of the grating fused-silica master, showing sections of the gratings used for green and red/blue primaries.

Equation (3) shows that subwavelength outcoupling gratings are needed for TIR light guides. Also, it can be seen that only one wavelength at a given incidence angle is outcoupled along the surface normal. Because we only have two different optimized grating periods for green and blue, the third wavelength band of red light will not emerge out from the light guide perpendicularly. The outcoupling angle for the red light is approximately

$$\sin \theta_R = (1 - \lambda_R / \lambda_B) n \sin \theta_i, \quad (4)$$

where λ_R and λ_B refer to red and blue wavelengths. The grating period for blue would be about 390 nm if the blue light is to be emitted perpendicularly, but in this case we can intentionally make the period smaller because then the intensity of red diffracted light becomes smaller. The blue emission deviates now from the normal at about 20° and red is at very high angles, more than 50°. The red emission from this grating is also weak. In optimal grating arrays, the red light needs its own outcoupling gratings, where the emphasis in design would be in weak blue outcoupling. This is one

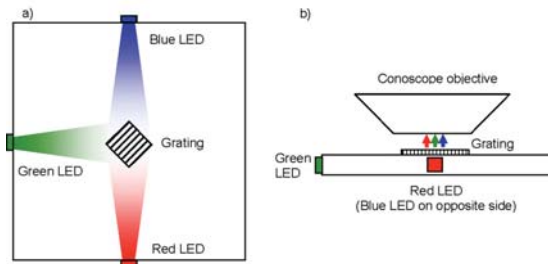


FIGURE 4 — Experimental setup (not to scale): (a) schematic view from above, (b) cross-sectional view.

TABLE 1 — Grating parameters and expected efficiency of the gratings.

Primary	Width (μm)	Depth (nm)	Grating period (nm)	Calculated efficiency of transmitted mode at $\theta_i = 55^\circ$, $\theta_t = 0^\circ$	
				TE	TM
Red and blue	118	220	450	0.150	0.040
Green	59	220	300	0.182	0.061
				0.204	0.044

possible way for spatial separation of blue and red wavelengths. The incoming angle θ_i should be selected so that the whole wavelength band of the LED emission will be confined inside the plate due to TIR. The angular distribution of the LED emission typically will be the dominating characteristic in the respective angular distribution of the output coupling, due to the relatively narrow wavelength bands of LED emission.

3.2 Model grating experiment

A small binary grating structure of 1 × 1-cm square, with 50% filling ratio, was fabricated on a plate of 1-mm-thick polymethyl methacrylate (PMMA) in a mold using UV-curable material SK9 at NanoComp Oy in Joensuu, Finland. The grating parameters as well as the theoretical outcoupled efficiencies for the gratings are shown in Table 1. The result is a stripe array with one grating used for both red and blue and one for green (Fig. 3). The red and blue light are directed to the grating from opposite corners of the grating area, and green perpendicularly to these. The grating directions are 45° and 135° with respect to the stripe orientation.

Osram LEDs were used as light sources.^{32,33} The LED parameters are shown in Table 2. Small, 0.6-mm-thick LEDs were used for efficient coupling of light into the sheet of PMMA.

Figure 4 shows the experimental setup. The LEDs were mounted on the sides of the grating plate, and ordinary butt-coupling was used to launch light into the plate of PMMA which then acted as a TIR light guide. The divergence of the LEDs was utilized to partially fan out the light across the grating area. The grating plate was placed in front of an Eldim EZLite 120 R conoscope and polar plots of light intensity were obtained for all individual colors as well as for the combined red, green, and blue LEDs all on.

TABLE 2 — LED parameters (Refs. 32 and 33).

Primary	Dominant wavelength (nm)	FWHM* (nm)	Luminous intensity at 20 mA (mcd)	Luminous efficiency (lm/W) (typical)
Red	625	19	180...900	43
Green	528	33	560...1800	36
Blue	460	25	90...280	11

*FWHM: Full width at half maximum.

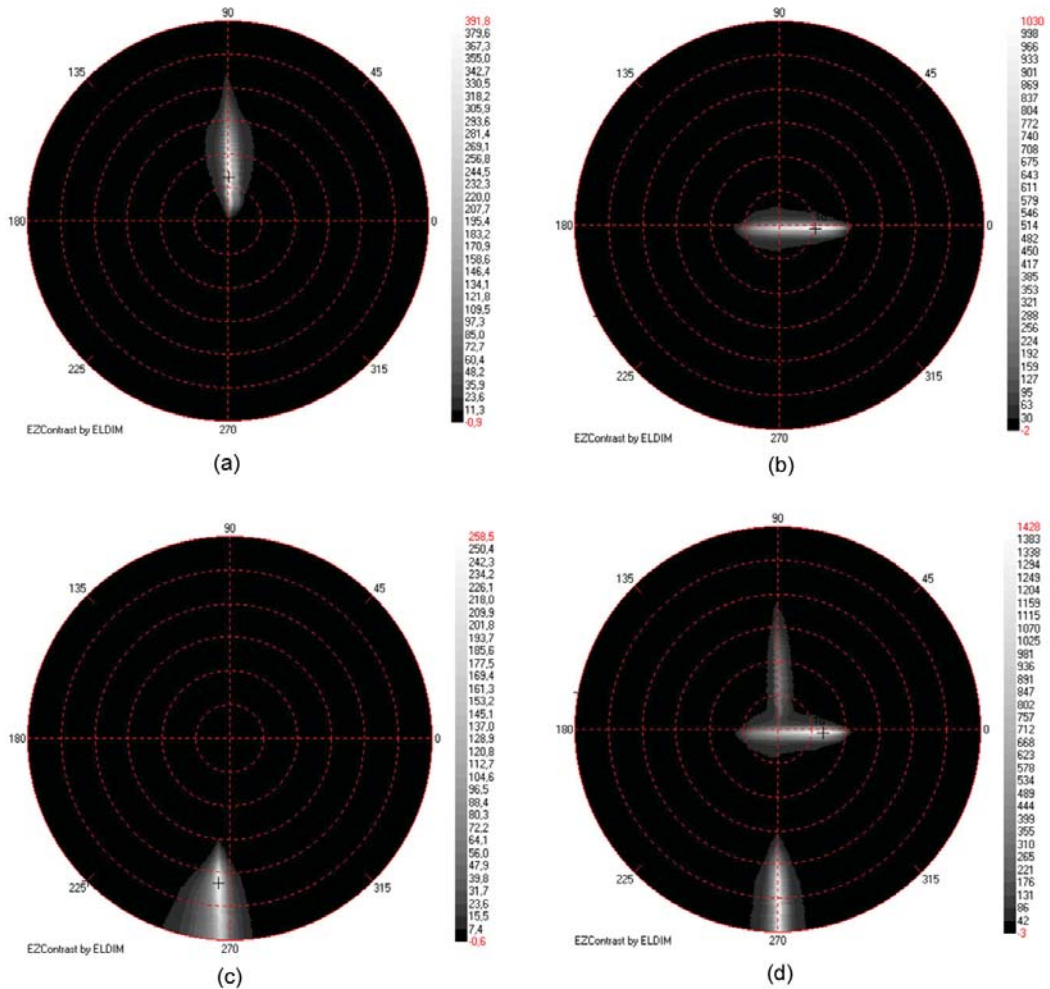


FIGURE 5 — Polar coordinate plots: (a) blue, (b) green, (c) red, and (d) all combined.

4 Results

Figure 5 shows the polar plots obtained with the Eldim EZContrast coscope. It was found that the joint grating for red and blue coupled out blue light, significantly better than the red, to the viewing direction. The red outcoupling was preferential in an oblique angle. The green outcoupling was also observed in an angular range directed effectively toward the viewer. The division of the outcoupling was clearly visible as can be seen from Fig. 6. The green light coupled out of the narrow grating stripes, and the blue and red coupled out of the double-width grating stripes. The red outcoupling could not be photographed because the light coupled out of the aperture of the microscope. Because we did not have a fan-out grating in this experiment, it is clear

that the uniformity of illumination was not very good. There was a visible streak of light in the middle of the structure for the blue and green primaries showing efficient outcoupling of light. The red emission streak was observed only by view-



FIGURE 6 — Microscope image of the outcoupled light from the grating array: (a) blue LED on, (b) green LED on, (c) blue and green LEDs on, and (d) optical microscope image.

TABLE 3 — Angles about the zenith of the outcoupling maxima in the model grating experiment.

Primary	Angle of maximum outcoupling (°)
Blue	15.0
Green	10.5
Red	58.0

ing the grating array obliquely from the LED side of the grating plate.

Table 3 summarizes the results of the measurement with the conoscope. Grating efficiencies were not characterized, but the luminance values in the conoscope results (over 1400 cd/m², all LEDs on) show that the emission from the gratings would be adequate for a mobile LCD BLU at least for the blue and green primaries, if properly arranged uniform lighting were to be implemented in a real BLU design.

Compared to the outcoupling characteristics expected from theory, it is evident that the angular range of outcoupling falls within the theoretical outcoupling range. The intensity distribution of outcoupled light shows that the conical grating theory explains the emission adequately. The outcoupling was very narrow in the azimuthal direction for the outcoupled bands of light for each primary color. The direction of the outcoupling for the red was near the maximum measurable angle of the conoscope (60°), and therefore the actual value is only estimated to be near that maximum angle. For an accurate analysis of the outcoupled distribution, comparing it to theory would require more extensive modeling. For the purpose of verifying the diffractive BLU concept, these experiments are adequate.

5 Conclusions

In principle, the results show that a diffractive BLU concept based on a pixelated structure of gratings with grating parameters selected for the respective primary colors of the backlight light sources is possible.

It is clear from the results that the blue and red grating used as a joint outcoupling structure is not effective for both bands of light. This was expected also from theory. Therefore, a dedicated grating for each primary color is needed. The original principle of separation of green and blue by having the green grating perpendicular to the red and blue grating was working, and the rejection of unwanted radiation from both gratings was observed.

With a fan-out grating, the directive effect of the light emission could be spread out throughout the structure, most likely giving good outcoupling characteristics and a good uniformity across the whole backlight module. A dif-fuser would be needed on top of the display stack to control the eventual viewing-angle characteristics of the display. Also, in an actual BLU based on grating arrays, a degree of modulation based on the diffraction efficiency or the pro-

portional area of the grating with respect to the intended subpixel needs to be designed in the BLU to improve the uniformity of the illumination.

The concept presented in this study could effectively reduce the display backlight power dissipation significantly to enable slimmer, smaller and smarter mobile phones with brighter video-capable displays. Ideally, compared to the state of the art, by directing the respective primary spectral bands of light from the red, green, and blue LEDs through their respective color subpixels, the efficiency of a display system could be increased from roughly 10% of today's to nearly 100%. Furthermore, by using dedicated primary color lights sources for red, green, and blue illumination, controlling the display color space and optimizing the power usage of the display would be easy to realize by software means. The resulting structure of the BLU would in principle also become simpler by using diffractive light guides because there is no need for collimating films between the BLU light guide and the LCD. However, there remains the need to register the BLU and LCD subpixels on top of each other, which adds an alignment step in manufacturing. In addition, for best efficiency and for best rejection of crosstalk, slanted gratings³⁰ would be required for all respective primary colors in the BLU array, making the master-grating-array manufacturing a complicated process.

Expanding the scope of pixelated diffractive BLUs beyond mobile-phone use would impose demands on alignment accuracy, and thermal-expansion issues in large-area systems such as in LCD-TV displays would especially require special attention.

We aim to further study larger structures based on more complicated and truly pixelated grating arrays. Also, a verification of a fan-out grating is needed to determine the feasibility of the concept to be integrable in a real display. Studies with actual displays in conjunction with these backlight structures are in the planning phase.

Acknowledgments

The authors thank Tampere University of Technology Optoelectronics Research Centre for the AFM image (Fig. 3), and NanoComp Oy for the grating manufacturing. Also, we thank Ms. Marja Salmimaa, Mr. Toni Järvenpää, and Dr. Pekka Äyräs of Nokia Research Center for their help in making the measurements for this study.

References

- 1 Y. Neuvo, "Cellular phones as embedded systems," *IEEE Solid-State Circuits Digest Tech. Papers (ISSCC)*, **1**, 32–37 (2004).
- 2 J. Kimmel, "Displays enabling mobile multimedia," *Proc. SPIE* **6507**, 650705-1–650705-11 (2007).
- 3 J. Bergquist and C. Wennstam, "Field-sequential-color display with adaptive gamut," *SID Symposium Digest Tech. Papers* **37**, 1594–1597 (2006).
- 4 G. Hooker and D. Smith, "Illuminated LCD apparatus," U.S. Patent No. 5,477,422 (1995).
- 5 A. G. Chen, K. W. Jelley, G. T. Valliath, W. J. Molteni, P. J. Ralli, and M. M. Wenyon, "Holographic reflective liquid-crystal display," *J Soc. Info. Display* **3**, 159–268 (1995).

- 6 J. Kimmel, J. Hautanen, and T. Levola, "Display technologies for portable communication devices," *Proc. IEEE* **90**, 581–590 (2002).
- 7 M. Suzuki, "Two approaches to the luminance enhancement of backlighting units for LCDs," *J. Soc. Info. Display* **7**, 157–161 (1999).
- 8 J. H. Min, H. Y. Choi, M. G. Lee, J. S. Choi, J. H. Kim, and S. M. Lee, "Holographic backlight unit for mobile LCD devices," *J. Soc. Info. Display* **11**, 653–657 (2003).
- 9 H. Y. Choi, M. G. Lee, J. H. Min, and J. S. Choi, "Hologram based light-guide plate for LCD-backlights," *Proc. Asia Display/IDW '01*, 521–524 (2001).
- 10 K. Kälantär, "Functional light-guide plate for backlight unit," *SID Symposium Digest Tech. Papers* **30**, 764–767 (1999).
- 11 K. Kälantär, S. Matsumoto, T. Onishi, and K. Takizawa, "Optical micro deflector based functional light-guide plate for backlight unit," *SID Symposium Digest Tech. Papers* **31**, 1029–1031 (2000).
- 12 S. Matsumoto, K. Kälantär, T. Onishi, and K. Takizawa, "Functional light-guide plate characterized by optical micro-structures for LCD backlight unit," *Proc. IDW '00*, 463–465 (2000).
- 13 K. Kälantär, Y. Nishiyama, A. Kakimoto, S. Matsumoto, and K. Takizawa, "Micro-structured light-guide plate for efficient backlighting transmissive LCDs used in mobile phones and PDAs," *Proc. Asia Display/IDW '01*, 645–647 (2001).
- 14 S. M. P. Blom, H. P. M. Huck, and H. J. Cornelissen, "Towards polarised light emitting back lights: Micro-structured anisotropic layers," *Proc. Asia Display/IDW '01*, 525–528 (2001).
- 15 H. J. B. Jagt, H. J. Cornelissen, and D. J. Broer, "Micro-structured polymeric linearly polarized light emitting lightguide for LCD illumination," *SID Symposium Digest Tech. Papers* **33**, 1236–1239 (2002).
- 16 H. J. B. Jagt, H. J. Cornelissen, D. J. Broer, and C. W. M. Bastiaansen, "Linearly polarized light-emitting backlight," *J. Soc. Info. Display* **10**, 107–112 (2002).
- 17 S. M. P. Blom, H. P. M. Huck, H. J. Cornelissen, and H. Greiner, "Towards a polarized light-emitting backlight: Micro-structured anisotropic layers," *J. Soc. Info. Display* **10**, 209–213 (2002).
- 18 H. J. Cornelissen, H. P. M. Huck, D. J. Broer, S. J. Picken, C. W. M. Bastiaansen, E. Erdhuisen, and N. Maaskant, "Polarized light LCD backlight based on liquid crystalline polymer film: A new manufacturing process," *SID Symposium Digest Tech. Papers* **35**, 1178–1180 (2004).
- 19 K.-W. Chien and H.-P. D. Shieh, "Design and fabrication of an integrated polarized light guide for liquid-crystal-display illumination," *Appl. Opt.* **43**, 1830–1834 (2004).
- 20 P. H. Yao, I. K. Pan, and T. H. Lin, "Micro-structure optical film with hybrid functions," *SID Symposium Digest Tech. Papers* **37**, 851–853 (2006).
- 21 "TPO bows 2.0-in. QVGA LTPS module," *Mobile Display Report*, No. 7, 31 (2007).
- 22 H. Dammann, "Color separation gratings," *Appl. Opt.* **17**(15), 2273–2279 (1978).
- 23 D. G. Pelka, C. C. Rich, J. M. Petersen, and K. H. Patel, "Replication of microstructured display films," *SID Symposium Digest Tech. Papers* **34**, 72–75 (2003).
- 24 J. Qi, J. Petersen, and K. Patel, "Tailored holographic micro-diffusers for display applications," *SID Symposium Digest Tech. Papers* **35**, 314–317 (2004).
- 25 J. Qi, J. Petersen, and C. Rich, "Tailored elliptical holographic diffusers for LCD applications," *J. Soc. Info. Display* **13**, 781–786 (2005).
- 26 D. R. Selviah and K. Wang, "Modeling of a color-separating backlight with internal mirrors," *SID Symposium Digest Tech. Papers* **35**, 487–489 (2004).
- 27 T. Levola, "Diffraction optics for virtual reality displays," *Proc. IDRC*, 542–545 (2005).
- 28 T. Levola, "Diffraction optics for virtual reality displays," *J. Soc. Info. Display* **14**, 467–475 (2006).
- 29 T. Levola, "Novel diffractive optical components for near to eye displays," *SID Symposium Digest Tech. Papers* **37**, 64–67 (2006).
- 30 T. Levola, and P. Laakkonen, "Replicated slanted gratings with a high refractive index material for in and outcoupling of light," *Opt. Express* **15**, 2067–2074 (2007).
- 31 R. Petit (ed.), *Electromagnetic Theory of Gratings* (Springer-Verlag, Berlin, 1980).
- 32 "Micro SideLED® Enhanced Optical Power LED (Thin GaN®), Blue/True Green," Osram Datasheet (2006).
- 33 "Micro SideLED® Enhanced Thin Film LED, Red," Osram Datasheet (2006).



Jyrki Kimmel received his M.Sc. and Licentiate of Technology degrees in electrical engineering from the Tampere University of Technology in 1986 and 1992, respectively. He is currently principal researcher at the Nokia Research Center in Tampere, Finland. He also lectures on display-related topics at Tampere University of Technology. Before joining Nokia in 1996, he was with the Technical Research Centre of Finland and was a Fulbright Scholar at the University of Utah. His current research interests relate to mobile displays, especially backlights. He has been active in SID, at Chapter- and Board-level duties. He was the European Regional Vice-President of SID during 2004–2006, and currently acts as the Chapter Formation Chair of SID.



Tapani Levola received his M.Sc. degree in 1976 from the University of Turku in physics and his Ph.D. degree from the University of Joensuu in 2005 in the field of diffractive optics. Before joining Nokia in 1996, he worked on the R&D of semiconductor manufacturing systems. He is now a Research Fellow at the Nokia Research Center in Tampere.



Pasi Saarikko received his M.Sc. degree in 1995 and his Post-Graduate degrees of Licentiate in Technology in 1997 and Doctor of Science in 2000 from Helsinki University of Technology. In 2001, he joined the Institute of Quantum Optics at the University of Hannover where he worked as a post-doctoral researcher on experimental Bose–Einstein condensation. In 2002, he moved to Philips Medical Systems MR Technologies Finland, to work as a R&D project manager on interventional magnetic-resonance imaging. Currently, he is working as a Principal Scientist at Nokia Research Center. His research interests include rigorous analysis of hybrid optical systems, including diffractive and refractive elements and their application to imaging devices.



Johan Bergquist received his M.S. and Ph.D degrees in physics from Chalmers University of Technology in 1988 and 1994, respectively. From 1988 to 1992, he worked as a staff scientist at the Quantum Electro-Optics Laboratory of Canon Research Centre and also spent 1 year as strategic R&D analyst at the company's R&D headquarters. After a post-doctorate period at the Electronics Engineering Department of the University of Electro-Communications, Tokyo, he joined the University of New Mexico's Asian Technology Information Program in Tokyo where he worked as senior technology analyst and manager of a DARPA-funded project on flat-panel-display technologies. In 1999, he joined the Visual Communications Laboratory of Nokia Research Center in Tokyo as senior research engineer and is currently principal scientist at the Display Research Group of Nokia Technology Platforms.

Publication [P3]

J. Kimmel, T. Levola, and P. Laakkonen, "Diffractive Backlight Grating Array for Mobile Displays," *JSID*, Vol. 16, No. 8, pp. 863-870, 2008.

Copyright © 2008 Society for Information Display.
Reprinted with permission.

Diffractive backlight grating array for mobile displays

Jyrki Kimmel (SID Member)

Tapani Levola (SID Member)

Pasi Laakkonen

Abstract — The display backlight unit (BLU) is the most power-consuming subunit in mobile liquid-crystal displays. The state-of-the-art BLUs utilize scattering, refractive, and reflective microstructures to generate a uniform distribution of white light through the display. More effective means of transmitting light through the display color filters could be obtained by using diffraction, but previously proposed diffractive backlights do not fully utilize all the possibilities to design gratings effectively for optimal color separation and outcoupling. This paper presents a new pixelated diffractive backlight grating array as an approach for overcoming these obstacles in BLU design. A model array was fabricated to couple out red, green, and blue primary colors from the respective subpixel locations. The results show that it is possible to manufacture such an array and that the light couples out as intended, giving a starting point to design mobile-display modules with low light-transmission losses.

Keywords — Active-matrix liquid-crystal display, backlight unit, diffractive grating array.

1 Introduction

Display backlights in mobile devices consume the majority of electrical power in the mobile-device user interface.^{1,2} For the best user experience, it is important to find solutions to reduce the power dissipation of mobile devices, and the backlight unit (BLU) is the most obvious subunit of interest in improving the power efficiency of mobile-display-module design. The demand to reduce the power consumption of mobile-phone displays is increasing also due to the new use models of mobile devices that have risen due to the adoption of new mobile services such as video telephony, imaging, gaming, and navigation. These applications generally demand a higher-resolution display while keeping the size of the display still pocketable; thus, pixel density is increased and the active aperture area of each color subpixel is reduced. This in turn means that the transmission of light through the display structure is getting proportionately lower.

Present state-of-the-art commercial BLU designs use scattering, refraction, or reflection for light outcoupling. The backlights are designed to provide a uniform distribution of white light that exits the BLU front face in a controllable manner. However, a lot of the available light is wasted, as this broad spectrum of essentially white light is spread along a pixel array of primary color filters that pass through light of their respective primaries, usually red, green, and blue.

Diffractive backlight concepts have been proposed recently where a grating pattern is formed on a backlight in a pixelated fashion.^{3–6} One of the objectives, besides improving the luminous efficiency of the display module, has been to design a BLU that allows a display module design with no color filters.³ In these previous studies, either the grating pattern diffracts the entire visible spectrum and has poor

control of the diffraction orders, resulting in a complicated structure with microlenses and micromirrors,³ or the gratings have been used in a spectrum-specific fashion but not in a fully pixelated way.^{4,5}

This paper builds on the previous study of Kimmel *et al.*,^{4,5} where a striped grating pattern was manufactured to demonstrate the feasibility of the diffractive-grating-array concept. This paper extends the striped grating pattern presented in Refs. 4 and 5 to a fully pixelated one. The expected benefits of this approach rely on results of a related study by Levola and Laakkonen that proved that it is possible to control the diffraction orders of incoming radiation of light in the visible range by using slanted gratings.⁷ These gratings have also been demonstrated to be replicable, giving a realistic outlook on manufacturing diffractive grating BLUs.⁷

A 1×1 -cm array of gratings, $56 \times 3 \times 56$ subpixels, representing a subsection of a proposed 2.8-in.-diagonal QVGA (320×240 pixels) display, was designed and manufactured by UV-embossing on an episulfide polymer light guide to verify the principle of the new backlight concept. The results show that it will be possible to design and manufacture a full mobile-display backlight using a similar array extending to the complete active area of the display. These results are applicable to displays that modulate the light from an external light source, in a manner that a liquid-crystal display (LCD) modulates the intensity of light from the BLU. Moreover, the diffractive approach is most beneficially suited for such displays where the active area is divided in subpixels that pass light corresponding to the selected primary colors of light, usually red, green, and blue. Other approaches, such as field-sequential displays (FSC) have been proposed to reduce power consumption,⁸ but since these displays modulate the color-specific subfields of light in a temporal fashion, the grating array approach will not

Extended revised version of a paper presented at EuroDisplay 2007 held September 17–20, 2007 in Moscow, Russia.

J. S. Kimmel and T. Levola are with Nokia Research Center, P.O. Box 1000, Visiokatu 1, 33721 Tampere, Finland; telephone +358-50-483-5484, fax +358-71-803-5322, e-mail: jyrki.kimmel@nokia.com.

P. Laakkonen is with NanoComp Ltd., Finland.

© Copyright 2008 Society for Information Display 1071-0922/08/1608-0863\$1.00

apply to FSC displays. An important category of mobile displays is the organic light-emitting diode (OLED) display.^{9,10} In these displays, the light emitted by the display is generated directly at each subpixel, and grating arrays will not be required in these displays either. The power consumption of OLEDs is highly dependent on the content to be displayed, as the electric power is transduced to emitted light for the most part only at the lit subpixels. The power consumption of LCDs does not, in the fundamental and most usually applied configuration, depend on the displayed content, and thus power reduction by use of the proposed subpixel-specific grating arrays is a widely applicable concept in mobile LCDs.

2 State of the art of backlight light guides and the pixelated BLU concept

2.1 State of the art of backlight light guides

The purpose of the backlight unit (BLU) is to gather the light from the available light sources, spread it along the BLU to form a uniform output pattern, and to launch the light into the display component itself. The light guide inside the BLU is the key component in the main tasks of the BLU. The input region of the light guide gathers the light from the light-emitting diodes (LEDs) or other suitable light sources and provides the initial direction to which the light is launched. Launching the light into the light guide requires careful engineering of the incoupling region to provide for minimal loss of light,¹¹ and already systems with adequate luminance for lighting a mobile display from only one LED have been proposed.¹² The light guide itself is a molded piece of transparent plastic that guides the light emitted by the light sources inside the light guide itself by total internal reflection (TIR). Outcoupling is generally distributed throughout one of the surfaces of the light guide in order to provide an efficient and uniform way for the light to enter the display component, in most cases the LCD.

The earliest voice-based applications for mobile phones only required the number to be called to be shown on the display. Simple segment or alphanumeric displays with icons were sufficient for this purpose, and these could be lit by monochrome LEDs. Therefore, the light-guide design was also very simple, most often only a roughened plate of molded transparent plastic was used. Possible hot-spots could be removed by dimming the reflector area close to the input coupling area of the LEDs.¹³ As the power constraints became more severe, and as the legibility of the display needed improvement, more advanced light-guide designs were required. Holographic reflectors were used to steer the glare of ambient-light sources away from the user,¹⁴ and groove patterns on the top of the light guide were beginning to be used.¹⁵ These approaches still satisfied the users of the second-generation mobile services, as even the games were very simple, and short message service (SMS) was the main feature of advanced communications in the phones.^{9,10} As the first color-screen phones appeared on

the market by the end of the 1990s, also wide spectrum light sources such as white LEDs and miniature cold-cathode fluorescent lamps (CCFLs) were used in more advanced products.^{9,10} The light-guide design also required better uniformity and spectrally independent output characteristics. Light guides quickly started to apply more advanced features such as statistically distributed scattering centers, reflecting and refracting output coupling designs,¹⁵ and, finally, microreflector and refractor arrays.^{16,17} This development, along with the application of collimating films, resulted in highly efficient light guides with good uniformity.¹⁸ However, these BLUs, when viewed through the entire display structure, could transmit only a few-percent transmission of the light from the LEDs to the viewer. This is because the light was treated as a uniform "sheet" of white light that then was steered through the LCD TFT array.¹⁵ There, the color filter, active aperture area, and the polarizing character of the LCD resulted in a total theoretical loss of 90% even when not counting in the material losses of the polarizers and the color filters.

Additional efficiency has been sought by studying polarizing backlights^{19–22} and diffractive backlights.^{3–6,11,23} Integration of several films in the backlight is now a trend, and hybrid functionality is employed in a single film, giving good potential to thinner display backlights.^{24,25} Total thickness of an LCD module below 1 mm has been reported, indicating rapid advancements in the integration of display modules.²⁶

2.2 The pixelated BLU concept

The pixelated BLU relies on a new diffractive light-guide structure that integrates the incoupling and outcoupling functions of the BLU light guide. In contrast to previous studies on diffractive light guides that are generally based on single-period, pixelated or uniform, gratings that extend under the entire display active area,^{3,6,11,23} the new diffractive light guide presented in this study is based on individual gratings that correspond to the display-component TFT-array subpixel structure. Previous studies by Levola and Laakkonen⁷ indicate that it is possible to manufacture small, slanted grating arrays and grating patterns where the slant directions even oppose each other. These structures have been proven experimentally to be replicable by UV-embossing. Up to over 500 replications from a single master grating has been demonstrated without degradation to either the master pattern or the replicated grating itself.⁷ This, and the previous study on striped grating arrays,^{4,5} lead to the conclusion that a fully pixelated array for mobile displays is possible to be manufactured.

Figure 1 shows the new BLU concept in broad detail. Light from red, green, and blue LEDs is launched into the BLU from different corners of the BLU. The light is then spread out into uniform beams propagating in the backlight, by fan-out gratings. A pixel array of gratings is then used for outcoupling the light toward the LCD pixel array. With

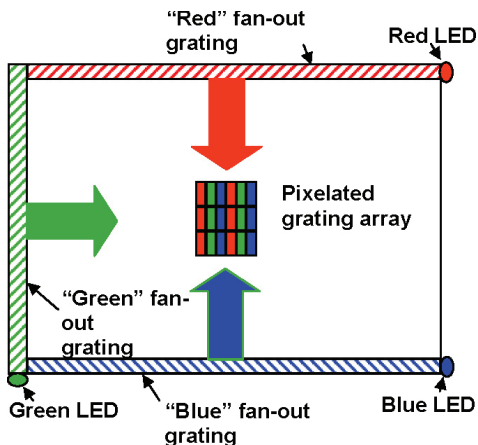


FIGURE 1 — Pixelated backlight concept, not to scale.

polarizing gratings, there would be no need for a polarizer between the BLU and the LCD. Also, by designing the BLU grating array to pass light through the active aperture area only, it is possible to prevent unwanted light from hitting the areas outside the active aperture of the LCD pixel, such as the transistor or reflector areas of transfective LCDs. Since separate gratings are used for red, green, and blue primaries, with good control of crosstalk, the light of the primary colors is only passed through the spectrally respective subpixels. An optimal design of these backlights can reduce the power consumption of the mobile-display backlight dramatically due to these inherent benefits of the diffractive BLU concept.

3 Grating-array design

A $56 \times 3 \times 56$ subpixel (1 cm^2) model array was designed for verifying the concept of the pixelated diffractive backlight. The individual grating structures had a 50% filling ratio, and the slanted gratings were designed using the principles presented in Ref. 7. To take in account a possible use in an LCD, the red and blue gratings were designed for TE polarization, and the green grating for TM (due to the orthogonal direction of propagation of the green light). The grating parameters are summarized in Table 1. Since episuifide was intended to be used as the substrate, the

TABLE 1 — Grating parameters.

Primary	Width (μm)	Depth (nm)	Grating period (nm)	Grating slant direction ($^\circ$)
Red (640 nm)	54	340	530	+45
Green (525 nm)	54	340	430	+20
Blue (460 nm)	54	240	375	-45

parameters were defined for the high refractive index ($n = 1.717$ at $\lambda = 525 \text{ nm}$) of this polymer.

The goal of the grating design is to maximize the out-coupling and to minimize the crosstalk of different colors. The groove orientation of the green grating with respect to blue and red grating grooves is 90° , which eliminates effectively any crosstalk between green and blue as well as green and red light. The crosstalk between blue and red is more problematic but can be solved reasonably well using slanted gratings that have their slanting angles at opposite directions. The polarization of the outcoupled light has a preferred direction and in this case it seems to be most convenient that blue and red are coupled out using TE coupling and green using TM coupling because the green grating vector is perpendicular to the blue and red ones, and therefore all the gratings produce the same polarization with respect to the pixel array. As the green outcoupling is well separated from the blue and red ones, it can be optimized by itself taking into account coupling efficiency and angular dependence. Generally, it is assumed, also in the cases of blue and red light sources, that the average angle of the beam inside the waveguide is 50° with respect to the plate normal. In practice, this would be achieved by cutting the edge of the light-guide plate to the desired angle and placing the light source at normal incidence to the cut edge. The beam has naturally some divergence, but this issue can be optimized by adjusting the grating shape.

In the design of the blue and red gratings, the main problem is the crosstalk of these colors. With the parameters in Table 1, the rigorous calculation reveals that diffraction efficiency of the blue light from the red grating is about 1/3 of the efficiency of diffraction of red light. The main part of this crosstalk is due to the second-order diffraction which alters the propagation direction of the beam. This second-order mode does not exist in the diffraction of red light from the blue grating. Therefore, the diffraction of red light from the blue grating is practically zero. Figure 2 shows the result of ray-tracing modeling for a blue point light source with a cosine law output radiation distribution, for several edge-cut angles of the light-guide plate, giving the output characteristics of the diffracted radiation from the "blue" and "red" gratings.

Finally, to fabricate the grating-array prototype, the dimensions of the individual subpixels in the grating-array design were intended to match a prospective pixel structure in an actual display, and taking in account the area required for the display pixel electronics and reflector structures, the individual subpixels were $54 \times 135 \mu\text{m}$ each, in a $177\text{-}\mu\text{m}$ -square matrix, arranged periodically to red, green, and blue subpixels.

4 Grating-array prototype and characterization

The grating master was manufactured on fused silica by Nanocomp Oy in Joensuu, Finland, using lithographic manufacturing methods.²⁷⁻²⁹ The starting point for the

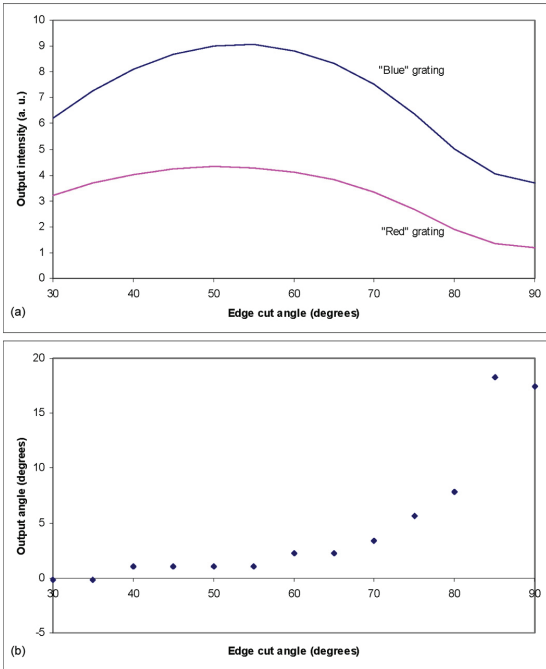


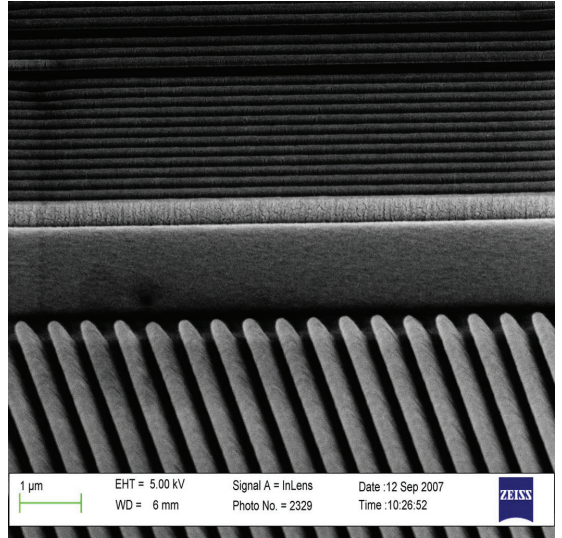
FIGURE 2 — Modeling of the output characteristics of the “blue” and “red” gratings for a blue point source with wavelength $\lambda = 460$ nm (a) Output intensity of blue radiation from the “blue” grating and “red” grating as a function of the edge-cut angle and (b) the output angle of the maximum intensity of outcoupling for blue light as a function of the edge-cut angle.

processing was a SiO_2 plate with a size of $5 \times 5 \times 0.09$ in. added with a 100-nm-thick chromium layer. On the top of the chrome a ZEP520 resist was spin coated to 200 nm thickness followed by the resist baking process. The resist exposure was performed by using a Gaussian electron-beam lithography process. After the resist development process with the resist manufacturer’s resist solutions, the resist grating on chrome was obtained. Then, the resist layer was transferred into the chrome layer by a standard chrome dry-etching process and a rigid grating structure for the following processes was obtained in chrome layer.

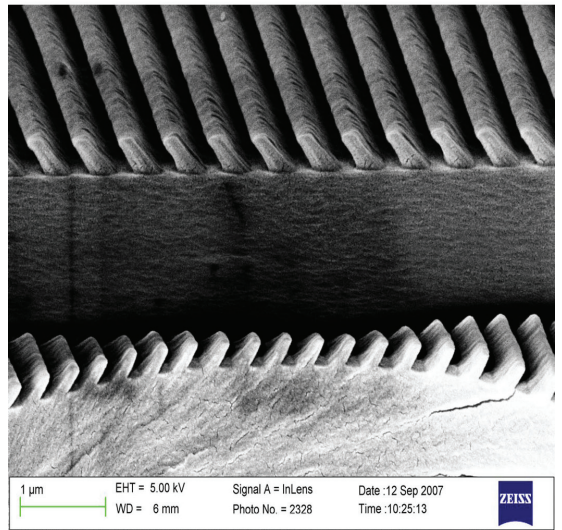
In order to manufacture gratings into three slanting angles, a masking process is needed. For this, three separate amplitude masks with a size of $6 \times 6 \times 0.09$ in. were manufactured by using the above-mentioned process. The only difference was that the grating apertures for R, G, and B pixels were transparent for light (and the other area in the amplitude mask was dark). In all masks the alignment marks were manufactured during the lithographic processing for the following alignment process.

After manufacturing the amplitude masks, the grating master was spin coated with a 500-nm-thick standard photoresist. Then a mask aligner with the manufactured amplitude mask was used and opened the “B” patterns from the resist (on the top of the chrome grating layer). The develop-

ment of the photoresist was made by using a standard NaOH developer solution. After opening the “B” pixels the mask was used in a reactive-ion e-beam etching equipment by adding fluorine compounds in the ion beam. This provides better than 10:1 selectivity between SiO_2 and Cr, and consequently the etching of the slant with an oblique incidence angle was easy and slanted gratings were obtained in SiO_2 . After the etching process, the photoresist was removed



(a)



(b)

FIGURE 3 — Scanning-electron-microscope images of the replicated grating array (a) “Green” grating lines at right angles to the “red” grating lines and (b) “blue” and “red” grating slanting directions in opposite directions to each other.

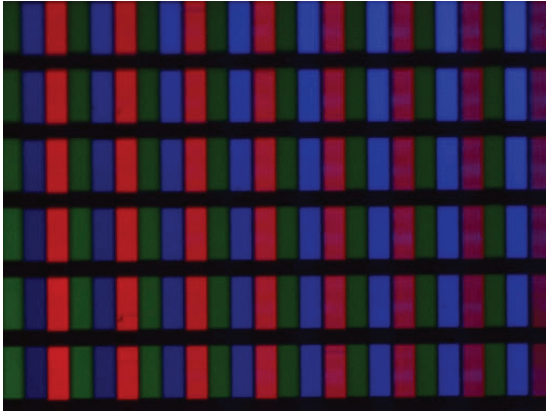


FIGURE 4 — Microscope image of the grating array.

by a strong NaOH solution and the process was repeated for “G” and “R” pixels. Finally, when all the gratings were etched into SiO₂, the remaining Cr layer was removed by a standard chrome wet-etching solution.

In order to manufacture replicas from the manufactured SiO₂ master, an anti-adhesion layer is needed. For this

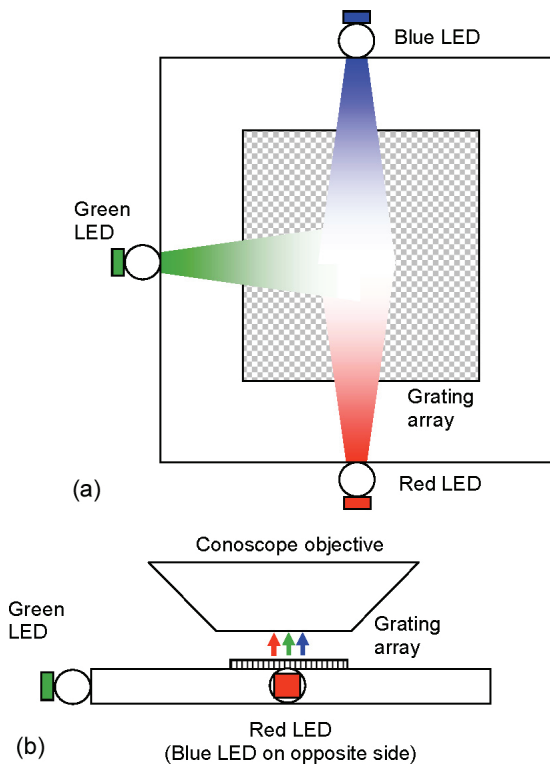


FIGURE 5 — Illumination setup for the conoscope measurements. (a) Top view, (b) side view.

TABLE 2 — LED parameters (Refs. 31 and 32).

LED	Dominant wavelength (nm)	FWHM (nm)*	Luminous intensity at 20 mA (mcd)
Red	625	19	180–900
Green	528	33	560–1800
Blue	460	25	90–280

*FWHM: Full width at half maximum.

the SiO₂ master mould was anti-adhesion treated with a standard process by immersing the sample in a 0.2% solution of tridecafluoro-1,1,2,2-tetrahydro-octyl-trichlorosilane by using methyl-nonafluoro-butylether as the solvent for 10 minutes and then immersing in pure methyl-nonafluoro-butylether for 10 minutes. The drying of the mask was done under nitrogen atmosphere. The chemical formula of tridecafluoro-1,1,2,2-tetrahydrooctyl-trichlorosilane is CF₃(CF₂)₅(CH₂)₂SiCl₃ and methyl-nonafluorobutylether was commercially available under the trade name “HFE-1700” by the 3M Minnesota Mining & Manufacturing Co. This anti-adhesion layer is suitable for hundreds of the replication processes with plastic epoxies.

The array prototype was manufactured by ultraviolet (UV) embossing on episulfide polymer (Mitsubishi Gas Chemicals) in the laboratory at Nokia Research Center in Helsinki. The grating substrate was an episulfide plate, about 1 mm thick, and the UV embossing was made in a Spectrolinker XL-1500 UV Crosslinker, on a hot plate heated to 60°C. After the anti-adhesion treatment, the slanted gratings with three angle directions were replicated from the SiO₂ mould.³⁰ Small parts of thermally cured episulfide material were used.⁷ The SiO₂ master mould was then placed on a metallic plate having uniform temperature of 60°C, and a small drop of UV-curable episulfide was dispensed with a pipette on the grating master. After this, the plastic substrate was placed on the UV-curable episulfide droplet without applying any pressure, and the whole assembly was cured with an UV energy of approximately 120 mJ/cm² (the UV lamp spectrum had the maximum at λ_{UV} = 360 nm). The replica was separated by peeling off with a knife from the plastic substrate edge and no separation problems were observed even though the individual gratings in the mould had slanting angles to the opposite directions. The resulting gratings could be replicated without visible degradation, as can be expected from Ref. 7. The obtained replication result proves that the slanted replication even with three directions is possible with good quality. Figure 3 shows SEM images of the replicated gratings. The gratings were scribed from the back of the sample and broken apart giving a sharp edge for SEM profile images.

Figure 4 shows an image where single 0.6-mm Osram LEDs (red, green, and blue^{31,32}), were placed at the edges of the display to illuminate the grating array. The light output of the LEDs was partially collimated toward the edge of

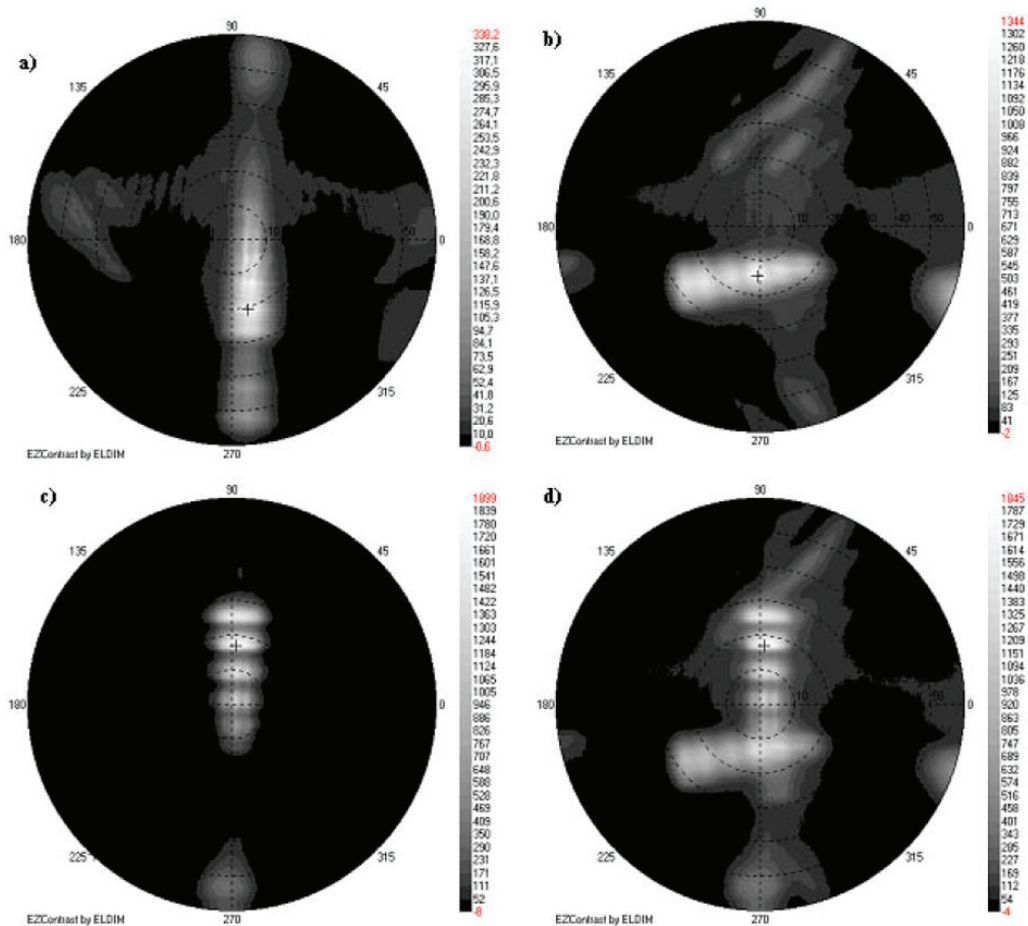


FIGURE 6 — Polar-coordinate plots from the conoscope measurement results (a) Blue, (b) green, (c) red, and (d) all colors combined.

the array plate by using 2-mm ball lenses (Edmund Optics). The image was taken with an Olympus digital camera mounted on a microscope. The LED parameters are shown in Table 2.

TABLE 3 — Angles about the zenith of the outcoupling maxima in the grating-array experiment.

Primary	Angle of maximum outcoupling (°)
Blue	20
Green	15
Red	17

The same illumination arrangement as in Fig. 4 was used in the characterization of the grating array (Fig. 5). The array was placed in front of an Eldim EZLite 120 R conoscope for measuring the angular distribution of the light output of the array. Conoscope measurements were performed for the individual primaries keeping the respective LED on, as well as for the “white” output keeping all LEDs on. The luminance levels with all LEDs off were negligible.

5 Results

The results of the characterization of the grating array show that the individual gratings used in the array performed as expected from the grating design. By visually examining the microscope image of the entire array, it can be seen that there is some leakage of blue into the red pixel, and in the

green illumination there is a slight shroud of light coupling out of the red and blue pixels. The exact amount of leakage was not measured. Figure 6 presents the results of the conoscope measurements. From these images, it is clear that the individual primaries are coupled toward the viewer quite effectively. Table 3 summarizes the conoscope measurement results. The individual color bands coupled out slightly obliquely, and the output distributions were narrow in cross section. A shroud of stray light was observed for all primary colors.

6 Discussion

There is a clear improvement over our previous results in the outcoupling of the individual primaries.^{4,5} Especially red is now directed toward the viewer instead of exiting in an oblique angle. This was expected due to the fact that the pixelated design includes an individual grating with a properly oriented slant angle for both red and blue primaries. Furthermore, from examining the microscope images of the grating output, it can be seen that the majority of the light is coupled out from the intended color-specific subpixel areas. Therefore, the light output is almost totally confined to the actual active area of the subpixel. The experimental results show a good correspondence with the modeling of the grating designs. Although we used a ball lens for improving the input coupling, the modeling results shown in Fig. 2 are not affected by the input coupling conditions to an appreciable degree. The effect of the edge-cut angle is much more prominent in affecting the output distribution.

Certain drawbacks are apparent in the initial design. Since the angular dependence of the light output is different for the individual colors, it is expected that a diffuser is required on the top of the display to reduce the color coordinate shift with viewing angle. This aspect requires further study. The output polar coordinate plots also show diffuse light output to unwanted directions, seen in Fig. 6 as dark-gray areas. The exact reasons for this have not been investigated, but the most likely reason is that since the LEDs were unpolarized, the uncoupled light of the unwanted polarization for each primary scattered into the viewing cone from the edge areas in the individual grating subpixels. In addition, since the grating input angle was optimized in the design of the gratings at 50°, the incoupling from the end face of the grating array was not the best possible one to achieve efficient outcoupling. Stray light from forward propagating modes that were not affected by the presence of the grating array may be one factor in the appearance of the extraneous light.

This is the first study to demonstrate the feasibility of using a slanted grating array in a BLU. It is planned to extend the studies of slanted grating arrays for BLUs to full-mobile-display-size grating arrays and to incorporate an effective fanout section for each primary color on the sides of the display to demonstrate the feasibility of the complete concept. The results of this study indicate that the pixelated

grating-array concept is a feasible one, and that by expending effort in proper design of the backlight unit it is possible to create a mobile display with improved power efficiency. Furthermore, the localization of the outcoupling of the primaries to the respective active areas of the subpixels makes it possible, by proper matching of the light sources and the gratings, to create BLU designs without a color-filter array in the display matrix itself.

Acknowledgments

The authors wish to thank Dr. Pekka Äyräs, Ms. Marja Salmimaa, and Mr. Toni Järvenpää for their help in making the measurements, as well as the entire Nokia Research Center display team for support. The authors also thank the Optoelectronics Research Center of the Tampere University of Technology for providing the SEM images (Fig. 3).

References

1. A. Iranli, W. Lee, and M. Pedram, "HVS-aware dynamic backlight scaling in TFT-LCDs," *IEEE Trans. VLSI Systems* **14**, 1103–1116 (2006).
2. Y. Neuvo, "Cellular phones as embedded systems," *IEEE Solid-State Circuits Conf. Digest of Technical Papers* **1**, 32–37 (2004).
3. D. R. Selviah and K. Wang, "Modeling of a color-separating backlight with internal mirrors," *SID Symposium Digest Tech. Papers* **35**, 487–489 (2004).
4. J. Kimmel, T. Levola, P. Saarikko, and J. Bergquist, "A novel diffractive backlight concept for mobile displays," *SID Symposium Digest Tech. Papers* **39**, 42–45 (2007).
5. J. Kimmel, T. Levola, P. Saarikko, and J. Bergquist, "A novel diffractive backlight concept for mobile displays," *J. Soc. Info. Display* **16**, 351–357 (2008).
6. S. R. Park, O. J. Kwon, D. Shin, S.-H. Song, H.-S. Lee, and H. Y. Choi, "Grating micro-dot patterned light guide plates for LED backlights," *Opt. Express* **15**, 2888–2899 (2007).
7. T. Levola and P. Laakkonen, "Replicated slanted gratings with a high refractive index material for in and outcoupling of light," *Opt. Express* **15**, 2967–2074 (2007).
8. J. Bergquist and C. Wennstam, "Field-sequential-color display with adaptive gamut," *SID Symposium Digest Tech. Papers* **37**, 1594–1597 (2006).
9. J. Kimmel, J. Hautanen, and T. Levola, "Display technologies for portable communication devices," *Proc. IEEE* **90**, 581–590 (2002).
10. J. Kimmel, "Displays enabling mobile multimedia," *Proc. SPIE* **6507**, 650705-1–650705-11 (2007).
11. J. H. Min, H. Y. Choi, M. G. Lee, J. S. Choi, J. H. Kim, and S. M. Lee, "Holographic backlight unit for mobile LCD devices," *J. Soc. Info. Display* **11**, 653–657 (2003).
12. A. Funamoto, Y. Kawabata, M. Ohira, and S. Aoyama, "Prism-sheetless high bright backlight system for mobile phone," *Proc. IDW '04*, 687–690 (2004).
13. G. Hooker and D. Smith, "Illuminated LCD apparatus," U.S. Patent No. 5,477,422 (1995).
14. A. G. Chen, K. W. Jelley, G. T. Valliath, W. J. Molteni, P. J. Ralli, and M. M. Wenyon, "Holographic reflective liquid-crystal display," *J. Soc. Info. Display* **3**, 159–268 (1995).
15. M. Anandan, "Progress of LED backlights for LCDs," *J. Soc. Info. Display* **16**, 287–310 (2008).
16. K. Kälantär, "Functional light-guide plate for backlight unit," *SID Symposium Digest Tech. Papers* **30**, 764–767 (1999).
17. K. Kälantär, S. Matsumoto, T. Onishi, and K. Takizawa, "Optical micro deflector based functional light-guide plate for backlight unit," *SID Symposium Digest Tech. Papers* **31**, 1029–1031 (2000).
18. K. Kälantär, Y. Nishiyama, A. Kakimoto, S. Matsumoto, and K. Takizawa, "Micro-structured light-guide plate for efficient backlighting transmissive LCDs used in mobile phones and PDAs," *Proc. Asia Display/IDW '01*, 645–647 (2001).

- 19 H. J. B. Jagt, H. J. Cornelissen, D. J. Broer, and C. W. M. Bastiaansen, "Linearly polarized light-emitting backlight," *J. Soc. Info. Display* **10**, 107–112 (2002).
- 20 S. M. P. Blom, H. P. M. Huck, H. J. Cornelissen, and H. Greiner, "Towards a polarized light-emitting backlight: Micro-structured anisotropic layers," *J. Soc. Info. Display* **10**, 209–213 (2002).
- 21 H. J. Cornelissen, H. P. M. Huck, D. J. Broer, S. J. Picken, C. W. M. Bastiaansen, E. Erdhuisen, and N. Maaskant, "Polarized light LCD backlight based on liquid crystalline polymer film: A new manufacturing process," *SID Symposium Digest Tech. Papers* **35**, 1178–1180 (2004).
- 22 K.-W. Chien and H.-P. D. Shieh, "Design and fabrication of an integrated polarized light guide for liquid-crystal-display illumination," *Appl. Opt.* **43**, 1830–1834, (2004).
- 23 H. Y. Choi, M. G. Lee, J. H. Min, and J. S. Choi, "Hologram based light-guide plate for LCD-backlights," *Proc. Asia Display/IDW '01*, 521–524 (2001).
- 24 A. Nagasawa, T. Eguchi, Y. Sanai, and K. Fujisawa, "A novel backlight system with the unified component," *Proc. IDW/Asia Display '05*, 1285–1288 (2005).
- 25 P. H. Yao, I. K. Pan, and T. H. Lin, "Micro-structure optical film with hybrid functions," *SID Symposium Digest Tech. Papers* **37**, 851–853 (2006).
- 26 "TPO Bows 2.0-in. QVGA LTPS Module," Mobile Display Report, No. 7, 31 (2007).
- 27 M. A. McCord and M. J. Rooks, "Electron beam lithography," in: *Handbook of Microlithography, Micromachining, and Microfabrication. Vol. 1: Microlithography*, P. Rai-Choudhury, ed. (SPIE Press, Washington, 1997), pp. 139–250.
- 28 H. J. Levison, *Principles of Lithography* (SPIE Press, Washington, 2005).
- 29 J. R. Sheats and B. W. Smith, *Microlithography: Science and Technology* (Marcel Dekker, New York, 1998).
- 30 M. T. Gale, "Replication," in: *Micro-optics*, H. P. Herzig, ed. (Taylor & Francis, London, 1997).
- 31 Micro SideLED® Enhanced Optical Power LED (Thin GaAN®), Blue/True Green. Osram Datasheet (2006).
- 32 Micro SideLED® Enhanced Thin Film LED, Red. Osram Datasheet (2006).



Jyrki Kimmel received his M.Sc. and Licentiate of Technology degrees in electrical engineering from the Tampere University of Technology in 1986 and 1992, respectively. He is currently Principal Researcher at Nokia Research Center in Tampere, Finland. He also lectures on display-related topics at Tampere University of Technology. Before joining Nokia in 1996, he was with the Technical Research Centre of Finland, and a Fulbright Scholar at the University of Utah. His current research interests relate to mobile displays, especially backlights. He has been active in SID, at the Chapter and Board levels. He was the European Regional Vice-President of SID during 2004–2006.



Tapani Levola is a Research Fellow at the Nokia Research Center in Tampere, Finland, working in the field of displays and optics. Tapani Levola graduated in physics from the University of Turku, Finland, in 1976. He received his Ph.D. degree in physics from the University of Joensuu, Finland, in 2005. Before joining Nokia in 1998, he worked in the ultra-high-vacuum industry.



Pasi Laakkonen received his M.Sc. in 1997 and Ph.D. in 2000 from the University of Joensuu, Department of Physics and Mathematics. He has published 22 articles in refereed journals and published 32 conference papers. He has also submitted several patent applications in the field of diffractive optics. His work interest are modeling, manufacturing, and commercialization of diffractive optical components. Currently, he is CTO of Nanocomp and is also a part-time Research Manager at the University of Joensuu, Department of Physics and Mathematics.

Publication [P4]

J. Kimmel, T. Levola, S. Siitonen, and T. Rytönen, "A New Diffractive Backlight for Mobile Displays," Proc. IDRC 2008, pp. 290-293, 2008.

Copyright © 2008 Society for Information Display.
Reprinted with permission.

15.4: A New Diffractive Backlight for Mobile Displays

Jyrki Kimmel*, Tapani Levola*, Samuli Siitonen**, and Tuomo Rytönen**

*Nokia Research Center, 33721 Tampere, Finland

**Nanocomp Ltd., 80710 Lehma, Finland

Abstract: Power efficiency of mobile terminals has become a limiting factor of user interface development, as consumers expect a full internet experience from their mobile multimedia terminals. The backlight unit is the most power-hungry subsystem in the mobile user interface, and improving the system efficiency of the displays by designing novel backlight light guide plates has great potential in enabling future mobile multimedia terminals. This study presents a diffractive optics approach with experimental characterization of a new backlight light guide plate with spectrum-specific gratings for each subpixel of the overlaying display.

Keywords: display backlights; diffractive optics; mobile displays.

Introduction

Recent developments in mobile communication terminals have made it possible to effectively utilize the mobile phone as a multimedia device [1], and the development of mobile networks and wireless broadband services support the data transfer of multimedia content both to and from the mobile terminals. Today's mobile user can expect a reasonable mobile internet experience, and consequently the user interface needs to support the consumption of and interaction with mobile multimedia. Power consumption has become a limiting factor of mobile multimedia use, as the display needs to be on for appreciably longer periods of time as compared to the basic telephone call function of the mobile device. The display backlight unit (BLU) is the most power-hungry subsystem of the user interface [2], and power savings in the BLU are an intensive area of research.

The backlights of the common liquid-crystal displays (LCDs) of today's mobile phones are usually based on a light guide plate (LGP) with scattering centers or microreflectors distributed statistically across one face of the LGP. Light traveling under total internal reflection (TIR) conditions scatters or reflects toward the display when impinging on these structures, and the user sees the image on the LCD as the incoming light is modulated by the display. Since most commonly the LCD is divided into subpixels designed to filter light of the respective color primaries, a lot of the light is wasted in the absorption of the color filter, as well as in absorption of the masked areas of the display. Kimmel *et al.* developed a concept based on diffractive optics to direct the light from red (R), green (G), and blue (B) light-emitting diodes (LEDs) into the spectrum-specific subpixels of the display matrix [3-6]. This concept was experimentally verified to be feasible by using 1 cm² sized model gratings. The full concept requires a BLU made to conform to a prospective display, as well as

fanout structures to spread the light into the whole LGP. In this study, both these advancements have been fabricated, to be implemented in a prospective 128 (x3) by 160 pixel mobile display.

Diffractive Backlight Design and Fabrication

Diffractive backlights have been previously proposed with a pixelated but uniform grating structure [7]. This approach and other studies in diffractive BLUs require additional microlenses, micromirrors, and even dedicated display matrices [8] to effectively utilize the spectral separation of the colors. This paper extends the work done on grating arrays published before by Kimmel *et al.* [3-6] in that for the first time, a full display sized diffractive LGP without mirrors or microlens structures was fabricated. A mobile display module with 128 by 160 pixels with red, green, and blue (R, G, and B) subpixels in portrait orientation was used as the basis for the design. For each subpixel, a slanted grating was designed to diffract light of the corresponding spectral band toward the respective subpixel. The display parameters are shown in Table 1, and the grating parameters are shown in Table 2. In order to achieve good uniformity across the LGP, area modulation was used in the subpixel structure so that pixels closer to the light source only used a small portion of the center of the subpixel transmission window as an active grating area, and this area was increased toward the end of the array, so that 100% modulation was achieved at the end farthest from the light sources. Fanout grating arrays in a double bowtie arrangement were provided along the sides of the LGP to spread the incoming light from the LEDs used as light sources. These gratings were binary, with 50 % fill factor. Figure 1 shows the design in detail.

Table 1. Prospective display parameters for the backlight grating array.

Resolution	128 (x3) by 160
Pixel size	222 μm by 222 μm
Active area	29 mm by 36 mm
Display glass thickness	0.63 mm

A 52 mm by 54 mm LGP for the BLU was fabricated in the clean room at Nanocomp Ltd. in Joensuu area, Finland, from a fused silica master, on a 0.65 mm thick episulfide polymer substrate. The active grating matrix as well as the fanout gratings were manufactured by ultraviolet embossing from episulfide on top and bottom of the substrate, respectively, similarly to grating arrays reported

in previous work [4, 6]. The edges of the LGP were beveled to 45 degrees to allow efficient coupling of LEDs to the LGP, in order to spread the light in the fanout structure.

Table 2. Grating parameters.

Primary	Width by length	Depth (nm)	Grating period (nm)	Grating slant direction (degrees)
Red (640 nm)	111 μm by 59 μm	340	530	+45
Green (525 nm)	59 μm by 111 μm	340	430	+45
Blue (460 nm)	111 μm by 59 μm	240	375	-45
Red fanout (Double bowtie)	10 mm by 36 mm	450	360	0
Green fanout (Double bowtie)	8 mm by 29 mm	370	290	0
Blue fanout (Double bowtie)	10 mm by 36 mm	320	250	0

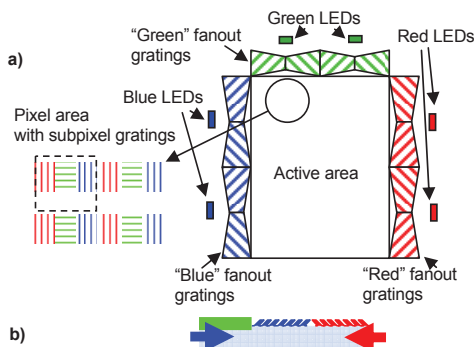


Figure 1. LGP layout. a) Grating arrangement from top, b) Direction of grating slants from the side ("green" slant perpendicular to both "blue" and "red" grating slants). The figures are not to scale.

Characterization Experiment

The experimental setup for the characterization is shown in Figure 2. The LGP was mounted on an X-Y translation stage. 0.6 mm thick Osram LEDs with dominant wavelengths of 625 nm (R), 528 nm (G), and 460 nm (B) [9, 10] were attached to supports that were cut and ground to a 45 degree angle to allow for effective incoupling of the light into the LGP. The LEDs were driven at the nominal 20 mA direct current. Two LEDs were used for each of the red, green, and blue primaries. This assembly was mounted

in front of a calibrated Eldim EZLite 120 R coscope at a location with maximum emission intensity. Polar plots of the outcoupled angular light distribution were obtained by the coscope for all individual primary colors as well as for all RGB LEDs on at the same time.

Results

By visual inspection, it was evident that the fanout gratings spread out the light only weakly, and streaks of light were prominently visible across the display from the incoupling points of the LEDs (see Figure 3). Figure 4 summarizes the coscope measurements. In addition, the angles of detected maxima of the angular distribution, as well as the measured full angular width of emission at half maximum intensity (FWHM) of outcoupled light are shown in Table 3.

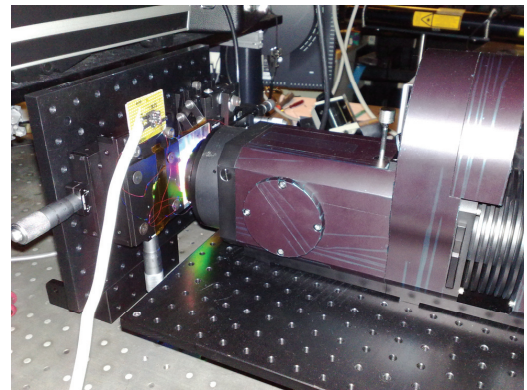


Figure 2. Experimental setup. Green LEDs illuminate the LGP from below.

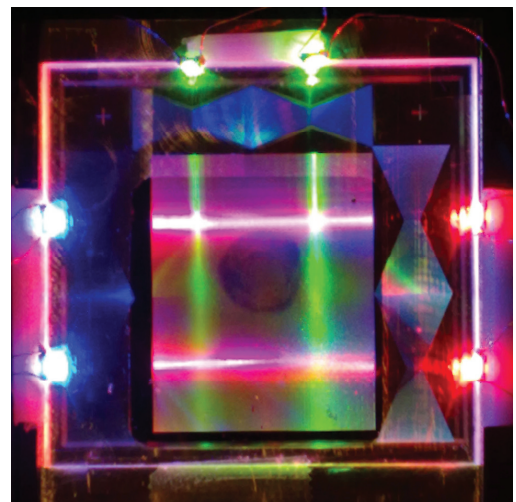


Figure 3. Diffraction LGP with all LEDs on.

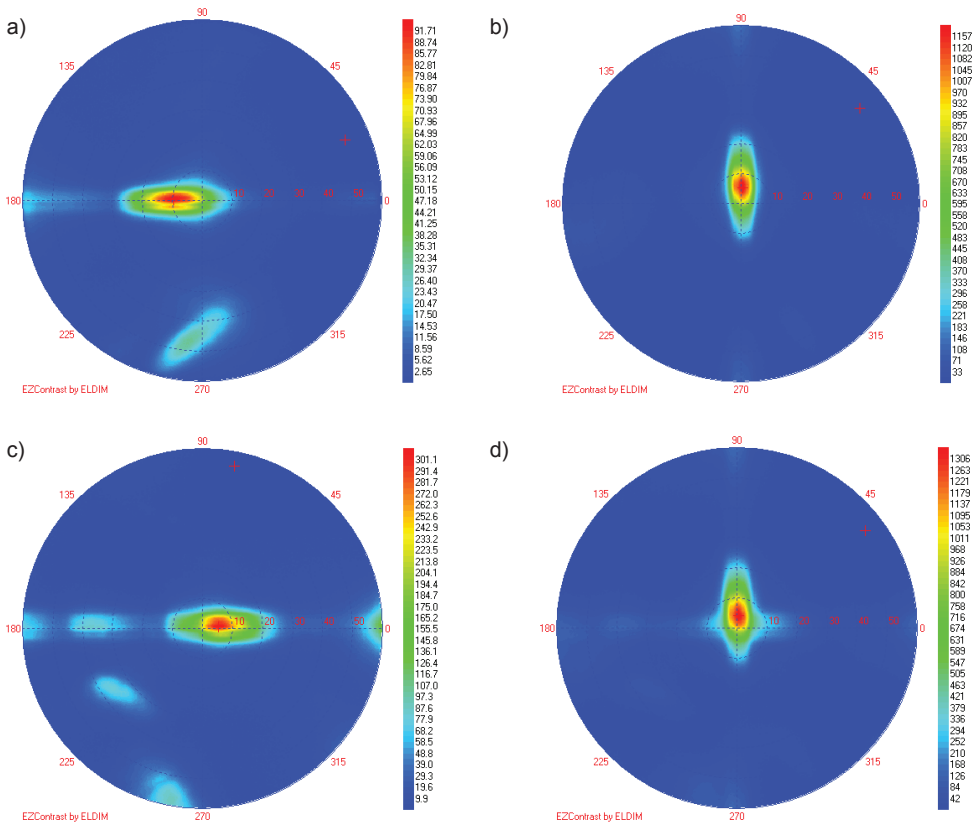


Figure 4. Polar coordinate plots: a) blue, b) green, c) red, d) all combined.

The measurements were repeated for polarized light. Only one of the LEDs for each primary color was used, and a thin (0.3 mm) foil of reflecting polarizer material was placed in between the LED and the beveled edge of the LGP to result in a transverse electric (TE) polarized emission for the red and blue wavelengths. To achieve the same direction of polarization for all colors, the “green” grating was designed to be preferentially diffracting for transverse magnetic (TM) polarized light, and thus the polarizer was cut at 90° orientation with respect to the polarizers used for the red and blue LEDs. The outcoupling distribution characteristics are very similar to those shown in Figure 4, but the intensity of maximum emission is roughly a sixth of the measured value for the unpolarized case for the green LED, and a half of the unpolarized case for blue and red LEDs. The “sidelobes” that are visible in Figure 4 a) and c) at the 270° region are missing from the measured polar plots for the polarized case. The angles of maximum outcoupling as well as the FWHM for each primary color are given in Table 3.

To examine the reason for the poor spreading of light in the fanout gratings, scanning electron microscope (SEM)

images were taken of surplus molds of the fanout gratings (See Figure 5). It can be seen that the profile of the fanout grating area for the red fanout section differs somewhat from the intended binary profile, and the same phenomenon is seen in the other fanout gratings as well. Similar images of the slanted grating areas show good correspondence to the design parameters given in Table 2. The depth of the replicated fanout grating for the red section is 416 nm, which is smaller than the intended depth of 450 nm. Similarly, the depth of the blue section is 278 nm as compared to the design value of 330 nm.

Conclusions

For the first time, a full display sized LGP incorporating a pixelated grating array, with fanout gratings, was presented. In principle, the results show that it is possible to direct light into the viewing area of the user by diffractive optics by using a full display sized grating array. There are artifacts that are visible from Figure 4 as “sidelobes” of outcoupled light distribution that are a result of the emission from the other LED of the respective color that was outside the intersecting path of the LEDs under the

objective of the conoscope. This sidelobe was not visible in the polarized case, due to the omission of one of the LEDs for each color in this measurement. Otherwise, the outcoupled intensity distributions were similar in both cases. The intensity values for the measurements done in the polarized case are not exactly comparable to the measurements done for the unpolarized case, as the experiment had to be taken apart and reassembled to insert the polarizers. Therefore, the location of the conoscope objective for making the measurements was not exactly the same as for the unpolarized case.

Table 3. Angles about the zenith of the outcoupling maxima and the FWHM of the emission in the grating experiment.

Primary	Angle of maximum outcoupling (degrees)		Full width at half maximum (degrees)	
	Unpolarized	Polarized	Unpolarized	Polarized
Blue	10	6	25	23
Green	5	5	18	18
Red	5	8	23	22

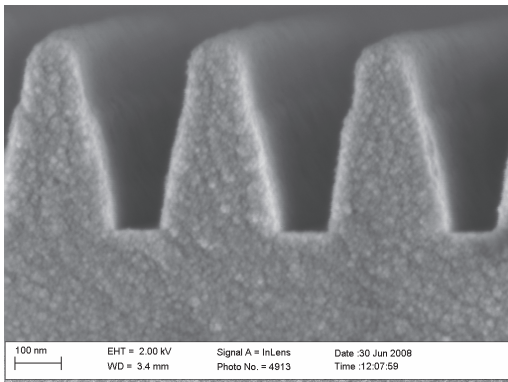


Figure 5. Scanning electron microscope image of the grating used for fanout of the red LEDs.

The fanout gratings were not as effective as was intended. In addition, the incoupling of LEDs was not optimized as of yet for this experiment. Less divergent light sources, coupled at precisely controlled angles, would help in this respect. The fanout grating profiles, as shown by electron microscopy, were not strictly binary, which may only partly explain the poor spreading of the light in the fanout sections. The waists of the bowtie structures in the fanout gratings were probably too narrow to spread the light. The fanout gratings require further study to verify the

contribution of the individual factors on spreading the light uniformly in the LGP.

Further work is planned to couple these backlights together with working displays to examine the energy efficiency and color gamut aspects of display design using diffractive backlights. There is great potential to improve the energy efficiency of mobile displays, and this study shows significant steps toward this goal.

Acknowledgements

The authors thank Ms. Marja Salmimaa, Mr. Markus Virta and Mr. Toni Järvenpää of Nokia Research Center for their help in preparing the experimental setup and the measurements for this study.

References

1. J. Kimmel, "Displays Enabling Mobile Multimedia", *Proc. SPIE* vol. 6507, pp. 650705-1-650705-11, 2007.
2. A. Iranli, W. Lee, and M. Pedram, "HVS-Aware Dynamic Backlight Scaling in TFT-LCDs", *IEEE Trans. VLSI Systems*, Vol. 14, pp. 1103-1116, 2006.
3. J. Kimmel, T. Levola, P. Saarikko, and J. Bergquist, "A Novel Diffractive Backlight Concept for Mobile Displays", *SID Symposium Digest*, Vol. XXXIX, Book I, pp. 42-45, 2007.
4. J. Kimmel, T. Levola, and P. Laakkonen, "Diffractive Backlight Grating Array for Mobile Displays", *Digest of Eurodisplay 2007 (International Display Research Conference)*, pp. 171-174, 2007.
5. J. Kimmel, T. Levola, P. Saarikko, and J. Bergquist, "A Novel Diffractive Backlight Concept for Mobile Displays", *JSID* Vol. 16, no. 2, pp. 351-357, 2008.
6. J. Kimmel, T. Levola, and P. Laakkonen, "Diffractive Backlight Grating Array for Mobile Displays", *JSID* Vol. 16, no. 8, pp. 863-870, 2008.
7. D.R. Selviah and K. Wang, "Modeling of a Color-Separating Backlight with Internal Mirrors", *SID Symposium Digest*, Vol. XXXV, Book I, pp. 487-489, 2004.
8. M. J. J. Jak, R. Caputo, E. J. Hornix, L. de Sio, D. K. G. de Boer, and H. J. Cornelissen, "Color-Separating Backlight for Improved LCD Efficiency", *JSID* Vol. 16, no. 8, pp. 803-810, 2008.
9. Micro SideLED® Enhanced Optical Power LED (Thin GaAN®), Blue/True Green. *Osram datasheet*, 2006.
10. Micro SideLED® Enhanced Thin Film LED, Red. *Osram datasheet*, 2006.

Publication [P5]

J. Kimmel, T. Levola, A. Giraldo, N. Bergeron, S. Siitonen, and T. Rytönen, "Diffractive Backlight Light Guide Plates in Mobile Electrowetting Display Applications," *SID Symposium Digest*, Vol. XV, pp. 826-829, 2009.

Copyright © 2009 Society for Information Display.
Reprinted with permission.

55.3: Diffractive Backlight Light Guide Plates in Mobile Electrowetting Display Applications

Jyrki Kimmel, Tapani Levola

Nokia Research Center, Tampere, Finland

Andrea Giraldo, Nicolas Bergeron

Liquavista BV, Eindhoven, The Netherlands

Samuli Siitonen and Tuomo Rytkönen

Nanocomp Ltd., Joensuu, Finland

Abstract

Power efficiency demands on mobile displays are increasing rapidly, as new multimedia services and applications are being adopted by users. Diffractive backlights and electrowetting displays have been proposed as some of the solutions to solve the poor efficiency of current mobile display systems. In this study, an electrowetting display was coupled with a pixelated, diffractive backlight light guide plate. This is to our knowledge the first time when a pixelated, diffractive backlight has been demonstrated in conjunction with an actual display. The results of the study show that the backlight and display panel need to be optimized as a system in order to obtain an applicable module for mobile use.

1. Introduction

Recent developments in mobile communication networks have made it possible for the mobile data services and applications to become a mainstream mode of interaction with mobile phones [1]. These services, such as mobile gaming, TV broadcasts, web browsing, and navigation, are getting very accessible due to the high information content screens employed in many modern mobile terminals. As the display in the mobile "smart phone" becomes larger in area and as it is manufactured with higher pixel density, the management of light throughput is becoming the limiting factor in power efficiency of mobile device user interfaces.

Kimmel *et al* have proposed a diffractive grating array based approach to solve the light throughput problem [2-7]. Whereas in the state-of-the-art of mobile display systems, white light-emitting diodes (LEDs) are used to launch an essentially uniform and spectrally broadband "sheet" of light into the light guide plate (LGP), which in return is directed toward the liquid-crystal display by means of brightness-enhancing films and diffusers [8], in the new concept, light from red, green, and blue LEDs is separated to be launched through the individual subpixels in the display so that each respective primary band of light travels only through the active aperture area of the respective subpixel. The system benefits for this approach arise from selecting the appropriate primary color of light for each subpixel, instead of filtering the broadband light through the display color filter array. In principle, a tenfold light throughput improvement can be realized with the new concept, if polarized light sources are used.

The latest experiments in the grating array design incorporated an active area array with 128 by 160 pixels, arranged in an RGB subpixel array [7]. The array was manufactured to correspond to a prospective display. Combining the backlight grating array with a display would then provide a platform for further research. Electrowetting (EW) displays that correspond mechanically to the subpixel matrix dimensions were used to investigate the

applicability of the pixelated diffractive LGPs in conjunction with an actual display. Since electrowetting displays are polarization insensitive, further power savings, as compared to liquid-crystal displays (LCDs), can be expected.

Conoscopic measurements on a color filterless EW display in conjunction with the pixelated LGP as well as with a color filter corresponding to the display matrix were performed. The results show poor contrast in using the electrowetting display, but measurements done with the color filter illustrate key aspects in color space engineering of diffractive backlight displays.

2. Diffractive Backlight Design and Fabrication

Diffractive backlights have been proposed with a pixelated but uniform grating structure [9, 10], where either a uniform, single-period binary or sinusoidal grating structure is used [9], or a similar structure is proposed to be pixelated [10]. These conceptual solutions have the drawback that the broadband light structures used in the studies diffract light to a wide range of angles, and microlens arrays as well as sometimes micromirror arrays, and in addition, even specialized pixel arrangements need to be used to fully exploit the diffraction. In a pixelated grating array with dedicated gratings for each subpixel, the direction of the diffracted beam can be optimized for each primary color. Furthermore, by using controlled grating profiles such as slanted gratings, the desired transmitted order of diffraction can be selected for each primary color, resulting in very high efficiency of output coupling [11].

In this study, a grating array, with a slanted grating for each subpixel [7], was applied in order to diffract light of the corresponding spectral band toward the respective subpixel. The EW display parameters are shown in Table 1, and the grating parameters are shown in Table 2. Area modulation was applied in the subpixel structure with increasing diffractive area in each subpixel toward the end of the array, in order to achieve good uniformity of light output across the display. Binary fanout grating arrays with 50 % fill factor, in a double bowtie arrangement, were provided along the sides of the LGP to spread the incoming light from the LEDs used as light sources.

Table 1. Display parameters for the experiment.

Resolution	128 (x3) by 160
Pixel size	222 μm by 222 μm
Active area	29 mm by 36 mm
Display glass thickness	0.63 (x2) mm

Figure 1 shows the LGP design in detail. As shown in [7], a 52 mm by 54 mm plate for the BLU was fabricated on a 0.65 mm thick episulfide polymer substrate at Nanocomp Ltd. in Joensuu area, Finland. The active grating matrix, as well as the fanout gratings, were manufactured using a fused silica master grating array by ultraviolet embossing from episulfide, on top and bottom of the substrate, respectively. The LGP edges were beveled to 45 degrees to allow efficient coupling of light from LEDs to the LGP.

Table 2. Grating parameters.

Primary	Width by length	Depth (nm)	Grating period (nm)	Grating slant direction (degrees)
Red (640 nm)	111 μm by 59 μm	340	530	+45
Green (525 nm)	59 μm by 111 μm	340	430	+45
Blue (460 nm)	111 μm by 59 μm	240	375	-45
Red fanout (Double bowtie)	10 mm by 36 mm	450	360	0
Green fanout (Double bowtie)	8 mm by 29 mm	370	0	
Blue fanout (Double bowtie)	10 mm by 36 mm	320	250	0

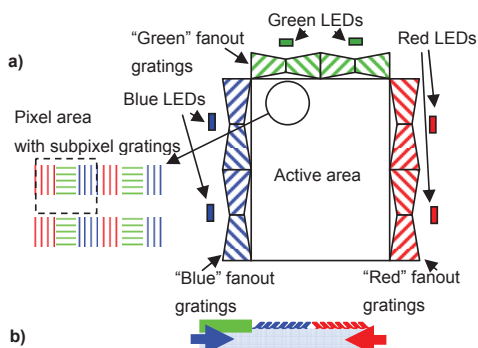


Figure 1. LGP layout. a) Grating arrangement from top, b) Direction of grating slants from the side (“green” slant perpendicular to both “blue” and “red” grating slants). The figures are not to scale.

3. Electrowetting Display Design and Manufacture

Electrowetting displays operate on electrostatic forces acting on an oil/electrolyte interface [12]. With oil containing a dye configuration with a specific absorption characteristic, movement of the interface along the substrate of a display blocks the light corresponding to the absorption spectrum of the oil. Electrowetting displays can be reflective, transmissive, or transmissive. In this experiment, a Liquavista panel with 128 (x3) by 160 pixels was used [13]. This panel was specially manufactured to be used as a transmissive display, without reflecting structures and color filters, so as to be applicable to be used with a diffractive backlight plate.

Each panel is processed starting from standard amorphous silicon active matrix substrates from a thin-film transistor liquid-crystal display (TFT-LCD) foundry. First the hydrophobic dielectric layer is deposited on the indium tin oxide (ITO) electrode and then the panel, coupled to a thin glass cover without color filter, is filled with two liquids: the oil with the absorbing dyes and the transparent liquid. Size reduction of the inter-pixel gaps and shielding with a black-mask configuration prevents undesired light leakage.

Once the panel is finished, the source and the gate integrated circuit (IC) drivers are bonded on the glass as well as the foil connecting the panel to the small driving board. The IC drivers provide for up to 6-bit grey scales per color to the panel with a pulse width modulation technique.

4. Experimental Characterization of the System

The display and the LGP were coupled together, to align the respective display and grating arrays, by means of a micromanipulator system. A similar arrangement was used to mount a striped RGB color filter in the place of the display to compare color space adjustment. The display was driven using a Nokia 3110 Classic mobile phone, with test screens stored in memory. The setup was then mounted in front of a calibrated Eldim EZLite 120 R conoscope to obtain polar plots of the outcoupling characteristics of light throughput. Osram LEDs [14, 15] were mounted at a 45 degree angle with respect to the face of the display arrangement to allow for effective incoupling of the light into the LGP. The drive current of the red and blue LEDs was varied, while keeping the green LED current at the nominal 20 mA, in order to control the effective color space available to the user. Table 3 shows the obtained maxima and full width at half maximum (FWHM) of the output angular distribution of light from the grating array, as reported in [7].

Table 3. Angles about the zenith and the FWHM of the outcoupling maxima in the model grating experiment.

Primary	Inclination (°)	FWHM (°)
Blue	10	25
Green	5	18
Red	5	23

5. Results

Figure 2 shows a polar coordinate plot of the output-coupled radiation when all LEDs are driven at 20 mA, with the display turned “on”. When the display pixels are turned “off”, the image looks quite similar, but the luminance level is slightly smaller. Averaging over the $\pm 60^\circ$ span of the conoscope aperture, along the azimuth angle at 0° , the luminance contrast ratio is only 1.6. The images also show a periodic structure in the output characteristics that can be attributed to crosstalk of the outcoupled light from the diffractive grating array through the neighboring subpixels of each full pixel. This is also seen in similar conoscopic measurements done in situations where each of the individual color LEDs were driven at 20 mA and varying the “on” and “off” conditions of the respective primary subpixels.

Measurements done with the color filter array do not exhibit appreciable crosstalk between the neighboring subpixels, which shows that the color filter blocks the unwanted output radiation quite well. Taking a cross section of the polar coordinate plots for different combinations of LED drive current conditions, at azimuth angle of 45° , where the contribution of the red and green primary colors will affect the output color space. The results of this experiment are also shown in Figure 3. As Figure 3 shows, it is possible to adjust the contribution of each respective primary color LED to the overall luminance by adjusting the drive current. This can be a starting point for effective color space engineering in mobile displays. In this experiment, the effect of the blue primary contribution was low in comparison to the effect of adjusting the red LED current.

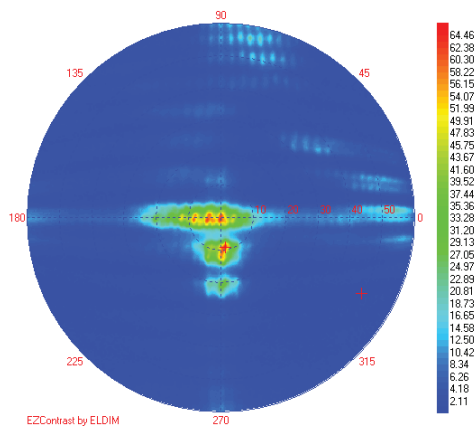


Figure 2. Polar coordinate plot of the electrowetting display coupled with the diffractive grating LGP.

6. Conclusions

For mobile display technology, it is important to reduce power dissipation of the display itself, and a radical redesign of the display module is required in order to make major inroads in reducing power consumption. In this study, the diffractive pixelated backlight has been applied to a display for the first time.

The results of this study illustrate the need to optimize the constituent technologies together as a system to achieve best performance. The EW display used in the study was a modified reflective display with accordingly engineered dye-electrolyte system that did not suit very well to the diffractive backlight technology. The display was also manufactured on too thick glass for optimal operation of the backlight, as the divergence of the output coupled light resulted in severe crosstalk between subpixels. Since there was no color filter in the display itself, in this experiment the color contrast could not be characterized. The results obtained with the color filter array only show that conceptually it is possible to adjust the white point and color space of displays equipped with diffractive LGPs by varying the drive current of the LEDs.

Further work is planned to couple the pixelated diffractive grating array designs with mobile LCDs to study the color space engineering aspects further and in more detail. As was already concluded in the earlier study on the LGPs [7], the fanout of the structure does not work very well, and other ways to realize the fanout are being investigated, to realize a viable mobile display system with improved light throughput efficiency.

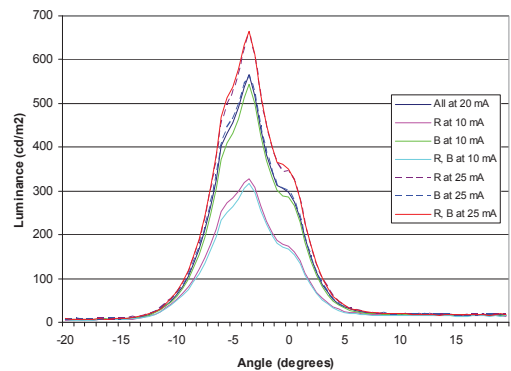


Figure 3. The effect of primary LED current to the overall luminance over a range of conoscopic characterization angles. The LEDs are driven at 20 mA, unless otherwise mentioned in the legend.

7. Acknowledgements

The authors would like to thank Mr. Toni Järvenpää and Mr. Markus Virta of Nokia Research Center for their help in the practical arrangements for making the measurements.

8. References

- [1] J. Kimmel, “Displays Enabling Mobile Multimedia”, Proc. SPIE vol. 6507, pp. 650705-1-650705-11, 2007.
- [2] J. Kimmel, T. Levola, P. Saarikko, and J. Bergquist, “A Novel Diffractive Backlight Concept for Mobile Displays”, SID Symposium Digest, Vol. XXXVIII, pp. 42-45, 2007.
- [3] J. Kimmel, T. Levola, and P. Laakkonen, “Diffractive Backlight Grating Array for Mobile Displays”, Digest of Eurodisplay 2007 (International Display Research Conference), pp. 171-174, 2007.
- [4] J. Kimmel, T. Levola, P. Saarikko, and J. Bergquist, “A Novel Diffractive Backlight Concept for Mobile Displays”, JSID Vol. 16, no. 2, pp. 351-357, 2008.

- [5] J. Kimmel and T. Levola, "Backlights in Mobile Display Power Management", SID Symposium Digest, Vol. XXXIX, pp. 1594-1597, 2008.
- [6] J. Kimmel, T. Levola, and P. Laakkonen, "Diffractive Backlight Grating Array for Mobile Displays", JSID Vol. 16, no. 8, pp. 863-870, 2008.
- [7] J. Kimmel, T. Levola, S. Siitonen, and T. Rytönen, "A New Diffractive Backlight for Mobile Displays", Proc. IDRC 2008, pp. 290-293, 2008.
- [8] M. Anandan, "Progress of LED Backlights for LCDs", JSID Vol. 16, No. 2, pp. 287-310, 2008.
- [9] D.R. Selviah and K. Wang, "Modeling of a Color-Separating Backlight with Internal Mirrors", SID Symposium Digest, Vol. XXXV, Book I, pp. 487-489, 2004.
- [10] M. J. J. Jak, R. Caputo, E. J. Hornix, L. de Sio, D. K. G. de Boer, and H. J. Cornelissen, "Color-Separating Backlight for Improved LCD Efficiency", JSID Vol. 16, no. 8, pp. 803-810, 2008.
- [11] T. Levola, and P. Laakkonen, "Replicated Slanted Gratings with a High Refractive Index Material for In and Outcoupling of Light", Optics Express, 15, 2967-2074, 2007.
- [12] R. A. Hayes and B. J. Feenstra, "Video-Speed Electronic Paper Based on Electrowetting", Nature, Vol. 425, no. 25, pp. 383-385, 2003.
- [13] A. Giraldo, J. Aubert, N. Bergeron, F. Li, A. Slack, and M. van de Weijer, "Transmissive Electrowetting-Based Displays for Portable Multi-Media Devices", paper to be presented at SID Symposium, 2009.
- [14] Micro SideLED® Enhanced Optical Power LED (Thin GaAN®), Blue/True Green. Osram datasheet, 2006.
- [15] Micro SideLED® Enhanced Thin Film LED, Red. Osram datasheet, 2006.

Publication [P6]

J. Kimmel and T. Levola, "Mobile Display Backlight Light Guide Plates Based on Slanted Grating Arrays," *Journal of Photonics for Energy*, Vol. 2, pp. 024501-1 - 024501-11, 2012.

Copyright ©SPIE 2012.
Reprinted with permission.

Mobile display backlight light guide plates based on slanted grating arrays

Jyrki Kimmel and Tapani Levola*

Nokia Research Center, Tampere Laboratory, P. O. Box 1000, 33721 Tampere, Finland
jyrki.kimmel@nokia.com

Abstract. Modern mobile communication devices have user interfaces that are dominated by high-quality displays. Increased multimedia use imposes high demands on the design of display modules, as the content available for mobile use becomes visually richer. Especially the power dissipation of the display can limit the amount of time available for multimedia consumption and interaction. In the mobile liquid-crystal display (LCD), the energy efficiency is determined by the backlight design. State-of-the-art backlights direct white light through a display subpixel array, with high uniformity and up to 90% efficiency in white light output. Therefore, it is difficult to obtain system-level energy savings by improving the backlight design alone. Diffractive backlights have recently been proposed to reduce the power dissipation of the display module, and slanted grating arrays are among the enabling optical features that allow for reduction in power dissipation beyond what is available in the state of the art. By the use of diffractive grating arrays, the required primary color (red, green, or blue) is directed through the LCD subpixel array with geometrical registration, instead of flooding the whole LCD with white light and filtering the primary colors through the subpixel color filter array. We present a study on grating structures based on slanted grating arrays fabricated in high refractive index materials. The grating design principles and grating outcoupling results are provided, and an outline of a new embedded system design is given. Emphasis is on grating array design aspects for future energy-efficient display system design. The results show that savings in power consumption can be expected with advanced display system design based on embedded slanted grating array backlight light guide plates. © 2012 Society of Photo-Optical Instrumentation Engineers (SPIE). [DOI: 10.1117/1.JPE.2.024501]

Keywords: mobile display; diffractive backlight; slanted grating array.

Paper 11189P received Jun. 9, 2011; revised manuscript received Oct. 27, 2011; accepted for publication Dec. 1, 2011; published online Mar. 12, 2012.

1 Introduction and Background

The mobile phone is no longer only a device to use to place a voice call to a person. The new uses of mobile phones derive from the multimedia capabilities of the devices and the enhanced digital networks that enable vast amounts of data to be transferred between the network and the device. Web browsing, gaming, video telephony, and navigation have become commonplace uses for mobile phones, and since many of these applications require high visual quality for enjoying these new services, the image quality demands on the mobile display have escalated. The mobile phone usage patterns are increasingly incorporating multimedia consumption and live interaction. Many visually demanding applications such as navigation, gaming, and social media require the display to provide the best image quality at all times. This means that power-saving techniques such as power-save modes and time-outs cannot be as effectively utilized as before.¹

Today, the majority of multimedia-capable mobile phone displays are active-matrix liquid-crystal color displays. Also, organic light-emitting displays (OLEDs) are taking a strong foothold on the mobile display market. Both varieties offer high image quality for the user, but of these, only the liquid-crystal display (LCD) can be made transfective, that is, in such

*Present address: Microsoft Oy, Keilaranta 7, 02150 Espoo, Finland.

a way that light reflecting from the ambient environment can also be utilized to show information to the user, although with reduced color gamut and contrast. While the OLED technology is emissive and does not need an external light source for operation, the prevalent technology in the mobile market, LCD, relies on its transmissive mode on a backlight to provide the light that the liquid-crystal material modulates to present high-quality visual information to the user.²

In modern mobile LCDs, the backlight plays the largest role in power dissipation.² The structure of a modern mobile display is essentially composed of a stack of optical films with the electro-optic LC material sandwiched between two plates of glass. The end result is a display with a very good image quality in the transmissive case. The backlight provides good light throughput and uniformity. The efficiency can be up to 90% and the uniformity about 80%.³ However, the light-guide plate (LGP) of the backlight unit (BLU) is designed to flood the display glass with white light. The light is then filtered in the color filter array (CFA) to red (R), green (G), and blue (B) subpixels. The eye and the human visual system then process the information shown on the display to an intelligible image for the human user.

In modern mobile displays, the resolution and pixel pitch are very high, over 300 pixels per inch (ppi) in some cases.⁴ This means that to effectively drive the display, the transistors themselves, the possible reflective area, and the black matrix in between the subpixels in the thin-film transistor (TFT) array span a large portion of the subpixel area. Furthermore, the CFA obviously blocks at least two thirds of the light throughput. Not even taking into account the material losses, the total system losses are on the order of 90%.⁵ There are several possible ways to improve the system efficiency of an LCD. One of these is to use temporal multiplexing of the primary color subpixels instead of spatial multiplexing. Using red, green, and blue light sources allows for fast field-sequential color (FSC) displays. Fast LC modes are required in this case, and in FSC displays, the temperature plays a large role in the speed of the LC and thus also in the viability of this approach, in any display that is to be used outdoors.⁶ Another way to circumvent the high losses in the current LCD structure is to separate the backlight output to the primary colors already in the backlight itself. This has been attempted by proposed designs with diffractive optical means to separate the primary colors into several output angles.^{7,8} In this approach, additional microlens arrays, and sometimes also micromirror structures, are required to avoid crosstalk between the subpixels.^{7,8} One possible way to separate the primaries without using additional microstructures is to apply RGB light sources on the periphery of the display panel and a spectrum-specific grating under each subpixel. The subpixel structure of the display panel is thus geometrically duplicated on the backlight LGP in the grating array. In this approach, light is selected instead of filtered, and there is a possibility to create a display that has radically better system efficiency than in the state-of-the-art LCDs.^{5,9-11}

Using a subpixel-level registered backlight structure under the LC glass requires a new paradigm for manufacturing LCDs. Depending on the thickness of the glass, the accuracy requirement of placement is in the order of micrometers, following the analysis of similar structures done previously.¹ It is obvious that the closer the backlight LGP is to the active electro-optic material, the better the throughput of light will be, and also crosstalk will then be more easily minimized. The LCD industry to date is geared to stacking the required optical films without such registration accuracy. In order to provide a solution for the registration requirement, it would be beneficial to integrate the LGP as a part of the actual display glass structure, which would result in a manufacturing paradigm that in accuracy closely resembles CFA manufacturing and alignment.

The work to date on pixelated diffractive LGPs has provided results on the color separation as a separate component in the display.^{1,5,9-11} In this work, the authors extend the previous work to embedded structures that can be thought of as a starting point for this new manufacturing paradigm. Concurrently, as it has become clear that the current state of the art in mobile display system design has reached a high degree of maturity, the need to reduce power dissipation in the mobile multimedia device has escalated. Therefore, a new system concept for mobile display design has been devised, based on slanted grating arrays.^{5,9} In previous studies, grating arrays ranging from 1 cm × 1 cm demonstration pieces^{5,9} to full mobile display-sized light guide plates^{10,11} have been shown. Figure 1 presents the basic principle of the backlight unit design. Instead of flooding the display subpixel array with essentially white light and filtering the desired primary colors through the color filter array of an LCD, a pixelated diffractive design selects the

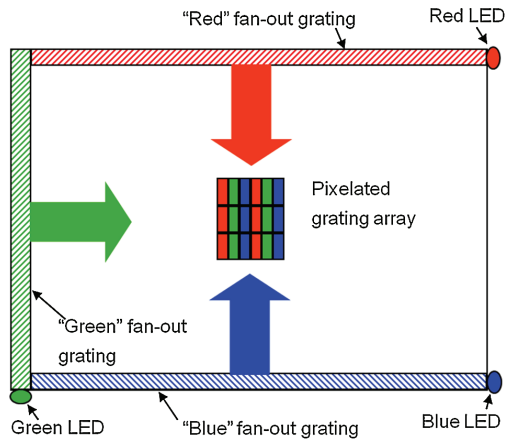


Fig. 1 Basic concept of a diffractive display backlight.^{5,7}

desired primary subpixels and directs the respective spectral band of light from red, green, and blue LEDs through this subpixel array, ultimately removing the requirement for a color filter array. This principle of backlight design can be used for all electro-optically modulating transmissive displays such as LCDs and electrowetting displays. The array of slanted gratings needs to correspond geometrically to the display subpixel array and an alignment step is required in display module fabrication. Previous results show that it is possible to direct the light efficiently,^{5,9} and with proper grating design it is also possible to obtain color purity adequate for removal of the color filter array.⁹ Current mobile display modules have glass thickness of up to 0.6 mm, and this means that the grating array needs to present very low divergence, if the grating array is behind the display glass. LED collimation is a limiting design factor, and with this glass thickness, it is impossible to eliminate crosstalk completely due to the Lambertian emission characteristics of current LED modules¹² and due to the diffraction from very small grating areas that spreads the light. Therefore, a new design, based on embedded gratings, is proposed. The slanted gratings have been manufactured in high—refractive index glass and a polymer has been deposited on this structure to act as a low-index cladding layer. This structure can then be used as the back glass substrate of an LCD or an electrowetting display. With the new design, significant advances in display module light throughput efficiency can be expected, especially since the integration of the backlight in the back substrate of the LCD removes the need to fabricate a dedicated backlight unit completely.

2 Grating Array Design and Fabrication

Based on the results of our previous research,^{9–11} similar slanted gratings were designed for the embedded pixelated LGP structure with red, green, and blue primary subpixels. The green subpixel gratings were oriented orthogonally to the red and blue subpixel gratings, and since the intended use was an LCD panel that requires the same polarization from all subpixel gratings, the polarization of the outcoupled light from the green subpixel was designed to be orthogonal (transverse magnetic [TM]) to the blue and red subpixel outcoupling (transverse electric [TE]). The modeling of the gratings was done using the *C*-method,¹³ the rigorous diffraction theory based on coordinate transformations, with the *S*-matrix algorithm for the layered structure.¹⁴ The grating design parameters are shown in Table 1.

The gratings were etched on a titanium oxide layer and were covered by a low—refractive index polymer having sufficient thickness. All the grating structures were binary, having a 45 deg slanting angle. This angle was sufficiently large to give an advantage of Bragg grating and was the same for all the gratings for practical reasons. The depth of the grating intended for the blue primary was tuned in such a way that the diffraction efficiency was high enough but as low as

Table 1 Grating array parameters.

Parameter/grating	“Red” subpixel grating	“Green” subpixel grating	“Blue” subpixel grating
Design λ (nm)	640	525	460
Grating period (nm)	450	370	325
Grating depth (nm)	250	240	150
Slant angle (degrees)	45	45	-45
Filling ratio (%)	50	50	50
Grating width (μm)	111	59	111
Grating length (μm)	59	111	59
Aperture of grating (%) ^a	13	13	13

^aThe aperture refers to the proportion of fabricated grating area of the total pixel area.

possible for the red light. The red light arrives from the opposite direction to the blue light, and thus the grating for blue is not a Bragg grating for the red primary light source. The design for the “red” grating was done using similar principles. The green light disturbs very little the blue and red primaries, as the green grating is oriented 90 deg in conical angle with respect to the blue and red light rays. The polarization of the incoming light was designed to be TE, that is, the electric vector parallel to the grating grooves. This condition is accurately met if the illumination is very well collimated, which is not the case when using LEDs. The light guide itself depolarizes the light somewhat due to the total internal reflections inside the light guide, and consequently there will be some amount of TM light in the light entering the grating. The diffraction from the gratings designed for the red and blue primaries thus produces mostly TE polarized light.

The design of the grating for the green light is based on TM polarization, because the outputs of all different colors must have the same polarization due to the LCD operation principle. The green light is only marginally scattered from the red and blue gratings, as they are in 90-deg conical orientation with respect to the green light. The depth of the green grating was designed to be slightly less than the depth of the maximum efficiency in order to tune the efficiency more suitably in this small sample.

The gratings were positioned on a 1.5-mm-thick glass plate, 10 cm \times 10 cm, in the center area. Altogether the array was 65 pixels wide (14.43 mm) and 81 pixels tall (17.98 mm), representing a hypothetical subsection of a mobile LCD backlight with 222 μm pixel pitch. The grating area in each subpixel was 59 μm wide and 111 μm tall. The grating array was fabricated by Nanocomp Oy (Lehmo, Finland) on a high refractive index (n) glass (LASFN46A, $n = 1.91$) with a 400 nm-thick titanium dioxide overlay fabricated by atomic layer deposition (ALD) at Beneq Oy (Vantaa, Finland). The gratings were etched, by reactive ion-beam etching, on the TiO₂ layer ($n = 2.2$), and a 500 nm-thick DuPont AF1600 low-index polymer layer ($n = 1.31$) was spin-coated on top, to form a cladding layer for the whole structure.

3 Experiment Design

Figure 2 shows the experimental setup in schematic form. The setup was mainly built on a Spindler & Hoyer mini rail frame, on an aluminum optical breadboard. The light sources were first aligned by means of two 0.6-mm-diameter apertures, and the remaining optical parts were then aligned using the green source as the reference. The light sources were a 4-mW green frequency-doubled diode laser pointer at 525 nm, a 6 mW red helium-neon laser at 632.8 nm, and a 0.4-mW blue frequency-doubled diode laser at 473 nm (as measured using a Edmund Optics LaserCheck detector). The green source was mounted at the beginning of the mini rail setup, and it could be removed when the red and blue sources were required. The light paths were aligned by means of the 0.6-mm circular apertures, which were about 240 mm apart. Therefore, the maximum angular error in the alignment was in the order of a minute of arc. Polarization control was achieved by a rotatable absorbing polarizer. A semi-transparent mirror reflected part of the light to a second mirror, which again directed the light to a BK7 prism for coupling the light into the LGP. This prism was placed under the light guide plate, and index-matching fluid was used to have the prism adhere to the LGP by capillary action. From the semitransparent mirror, part of the light was let through to the aperture at the end of the

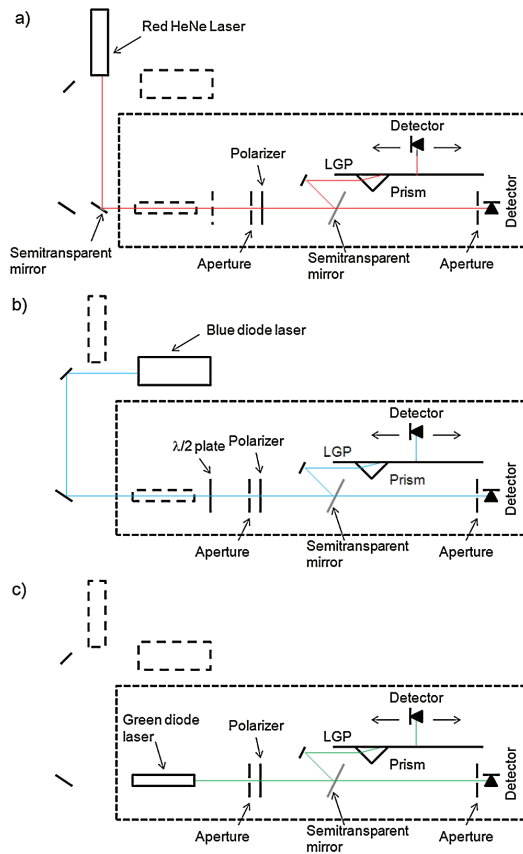


Fig. 2 Schematic of the experiment design: (a) red light source, (b) blue light source, (c) green light source.

mini rail, in order to maintain alignment of the experiment through the series of the measurements. A reference detector was placed after the aperture.

The detectors used for the measurements were Siemens SFH 217 photodiodes¹⁵ mounted on a micromanipulator stage arrangement, and a simple operational amplifier circuit was used to convert the photocurrent from the photodiode to a voltage signal. The voltage was measured with two Hewlett-Packard 34401A digital multimeters. For each separate light source, a reference measurement was done first to acquire the signal level for a theoretical value representing 100% outcoupling from a single point on the LGP. This was achieved by placing a mirror on the path of light and directing the beam of light to the main detector. At the same time, the voltage signal for the beam of light propagating from the semitransparent mirror to the reference detector was recorded.

For each light source, measurements were done for the TE and TM polarization states of light entering the prism. First, the maximal intensity of the outcoupled light was sought by adjusting the position of the detector on top of the LGP. After this, the detector was moved along the sample and the outcoupled light signal was recorded. Next, the polarizer was rotated 90 deg and the outcoupling for the orthogonal state of polarization was recorded, to account for the polarization sensitivity of outcoupling. These experiments were repeated for all light sources for the three respective principal orientations of the LGP. In some cases, a neutral density filter and an additional semitransparent mirror were used to reduce the amount of light in calibration

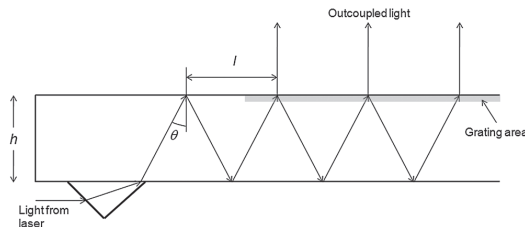


Fig. 3 Light propagation in the light guide plate (not to scale).

and during the experiment, if one of the detectors was near or at maximum voltage level. A Thorlabs $\lambda/2$ plate was used with the blue laser to turn the polarization prior to the absorbing polarizer, when required.

Figure 3 depicts the light propagation in the LGP schematically. It can be seen from the geometry of the experiment that the light coupled into the LGP is guided in a zig-zag fashion, with the distance between points of reflection becoming $l = 2h \tan \theta$. Since the design for the grating array was done for $\theta = 50^\circ$, for the plate thickness $h = 1.5$ mm, the expected distance $l = 3.58$ mm. Once the light enters the grating area, the light is then coupled out at points on the front surface of the LGP, and the distance between outcoupling points is therefore also l .

4 Results

Figure 4 shows a scanning electron microscope (SEM) image of a model grating, similar to the one used for the measurements, from a cladding deposition trial. The cladding polymer lifts off in the preparation process for SEM, but it can be seen that the thickness of the cladding layer is on the order of 500 nm. It can also be seen from Fig. 4 that the grating fabrication is feasible in TiO_2 . The 400 nm-thick TiO_2 layer is not resolvable in the SEM image. Since only one sample was fabricated for this study, it could not be sacrificed for a SEM study, but the results shown in Fig. 4 are considered to be representative of the fabrication technique.

Figures 5–7 show the measured intensity curves, normalized to the maximum value of outcoupling, after Fresnel losses,¹⁶ in the prism coupling arrangement, of the measurements along the surface of the LGP. As was expected, several peaks along the grating area were observed for each light source and polarization. The locations of the maxima of these curves show that the distance between the outcoupling peaks was 3.6 mm on the average, which agrees with the expected design incidence angle of the gratings, within the measurement accuracy (the detector was moved with 0.25 . . . 0.50 mm steps). The full width at half maximum (FWHM),

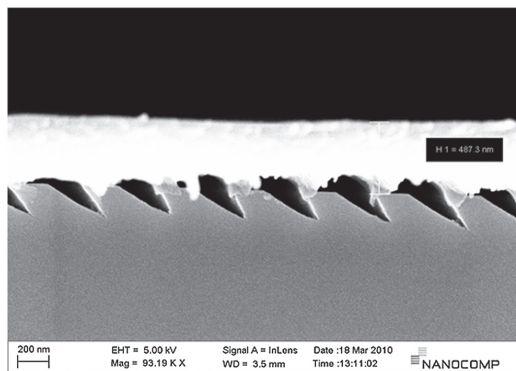


Fig. 4 Scanning electron microscope (SEM) image of a grating structure similar to the one used in the study. The polymer cladding lifts off in the preparation process for SEM.

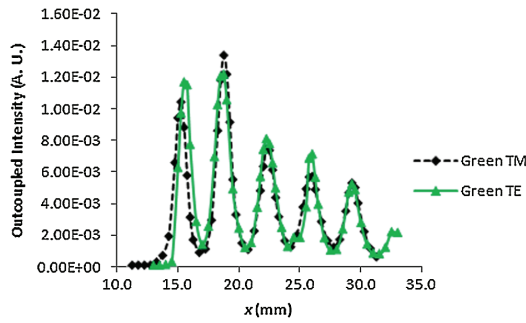


Fig. 5 Normalized intensity for green outcoupling.

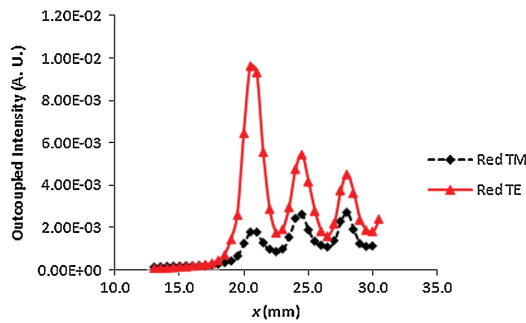


Fig. 6 Normalized intensity for red outcoupling.

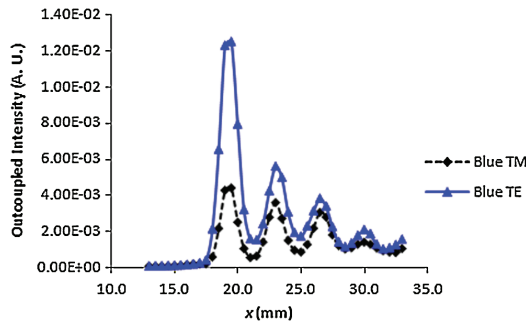


Fig. 7 Normalized intensity for blue outcoupling.

measured separately for selected outcoupling peaks with 0.25 mm resolution in detector placement, was about 1.5 mm for all light sources. Also, one G peak was scanned by varying the angle of the detector, centered at the point of outcoupling. In this measurement, the FWHM of the peak was about 3° . Both these measurements actually represent a convolution of the detector function and the beam characteristics.

In order to verify that the backlight function can be done using divergent light sources, a verification experiment was performed with a red laser diode (wavelength about 630 nm) that had an adjustable lens at the front. The spreading of the outcoupled beam of the TM mode was verified as shown in Fig. 8. The intensity values in this experiment were not referenced

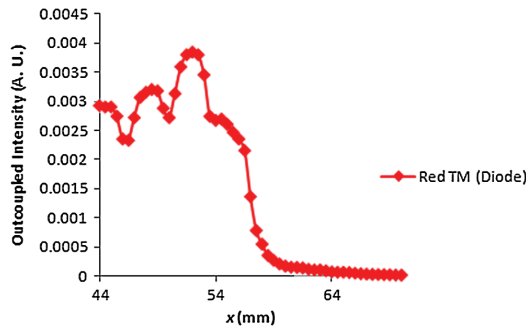


Fig. 8 Normalized intensity for a divergent red laser diode beam. TM mode only shown.

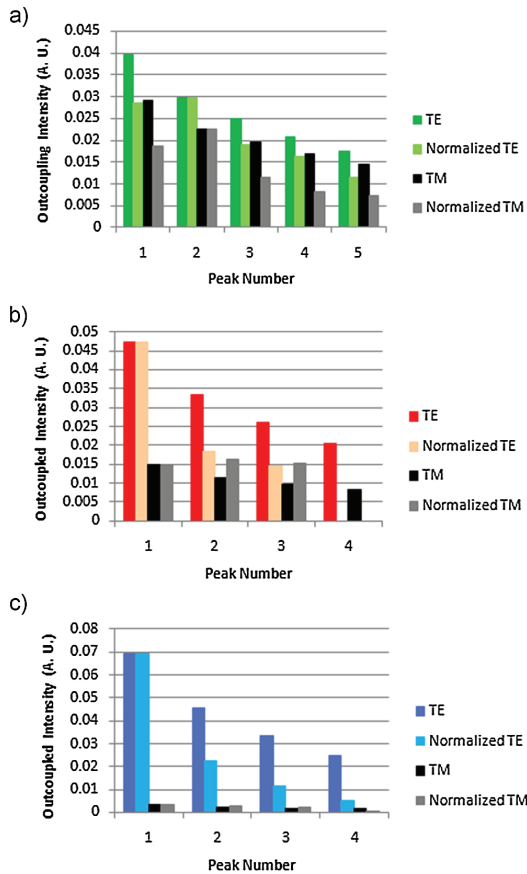


Fig. 9 Comparison of theoretical decay and experimental results for the outcoupled peak intensities: (a) green outcoupling, (b) red outcoupling, (c) blue outcoupling.

to any specific calibration value of outcoupling, and the zero point for the x -coordinate was also different than for the main experiment. The TE mode behaves similarly to the TM outcoupling in the divergent case.

5 Discussion

The results show that the light is outcoupled as expected, with intensity of outcoupled light decreasing with the distance from the incoupling point (with the green light source the decrease starts from the second peak, since evidently the incident beam hits the grating only partially, leaving the first outcoupled peak incomplete). This is understandable, since there is no area modulation in the grating array to take into account the already outcoupled energy along the propagation path of the light. Scattering from the grating array layout amounts to about 10% of incident intensity, as calculated from scalar diffraction theory, and this is evidenced from the decay of the peaks and due to the appearance of a background outcoupling, detected between the peaks in Figs. 5–7. Scattering contributes partially to the total outcoupled energy. Figure 9 presents the comparison of the theoretical decay characteristics of the outcoupling peaks with experimental findings. The theoretical outcoupled peaks are normalized to the first detected outcoupled peak intensities, except for the green outcoupling, as it was evident that the first incoming beam only hit the edge of the grating array, resulting in partial outcoupled intensity. The results show that in the experiment, the outcoupling decays more rapidly than predicted, indicating that some of the scattering losses have not been taken fully in account.

The polarization sensitivity of outcoupling varied, with the green TE outcoupling 7% higher than the TM outcoupling, red TE coupling out 206% stronger than TM, and blue TE 78% more intense than the respective TM polarization state. The coupling from the green TM mode could reach higher values with different grating design, but in this experiment the present outcoupled intensity values were considered to be adequate. The outcoupling efficiency is controlled by grating area and with smaller area the scattering from the small structures increases. The discrepancy in the green outcoupling polarization state to the design objective can be explained by a further modeling result where a grating depth of 250 nm gives similar results to the measured values. In addition, the deviations of the experimental groove shape from the designed one can explain this. Fabricating much deeper grooves would improve the situation. This means that when modeling the grating parameters, the depth of the grating is in the “shallower side” of the efficiency maximum, but it could also be in the “deeper side.” However, this would result in a groove depth exceeding 400 nm, and this means that a thicker titanium oxide layer ought to be used in this case.

6 Conclusions

The outcoupling pattern from the grating array was as expected from the geometry of the sample LGP, for native laser light sources. Diverging or focusing the light along the light path would result in a larger angular and lateral spread of incoupling, and thus the observed peaks would subside and the output distribution would be more even. This would also be the case with LEDs as light sources, as in a typical mobile display. These assumptions were confirmed by a verification experiment using a spread-beam red diode laser.

The outcoupling polarization sensitivity did not follow the design objectives for the “green” grating, but by running a simulation with a 10-nm deeper grating than in the original design, the measured values agreed with the model. This means that the actual fabricated grating depth for the green subpixels was deeper than the design value. The actual height of the cladding layer also affects the outcoupling somewhat, but the actual calculation is outside the scope of this paper. In a possible LGP manufactured for display use, the cladding must be thick enough (about 700 nm) so that the evanescent field of the light at the grating array interface will not be disturbed by materials outside the cladding proper.

It was shown in this study that outcoupling of light is possible for embedded gratings, etched in glass. Furthermore, it was shown that the low—refractive index polymer cladding did not deter the outcoupling. Therefore, it can be said that for an embedded backlight concept, an

etched grating array approach is possible. In this approach, the pixelated grating array can be fabricated right next to the electro-optically active LC layer, and maximum throughput of light, for this backlight concept, can be achieved with the associated savings in expended energy for a given display luminance.

A mobile display system can be created by this approach with the backlight integrated in the back substrate. The final back substrate structure would require transparent electrodes, such as indium tin oxide (ITO), as an additional layer on top of the cladding. A display-oriented investigation of embedded backlight light guide plates is in the planning phase, and this involves adding an LC layer and a color filter array on top of the LGP, for full color contrast measurement with red, green, and blue LEDs as light sources.

The economic implications of changing to a new display module manufacturing paradigm are unknown, and it remains to be seen whether the display industry can embrace a new system module design concept such as the one proposed in this study. In particular, the concept calls for manufacturing a grating array on the back substrate of each display manufactured on a large multi-display substrate glass plate. In this study, a single etched grating array was used. In a practical application, a replication technique should be used instead, to achieve an economic way to fabricate displays with diffractive grating arrays. Furthermore, for many backplane configurations, the cladding layer should be such that a layer of ITO or other transparent conducting material can be deposited on top. Such polymers are available, but could not be used for this research. Finally, most likely, the transistor layer of an active-matrix display should be on the top substrate. While this is not impossible to achieve, the shielding properties of the transistor array and the reflecting structures for transfective use must be designed accordingly.

Acknowledgments

The authors thank the following Nokia Research Center colleagues: Dr. Pekka Äyräs, Dr. Martin Schrader, Ms. Marja Salmimaa, and Dr. Pasi Saarikko for assistance and helpful discussions, as well as Mr. Markus Virta for his help with additional mechanical parts required for the measurement setup. The authors also extend their thanks to Samuli Siitonen of NanoComp Oy for the SEM image of the model grating array (Fig. 4), and to Luc D'Haenens of DuPont Corp. for donating the AF 1600 polymer for this study.

References

1. J. Kimmel and T. Levola, "Backlights in mobile display power management," *SID Int. Symp. Digest Tech. Papers* **39**, 1594–1597 (2008).
2. Z. Li, A. K. Bhowmik, and P. J. Bos, "Introduction to mobile displays," Chapter 1, in *Mobile Displays: Technology and Applications*, A. K. Bhowmik, Z. Li, and P. J. Bos, eds., pp. 1–22, Wiley, Chichester (2008).
3. A. Funamoto and S. Aoyama, "LED backlight system with double-prism pattern," *JSID* **14**(11), 1045–1051 (2006), <http://dx.doi.org/10.1889/1.2393029>.
4. Apple, Inc. (Specifications for the iPhone.), <http://www.apple.com/iphone/specs.html> (accessed June 8th, 2011).
5. J. Kimmel et al., "A novel diffractive backlight concept for mobile displays," *JSID* **16**(2), 351–357 (2008), <http://dx.doi.org/10.1889/1.2785221>.
6. Z. Ge and S.-T. Wu, "Color sequential mobile LCDs," Chapter 5, in *Transflective Liquid Crystal Displays*, pp. 189–211, Wiley, Chichester (2010).
7. D. R. Selviah and K. Wang, "Modeling of a color-separating backlight with internal mirrors," *SID Symp. Digest Tech. Papers* **35**, Book I, pp. 487–489 (2004), <http://dx.doi.org/10.1889/1.1831020>.
8. M. J. J. Jak et al., "Color-separating backlight for improved LCD efficiency," *JSID* **16**(8), 803–810 (2008), <http://dx.doi.org/10.1889/1.2966441>.
9. J. Kimmel, T. Levola, and P. Laakkonen, "Diffractive backlight grating array for mobile displays," *JSID* **16**(8), 863–870 (2008), <http://dx.doi.org/10.1889/1.2966448>.

10. J. Kimmel et al., "A new diffractive backlight for mobile displays," *Proc. of the 28th International Display Research Conference (IDRC) 2008, Orlando, Florida*, pp. 290–293 (2008).
11. J. Kimmel et al., "Diffractive backlight light guide plates in mobile electrowetting display applications," *SID Int. Symp. Digest Tech. Papers* **40**(1), 826–829 (2009), <http://dx.doi.org/10.1889/1.3256921>.
12. M. Anandan, "Progress of LED backlights for LCDs," *JSID* **16**(2), 287–310 (2008), <http://dx.doi.org/10.1889/1.2841864>.
13. J. P. Plumey and G. Granet, "Generalization of the coordinate transformation method with application to surface-relief gratings," *JOSA A* **16**(3), 508–516 (1999).
14. L. Li, "Formulation and comparison of two recursive matrix algorithms for modeling layered diffraction gratings," *JOSA A* **13**(5), 1024–1035 (1996).
15. SFH217, daylight filter SFH 217F silicon PIN photodiode," in *Optoelectronics Data Book 1993–1994*, 8-71-8-72, Siemens (1993).
16. M. Born and E. Wolf, *Principles of Optics*, 7th ed., Cambridge University Press, Cambridge (2002).



Jyrki Kimmel received the MSc and Licentiate of Technology degrees in electrical engineering from the Tampere University of Technology in 1986 and 1992, respectively. He is currently Distinguished Researcher in Nokia Research Center in Tampere, Finland. He also lectures on display-related topics at Tampere University of Technology. Before joining Nokia in 1996, he was with the Technical Research Centre of Finland, and as a Fulbright Scholar in University of Utah. His current research interests relate to mobile displays, especially backlights. He is a Member of SPIE.



Tapani Levola received his MSc degree in 1976 from the University of Turku in physics, and the PhD degree from the University of Joensuu in 2005 in the field of diffractive optics. Before joining Nokia in 1996, he worked in R&D of semiconductor manufacturing systems. He was a Distinguished Scientist in Nokia Research Center in Tampere, Finland until October, 2011, after which he worked in Vuzix Corporation. In January 2012, he joined Microsoft Oy in Espoo, Finland. He has scientific interests in rigorous modeling of gratings and in 3D display technologies.

Tampereen teknillinen yliopisto
PL 527
33101 Tampere

Tampere University of Technology
P.O.B. 527
FI-33101 Tampere, Finland

ISBN 978-952-15-2844-6
ISSN 1459-2045